Exploring the role of the iron sulphur cluster regulator IscR in *Yersinia*

Clair Brooks, BSc (Hons)

June 2020

Thesis submitted to the University of Nottingham

for the degree of Doctor of Philosophy

Declaration

I declare that the thesis is the result of my own work which has been undertaken during my period of registration for this degree at The University of Nottingham. Unless otherwise acknowledged, the work presented in this thesis is entirely my own. No part has been submitted for another degree in The University of Nottingham or any other institute of learning.

Clair Brooks

June 2020

Abstract

Yersinia pseudotuberculosis is an enteropathogen that is transmitted through contaminated food or water and results in self-limiting fever and gastroenteritis. *Y. pseudotuberculosis* is closely related to *Yersinia pestis,* the cause of bubonic, pneumonic and septicaemic plague. Despite causing vastly different diseases, virulence and in particular, type three secretion (T3S) as well as biofilm formation, motility, and aggregation are controlled in both species by several interrelated regulatory systems including quorum sensing (QS). The latter depends on an *N*-acylhomoserine lactone (AHL) system that incorporates two AHL synthases (YpsI and YtbI) and two LuxR-type response regulators (YpsR and YtbR).

Recently a novel component of this network has emerged, the iron-sulfur cluster regulator, IscR. IscR is a transcription factor best understood for its role in regulating the formation of Fe-S cluster containing proteins in *E.coli*. It is now known that in *Y. pseudotuberculosis* IscR regulates type three secretion, a key virulence mechanism employed by pathogenic *Yersinia* spp. to inject effector proteins into host cells, which have a range of effects including dampening the immune response and inducing apoptosis.

Considering the links between QS, T3S and other QS mediated phenotypes, this study set out to investigate how IscR contributes to this regulatory network, by creating a series of knock-out mutants in *Y. pseudotuberculosis* and *Y. pestis*. Yop secretion assays confirmed that IscR regulates T3S in *Y. pseudotuberculosis* and using chromosomal promoter:*lux* this fusions was found to be via action on *yscW-lcrF* and *lcrF* specific promoters. Further Yop assays showed that IscR's effect on Yop secretion was lost in a QS response regulator gene mutant background, suggesting that IscR may further regulate T3S via the QS system. This was further supported by

promoter:*lux* fusion data that showed that IscR positively regulated the expression of *ypsR* and *ytbR.* However, IscR did not affect expression of either of the AHL synthase genes (*ypsI* and *ytbI*). Whether IscR affects the production of AHL signalling molecules remains inconclusive.

Phenotypic characterisation of the mutants showed that IscR did not affect colony morphology, growth rate or biofilm formation on *C. elegans* in *Y. pseudotuberculosis* or *Y. pestis*. Nor did IscR have an effect on the iron scavenging abilities or motility of *Y. pseudotuberculosis*. The *iscR* mutant did show attenuation of biofilm formation on glass at 22^{o}C, which was not influenced by QS-mediated repression. Mutating *iscR* also resulted in faster killing in a louse infection model which has been linked to dysregulation of biofilm production within the louse gut. A further link between IscR and T3S was identified through auto-aggregation, as this is significantly reduced in an *iscR* mutant. Interestingly, this trend was also observed in QS mutant backgrounds, which did not correspond to levels of Yops secreted, suggesting an alternative mechanism of regulation of auto-aggregation separate from T3S which is IscR-dependent.

Considering these results, the regulation of T3S by IscR has been confirmed, and there is strong evidence for a regulatory link between IscR and QS. This places IscR as a key regulator of many virulence associated phenotypes, including T3S, QS, biofilm formation and aggregation. As a virulence regulator IscR could be a future target for alternative antimicrobial therapies, a necessity given the threat of multidrug resistance and the classification of *Y. pestis* as a re-emerging pathogen.

To my wonderful Grandad,

Always the biggest supporter of my education and passion for Science.

This thesis is for you, I hope you would have been proud.

William and Deanna Brooks, 1961

Acknowledgements

Firstly, I must thank my supervisors, Dr Steve Atkinson and Professor Paul Williams for taking me on as their student, and for their contribution of time and research ideas. Your help and support has been invaluable. I am grateful to Jeni Luckett, Ewan Murray, Phil Barderlang and Nigel Halliday for their technical support and advice. A huge thank you to Vanina Garcia for all of your help through the years, in particular with training me in the CL3 laboratory and supporting me when I was less than comfortable with certain insects!

The *Yersinia* 'dream team' have made my PhD particularly special; Amy Slater, Natalie Barratt, Linzy Elton and Carolina Paiva, thank you for all of the memories, I will see you in Georgia one day! My friends have made the last four years unforgettable, particularly William Richardson and Dean Walsh, thank you for always trying to keep me sane.

I wouldn't be where I am today without the love and support of my family. Thank you to my parents for their endless support and encouragement, and my lovely Grandma for always being there for a drink and a chat when needed. Mum, it is safe to say I would not have finished this PhD without your constant motivation and comfort, thank you for putting up with all of my complaining!

Table of Contents

List of tables

List of figures

Abbreviations

<	Less than
>	Greater than
≤	Equal to or greater than
≥	Equal to or less than
µg	Microgram
µl	Microlitre
µM	Micromolar concentration
AAg	Auto-aggregation
AHL	*N*-acylhomoserine lactone
AI-2	Autoinducer-2
Ail	Adherence-invasion locus
Amp	Ampicillin
ANOVA	Analysis of variance
APS	Ammonium persulfate
BHI	Brain heart infusion media
bp	Base pair
BSA	Bovine serum albumin
BSI	Biofilm severity index
Ca^{2+}	Calcium
CL2	Containment level 2 laboratory
CL3	Containment level 3 laboratory
CLSM	Confocal laser scanning microscopy
Cm	Chloramphenicol
CO92	Colorado (1992) *Y. pestis* strain
CR-MOX	Congo Red Magnesium Oxalate agar
dH_2O	Distilled water
DMSO	Dimethyl sulfoxide
DNA	Deoxyribonucleic acid
dNTP	Deoxynucleotide
DTT	DL-Dithiothreitol
ECM	Extracellular matrix
EDTA	Ethylenediaminetetraacetic acid
Erm	Erythromycin
EtOH	Ethanol
g	Gram(s)
gDNA	Genomic DNA
GFP	Green fluorescent protein
GlcNAc	*N*-acetyl-D-glucosamine
GlcNAc-6-P	*N*-acetyl-D-glucosamine-6-phosphate
GMO	Genetically modified organism
Gm	Gentamicin
hms	Haemin storage locus
Kan	Kanamycin
kb	Kilobase
kDa	KiloDalton
KIM	Kurdistan Iranian Man *Y. pestis* strain
Km	Kanamycin
kV	Kilovolt
L	Litre
LB	Luria Bertani
LC-MS/MS	Liquid Chromatography – Mass Spectrometry

Log	Logarithmic
M	Molar
min	Minute
ml	Millilitre
mM	Millimolar
mm	Millimetres
MSC	Microbiological safety cabinet
Nal	Nalidixic acid
ng	Nanograms
NGM	Nematode Growth Medium
ºC	Degrees Celsius
OD	Optical Density
PBS	Phosphate Buffered Saline
pCD1	*Yersinia pestis* virulence plasmid
PCR	Polymerase chain reaction
PEG	Polyethene glycol
PFA	Paraformaldehyde
pFra (pMT1)	CO92 Murine toxin plasmid (KIM strain name)
pH	Potenz (power) of hydrogen
pPst (pPCP)	CO92 pesticin, coagulase and plasminogen activator plasmid (KIM name)
QS	Quorum sensing
R	Resistance
RBS	Ribosome Binding Site
RLU	Relative Light Units
RLU/OD_{600}	Relative light units per cell population density
RNA	Ribonucleic acid
rpm	Revolutions per minute
SAM	*S*-adenosylmethionine
SD	Standard Deviation
SDS	Sodium dodecyl sulphate
SDS-PAGE	Sodium dodecyl sulphate polyacrylamide gel electrophoresis
Sm	Streptomycin
Spp.	Species
T3S	Type III secretion
TAE	Tris-acetate-EDTA buffer
Tc	Tetracycline
TCA	Trichloroacetic acid
Tris	Tris hydroxymethyl aminomethane
V	Volts
v/v	Volume to volume ratio
w/v	Weight to volume ratio
WGA	Wheat germ agglutinin
x	Times
x g	Times gravitational force
X-gal	5-bromo-4-chloro-3-indolyl-β-D-galactopyranoside
YDMM	*Yersinia* defined minimal medium
Yop	*Yersinia* outer protein
YPIII	*Yersinia pseudotuberculosis III* strain
YSA	*Yersinia* selective agar
Ysc	*Yersinia* secretion complex
Δ	Mutant
Ω	Ohm
MOPS	3-(*N*-morpholino)propanesulfonic acid
n/a	Not applicable

Introduction

1.1 The Pathogenic *Yersiniae*

The genus *Yersinia* is made up of eleven Gram negative species (Chen, Cook, Stewart, *et al*., 2010), three of which are important human pathogens: *Yersinia pestis*, the causative agent of bubonic, pneumonic and septicaemic plague, and *Yersinia enterocolitica* and *Yersinia pseudotuberculosis*, which cause gastoenteritis.

Enteropathogenic *Yersinia* typically cause self-limiting fever and gut associated symptoms, including diarrhoea and abdominal pain often referred to as Yersiniosis. Infections are rarely fatal, although complications can arise such as reactive arthritis and septicaemia (Koornhof, Smego, and Nicol, 1999). Human infection usually occurs *via* the fecal-oral route, with infected food or water often acting as a reservoir. Raw or poorly cooked pork or unwashed vegetables such as lettuce are a common source of infection (Bottone, 1997). *Y. pseudotuberculosis* and *Y. enterocolitica* have been found to exist in a range of conditions but thrive in moist natural environments, such as soil.

Y. pestis causes plague, a severe illness, which in the absence of effective antimicrobial therapy is often fatal. Plague can present in three forms, pneumonic, bubonic or septicaemic (Reviewed in (Perry and Fetherston, 1997)) and is usually transmitted to humans from an infected mammal *via* an intermediate vector, such as a flea. Person to person transmission can then occur, usually as a result of the aerosol transmitted pneumonic plague. Bubonic plague often results when *Y. pestis* enters the host through a skin lesion, either via an open wound or flea bite, and if the organism migrates to the blood stream, the infected individual may present with septicaemic plague. Pneumonic plague can either be a primary infection, caught by inhaling infected aerosols, or a secondary infection as a result of the bacteria spreading to the lungs from a bubonic or septicaemic infection (Perry and Fetherston, 1997).

Bubonic plague presents between two and eight days after initial infection with symptoms including fatigue, headache, fever and the appearance of buboes due to swelling of

regional lymph nodes. Septicaemic plague presents as a typical Gram-negative septicaemia with fever, chills, headaches and gastrointestinal disease and has a very high mortality rate (Crook and Tempest, 1992; Perry and Fetherston, 1997). Pneumonic plague starts wth flu-like symptoms and progresses to serious pneumonia, with the majority of untreated cases resulting in death within 24-36 hours (Crook and Tempest, 1992; Pechous, Sivaraman, Stasulli, and Goldman, 2016).

Y. pestis is infamous as the cause of three historic pandemics, including the fourteenth century 'Black Death' responsible for reducing Europe's population by around a third (Cohn, 2008). However, plague is not just of historical interest as infections still persist today (Zietz and Dunkelberg, 2004) with natural plague foci in a number of countries including Madagascar, the Democratic Republic of the Congo and Peru (Figure 1.1). Sporadic cases are also observed annually in the United States (Kugeler, Staples, Hinckley, Gage, and Mead, 2015), Russia and adjacent countries. *Y. pestis* is also of increasing concern as several of its properties, including aerosol transmission, rapid disease progression and high mortality rates, make it an attractive agent for use in bioterrorism (Inglesby, Dennis, Henderson, *et al*., 2000).

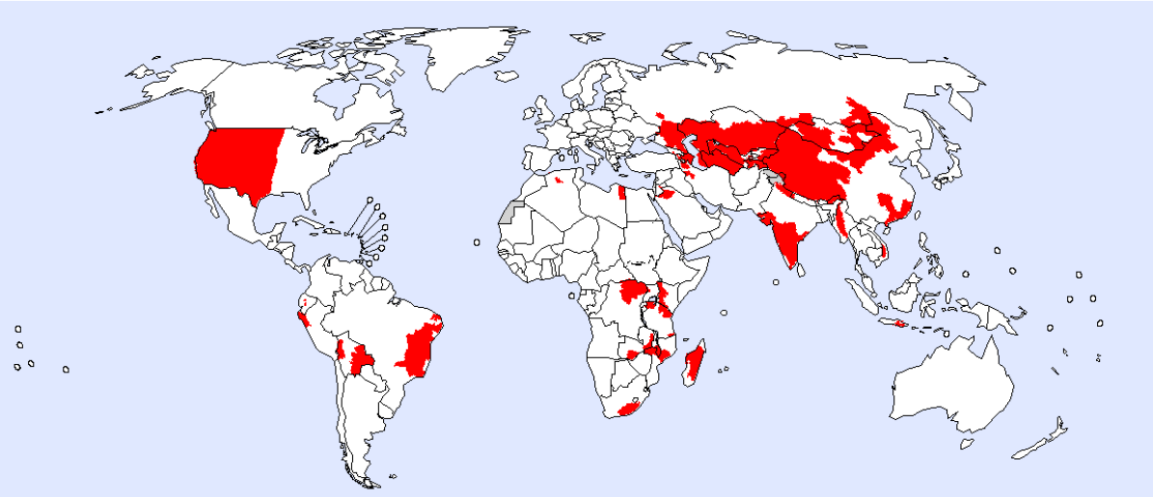

Figure 1.1 Global distribution of natural plague foci as of March 2016.

Red areas show potential plague natural foci based on historical data and current information. Source: WHO/PED as of March 2016.

Y. pestis and *Y. pseudotuberculoisis* share strong DNA sequence homology, such that they are indistinguishable by DNA hybridisation methods and share 99.7% sequence identity in 16s rDNA studies (Bercovier, Mollaret, Alonso, *et al*., 1980; Ibrahim, Goebel, Liesack, Griffiths, and Stackebrandt, 1993). Evidence indicates that *Y. pestis* evolved from *Y. pseudotuberculosis* as recently as 1500 – 2000 years ago, just before the first recorded human plague pandemic (Achtman, Zurth, Morelli, *et al*., 1999; Achtman, Morelli, Zhu, *et al*., 2004)[,]. The most obvious genetic difference is in the acquisition of two additional plasmids by *Y. pestis*, pPCP (also known as pPla, pYP and pPst) and pMT, (otherwise known as pFra and pYT) (Ferber and Brubaker, 1981). In addition, the chromosome of *Y. pestis* has acquired a number of mutations and deletions. Based on these relatively few genetic differences, the differences in pathogenicity between the two species are striking (Hinnebusch, 1997).

1.2 Pathology of *Yersinia* Infections

The disease progression of the enteropathogenic *Yersinia* is markedly different to that of *Y. pestis*, with the former resulting in a chronic infection and plague an acute infection that kills its host relatively quickly. This difference is indicative of their modes of transmission, as a chronic infection ensures *Y. pseudotuberculosis* can be excreted for long periods of time. *Y. pestis* however favours a rapid, acute infection where the bacteria can quickly disseminate from the initial infection site and reach the vascular system, where its presence ensures access to the flea vector and the fatality of the host, forcing the flea to search for a new host and spread the bacteria (Brubaker, 1991). Despite clear differences in transmission routes and pathologies, all three human pathogenic *Yersinia* have common virulence features, including a tropism for lymphatic tissues and an enhanced ability to resist the innate immune response (Bliska, Wang, Viboud, and Brodsky, 2013).

Upon consumption of contaminated food, the enteropathogenic *Yersinia* adhere to the small intestinal epithelial cells, and eventually cross the intestinal barrier *via* the antigen

sampling M cells (Galindo, Rosenzweig, Kirtley, *et al*., 2011; Grutzkau, Hanski, Hahn, and Riecken, 1990). The bacteria then replicate in Peyer's patches. M cells, also known as microfold cells, are important factors in the immune response as they transport vesicular enclosed bacteria to antigen presenting cells in gut lymphoid tissue (Clark, Hirst, and Jepson, 1998). However, as *Yersinia* are not enclosed in vesicles when they are transported into Peyer's patches, localisation relies on a number of adhesive and invasive virulence factors instead. These are essential to promote contact with and invasion of host cells, as are anti-phagocytic virulence factors needed to inhibit uptake by cells of the host immune system. The adhesins are essential to ensure close host contact and several have been identified, both chromosomally and plasmid encoded (Reviewed by Atkinson and Williams, 2016). Not all of the *Yersinia* adhesins are shared by the three human pathogens, but combinations act in each species to allow contact with host cells, helping to promote invasion or ensure successful delivery of effector proteins into the host.

As enteropathogens, the ability to specifically adhere to and invade cells lining the surface of the gut is crucial for *Y. pseudotuberculosis* and *Y. enterocolitica* and two adhesins, Invasin and YadA, are vital for this process. Invasin, a chromosomally encoded outer membrane protein, plays a major role in allowing *Y. pseudotuberculosis* to pass into the lymphatic system via M-cells by binding to β1-integrins causing them to associate into clusters and resulting in cytoskeletal rearrangements (Clark *et al*., 1998) that promote internalisation of the bacteria by the epithelial cells and subsequent transfer into the lymphatic system. YadA, encoded on the virulence plasmid pYV, is the major adhesin responsible for contact with submucosal cells (Mühlenkamp, Oberhettinger, Leo, Linke, and Schütz, 2015) which along with invasin is primarily concerned with enteropathogenicity. It is therefore unsurprising that are both found as pseudogenes in *Y .pestis* (Parkhill, Wren, Thomson, *et al*., 2001).

Ail is a 17 kDa chromosomally encoded protein present in all three human pathogenic *Yersinia* (Miller, Bliska, and Falkow, 1990; Miller and Falkow, 1988). In all three species Ail has cell adhesion properties as well as providing resistance to complement mediated killing

(Miller and Falkow, 1988; Felek and Krukonis, 2009; Bartra, Styer, O'Bryant, *et al*., 2008; Ke, Chen, and Yang, 2013). In *Y. pestis*, Ail is thought to facilitate attachment to host cells through binding to laminin and fibronectin, two components of the extracellular matrix (Tsang, Felek, and Krukonis, 2010). Interestingly, Ail from *Y. pseudotuberculosis* confers different adhesion and invasion functions to that of *Y. pestis*, which has been attributed to two amino acid substitutions (Miller, Beer, Heusipp, Young, and Wachtel, 2001; Ke *et al*., 2013)'. It is perhaps unsurprising that Ail plays a more prominent role in *Y. pestis* virulence when compared to *Y. pseudotuberculosis*, considering the functional redundancy between Ail and other virulence factors encoded by the enteropathogenic *Yersinia* which are not active in *Y. pestis* (Atkinson *et al*., 2016).

Another adhesin found in all three human pathogenic *Yersinia* is the chromosomally encoded pH6 antigen (Psa) which was first identified in *Y. pestis* where it was shown to coat bacteria with a fibrillar matrix (Ben-Efraim, Aronson, and Bichowsky-Slomnicki, 1961, Lindler and Tall, 1993). In *Y. pseudotuberculosis*, (where it is known as MyfA), it has been shown to promote attachment to tissue culture cells (Yang, Merriam, Mueller, and Isberg, 1996) and has also been shown to have anti-phagocytic effects (Huang and Lindler, 2004), perhaps through its ability to bind to β1-linked galactosyl residues in glycosphingolipids and *apoB*-containing LDL in human plasma (Payne, Tatham, Williamson, and Titball, 1998; Makoveichuk, Cherepanov, Lundberg, Forsberg, and Olivecrona, 2003; Ke *et al*., 2013). The differences in virulence between *Y. pestis* and *Y. pseudotuberculosis* is largely down to the acquisition by *Y. pestis* of two plasmids, pPCP and pMT, which possess additional virulence factors. The protease Pla, or plasminogen activator, which is encoded on pPCP allows *Y. pestis* to rapidly invade host tissue and disseminate from peripheral sites of infection as it converts plasminogen to plasmin, which subsequently degrades the extracellular matrix (Degen, Bugge, and Goguen, 2007). Pla has other activities that enhance *Y. pestis* migration and dispersal, including acting as an adhesin and preventing blood clotting through its fibrinolytic activity (Kienlel, Emody, Svanborg, and O'Toole, 1992; Lähteenmäki, Kukkonen, and Korhonen, 2001)'. pPCP also encodes the bacteriocin

pesticin, and a pesticin immunity protein, which are used by bacteria to defend a niche environment from closely related species (Hu and Brubaker, 1974). Pesticin exhibits *N*-acetylglucosaminidase activity, which is active against some strains of *Y. pseudotuberculosis* and *Y. enterocolitica*, as well as sensitive *Y. pestis* cells that have been cured of the pPCP plasmid (Hu and Brubaker, 1974; Ferber and Brubaker, 1979; Rakin, Boolgakowa, and Heesemann, 1996).

pMT encodes the virulence factor fraction 1 (F1) antigen, made up of the fraction 1 capsular antigen (Caf1) subunit (Zavialov, Berglund, Pudney, *et al*., 2003). Similar to Psa, F1 forms fimbrial structures on the bacterial surface that have anti-phagocytic activity and enhance extracellular survival (Du, Rosqvist, and Forsberg, 2002). pMT also encodes the *Yersinia* murine toxin (Ymt), a phospholipase D homologue, named because of its highly toxic effects in mice (Schar and Meyer, 1956). The toxin is crucial for survival in the flea mid-gut and subsequent colonisation by *Y. pestis* (Hinnebusch, Fischer, and Schwan, 1998; Hinnebusch, Rudolph, Cherepanov, *et al*., 2002). The phospholipase D activity is believed to protect the bacteria from a flea-derived cytotoxin and although the mode of action is unknown, two models have been proposed. The prophylaxis model proposes that Ymt modifies components of the bacterial membrane to make it impenetrable to the cytotoxin , and the antidote model suggests that Ymt directly or indirectly neutralises the cytotoxin upon contact with the bacteria (Hinnebusch *et al*., 2002).

Although pPCP and pMT are *Y. pestis* specific, all three human pathogenic *Yersinia* possess an approximately 70 kb virulence plasmid known as pYV in *Y. pseudotuberculosis*, pCD1 in *Y. pestis* and pYVe in *Y. enterocolitica* (Gemski, Lazere, Casey, and Wohlhieter ', 1980; Laroche, van Bouchaute, and Cornelis, 1984)'. The plasmid was often referred to as the low calcium response plasmid (Lcr), due to the observation that in sub-millimolar concentrations of calcium, *Yersinia* strains carrying the virulence plasmid show growth arrest at 37^{o}C (Mehigh, Sample, and Brubaker, 1989; Straley, Plano, Skrzypek, Haddix, and Fields, 1993). These conditions are believed to mimic the effect of host cell contact and offer a convenient way to study T3S *in vitro*. At Ca^{2+} concentrations less than 2.5mM

and at 37^{o}C the virulence factors encoded on pYV are synthesised. High Ca^{2+} and lower temperatures resumes vegetative growth and represses expression of genes on the plasmid (Sample, Fowler, and Brubaker, 1987a; G R Cornelis, Boland, Boyd, *et al*., 1998). At the DNA level, the three pYV plasmids share a high degree of homology but the response to low Ca^{2+}, such as the shut off of cell division, is amplified in *Y. pestis* (Carter, Zahorchak, and Brubaker, 1980; Brubaker, 1991).

Virulence factors encoded on this plasmid include the *Yersinia* outer proteins, or Yop effectors, which are injected directly into host cells. Yops primarily target the actin cytoskeleton and important signalling pathways which dampen the immune response. pYV also codes for the V antigen, or LcrV, a protein with multiple functions including modulation of the immune response and secretion control (Fields, Nilles, Cowan, and Straley, 1999). The plasmid also encodes a specialised apparatus used to secrete these virulence factors, known as the Type Three Secretion (T3S) system. Strains lacking this plasmid exhibit either a severe reduction or a complete attenuation of virulence (Portnoy and Falkow, 1981; Portnoy, Moseley, and Falkow, 1981).

1.3 Type Three Secretion

1.3.1 The Injectisome

The mechanism for delivering virulence effectors into host cells comes in the form of the pYV encoded type T3S system. T3S systems are analogous to a hypodermic needle (injectisome), injecting the effectors directly into the cytosol of the host cell. The T3S system is closely related to the flagellum, has a core of 8 proteins that are similar to components of flagella export apparatus (Van Gijsegem, Gough, Zischek, *et al*., 1995). However, there is still debate over whether the injectisome is derived from flagellum or rather that they share a common ancestor (Gophna, Ron, and Graur, 2003).

T3S systems are not limited to *Yersinia*, and the injectisome is both structurally and functionally conserved in over 25 different negative species (Troisfontaines and Cornelis, 2005). The T3S system is usually encoded in a single gene cluster on a mobile genetic element, be it a plasmid or pathogenicity island (Guy R Cornelis, 2006; Schmidt and Hensel, 2004)[1]. Evidence suggests that the injectisomes have evolved by lateral gene transfer into seven different families, with subtle differences between them (Gophna *et al*., 2003). The archetypal system is the Ysc (*Yersinia* secretion) system found in *Yersinia* spp., and this will be discussed from here onwards.

The injectisome is assembled from 21 Ysc proteins and the entire complex spans the inner and outer bacterial membranes, the extracellular space and the cellular membrane of the host, resulting in a direct and uninterrupted path for effectors to be delivered from bacterial cytoplasm into the host cytosol (Yip and Strynadka, 2006). The injectisome can be divided into three components: the basal body, needle and tip complex (Figure 1.2).

The basal body is cylindrical in shape, similar to the flagellar basal body, and consists of two pairs of rings joined by a rod that span both the inner and outer bacterial membranes. The outer rings are associated with the outer membrane and peptidoglycan layer and consist of a 12-14mer of the secretin YscC. YscC belongs to a multifunctional family of proteins that are able to form pores in outer membranes and so participate in a variety of transport processes (Koster, Bitter, de Cock, *et al*., 1997). An outer membrane protein, YscW, assists with the oligomerisation and insertion of YscC into the outer membrane (Burghout, Beckers, de Wit, *et al*., 2004). The second ring, anchored to the inner membrane, is termed the MS (membrane and supramembrane) ring, and is composed of YscD and YscJ (Silva-Herzog, Ferracci, Jackson, Joseph, and Plano, 2008; Ross and Plano, 2011). The basal body complex is completed by a number of proteins in association with the rings (Dewoody, Merritt, and Marketon, 2013). This includes a set of five integral membrane proteins that form the export apparatus YscRSTUV which assembles separately to the scaffold proteins that make up the rings (Diepold, Wiesand, and Cornelis, 2011). The final two components are the ATPase complex YscNKL involved in producing the proton

motive force needed for export, and a component analogous to the flagellar C ring comprised of YscQ (Blaylock, Riordan, Missiakas, and Schneewind, 2006, Bzymek, Hamaoka, and Ghosh, 2012).

The basal body then forms a platform for the assembly of the rest of the injectisome. The next part of the system is the needle, which is made up of around 100-150 helically polymerised subunits of YscF (Hoiczyk and Blobel, 2001). The needle is hollow, approximately 60-80 nm long and has an inner diameter of around 25Å. The length of the needle has been evolutionary adjusted relative to the size of other structures on the bacterial surface and so varies between different species, and even amongst different strains there can be as much as 20% difference (Guy R Cornelis, 2006). Precise needle length is essential and this is regulated by YscP, often known as a molecular ruler, which enforces a substrate specificity switch once the needle has reached the correct length, terminating YscF export (Payne and Straley, 1999; Journet, Agrain, Broz, and Cornelis, 2003; Agrain, Callebaut, Journet, *et al*., 2005)'.

At the end of the needle is the LcrV (V-antigen) tip complex or translocation pore which once secreted polymerises at the end of the YscF needle, forming a pentamer (Mueller, Broz, Müller, *et al*., 2005). This then acts as a platform allowing two pore proteins, YopD and YopB, to insert into the host cell membrane (Goure, Pastor, Faudry, *et al*., 2004; Mueller, Broz, and Cornelis, 2008). It is through this completed pore that effectors are transported across host cell membrane and into the cytosol.

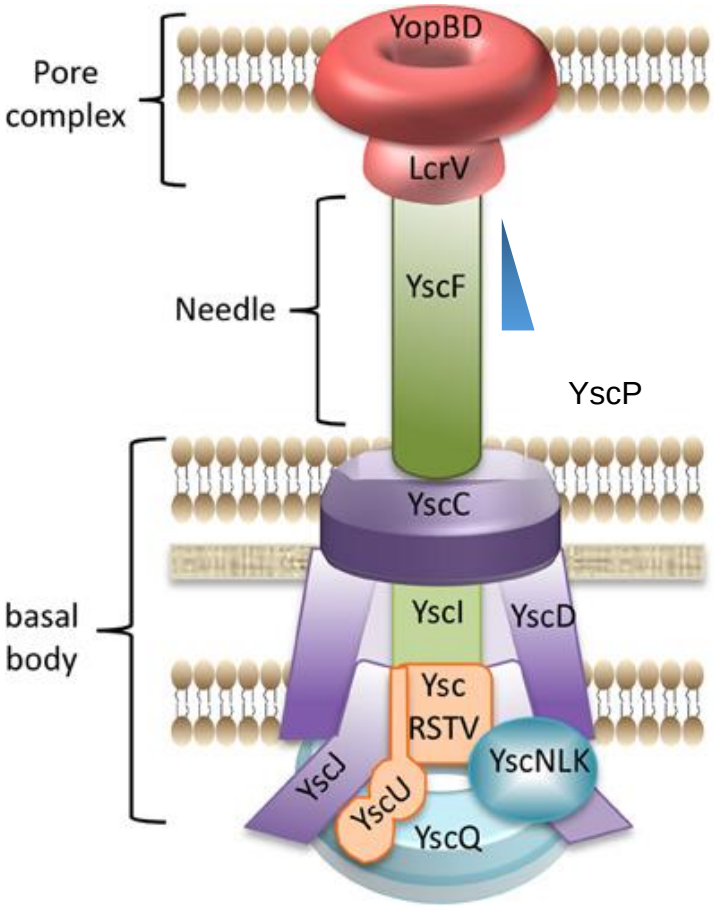

Figure 1.2 The type three secretion injectisome of *Yersinia* species.

Purple denotes scaffold proteins: YscC, YscD, YscJ; orange shows proteins comprising the export apparatus: YscR, YscS, YscT, YscV, YscU; Blue shows cytoplasmic proteins: YscN, YscL, YscK, YscQ; Red shows the needle tip complex comprised of LcrV and the translocation pore consisting of YopB and YopD. Figure from (Dewoody *et al*., 2013)

1.3.2 Yop effectors

Whilst the injectisome structure is relatively conserved across species, over 100 effectors have been identified, with each pathogen using a distinct set. Their modes of action vary with target systems including those involved in phagocytosis, the inflammatory response, apoptosis and autophagy. In *Yersinia* spp. there are five effectors, YopH, YopM, YopE, YopO and YopJ/P. Three target the actin cytoskeleton and the other two reduce the immune response by interfering with signalling pathways (Trosky, Liverman, and Orth, 2008).

YopH is a potent tyrosine phosphatase that targets focal adhesion proteins and other targets required for effective phagocytosis, dampening the immune response (Viboud and Bliska, 2005; Fällman, Persson, Schesser, and Wolf-Watz, 1998). YopE is a GTPase activating protein that disrupts the actin cytoskeleton by targeting and inhibiting members of the Rho family of small G-proteins including RhoA, Rac1 and Cdc42 (Von Pawel-Rammingen, Telepnev, Schmidt, *et al*., 2000). YopM is the only effector with no known catalytic activity but it has been proposed to act as a scaffold protein, mediating protein-protein interactions between two important cellular kinases, allowing Rsk1 to activate Prk2 (McDonald, Vacratsis, Bliska, and Dixon, 2003). However, its full role in *Yersinia* virulence is still unclear. YopO, sometimes known as YpkA, is a multifunctional protein with both serine/threonine kinase and GDI (guanidine nucleotide dissociation inhibitor) domains, that are believed to act together to disrupt the actin cytoskeleton and impair phagocytosis (Lee, Grimes, and Robinson, 2015). YopJ is a serine/threonine acetyltransferase that inhibits several signalling pathways, including the Mitogen-activated protein kinase (MAPK) pathway, which dampens the immune response (Orth, Palmer, Bao, *et al*., 1999).

1.3.3 Regulation of Type Three Secretion

Both *Y. pestis* and *Y. pseudotuberculosis* exhibit biphasic lifestyles, with *Y. pseudotuberculosis* alternating between soil or aquatic environments and the mammalian gastrointestinal tract and *Y. pestis* needing to survive in the insect vector and mammalian host (Martínez-Chavarría and Vadyvaloo, 2015; Eisen and Gage, 2009). Virulence factors only need to be expressed when in a host and so both an increase in temperature to 37ºC and host cell contact is needed to induce expression of the T3S system. The tight regulation of T3S is largely down to two transcriptional regulators, LcrF and YmoA.

LcrF is an AraC-like transcriptional activator, encoded on pYV/pCD1, and highly conserved amongst all human pathogenic *Yersinia*. It is named due to the observation that mutations in this gene alter the low calcium response (lcr) phenotype (G R Cornelis, Biot, Lambert de

Rouvroit, *et al*., 1989). The lcr is characterised by restricted growth and synthesis of Lcr plasmid-encoded virulence functions in low Ca^{2+} concentrations and at 37ºC (Mehigh et al., 1989).

At 37ºC *lcrF* expression increases and activates transcription of the T3S system and associated Yop genes (G R Cornelis and Wolf-Watz, 1997; Hoe and Goguen, 1993). However, LcrF does not trigger translocation of effectors (Wattiau and Cornelis, 1994). *lcrF* expression is subject to thermoregulation, via a short stem loop structure or 'RNA-thermometer' which at environmental temperatures conceals the *lcrF* ribosome binding site and prevents translation. It has been proposed that when temperature increases, hydrogen bonds in the AT-rich thermometer melt, unmasking the RBS and initiating *lcrF* translation (Hoe and Goguen, 1993; Böhme, Steinmann, Kortmann, Seekircher, Heroven, Berger, Pisano, Herbst, *et al*., 2012).

The RNA thermometer is located in an intergenic region between *lcrF* and the T3S system chaperone *yscW*, which lies 123 bp upstream of *lcrF*, in the same operon and under the control of the same promoter (Böhme, Steinmann, Kortmann, Seekircher, Heroven, Berger, Pisano, Herbst, *et al*., 2012). In addition to the translational regulation, this operon is under the control of the transcriptional repressor, YmoA (*Yersinia* modulator). YmoA is a histone-like protein that is proposed to prevent expression of *lcrF* at low temperatures through influencing DNA topology, such as compaction of chromatin and impacting on DNA supercoiling (G R Cornelis, Sluiters, Delor, *et al*., 1991; G R Cornelis, 1993). At 37ºC the repressor activity of *ymoA* falls and allows for the assembly of the T3S system. This is partly due to ClpXP and Lon mediated proteolysis of YmoA, temperature-induced topological changes of the promoter and conformational changes in the regulatory proteins (Jackson, Silva-Herzog, and Plano, 2004; Ono, Goldberg, Olsson, *et al*., 2005). Several chromosomally encoded genes have also been identified as being necessary for effective regulation of T3S in *Y. pestis* including those involved in the biosynthesis or integrity of the cell envelope and in LPS biosynthesis (Houppert, Kwiatkowski, Glass, *et al*., 2012). Recent

lux promoter fusion studies in *Y. pseudotuberculosis* showed that *ymoA* expression is upregulated by QS and *lcrF* is downregulated, highlighting another regulatory mechanism for T3S (Slater, 2017). When studying *lcrF* promoter activity in QS mutant backgrounds, significant repressive activity of *ytbR/ysR* was observed supporting the phenotypic observations of a negative role for QS on T3S (Slater, 2017; Atkinson, Goldstone, Joshua, et al., 2011; Atkinson, Chang, Sockett, et al., 2006). Further promoter::*lux* fusions showed that YpsI/YtbI and YpsR/YtbR both activated *ymoA* expression. As YmoA represses T3S through *lcrF,* activation of *ymoA* by QS indirectly represses the T3S system (Slater, 2017).

1.4 Quorum Sensing

Until the early 1990's it was generally accepted that individual bacteria in a population were autonomous entities. However, this belief has been superseded by the realisation that a bacterial community is capable of complex coordinated social interactions, facilitated by the release of extracellular signal molecules. The signal molecules are usually released in response to environmental challenge which results in a change in gene expression, and a coordinated change in community behavior. The ability to coordinate gene expression in this way can confer a number of advantages and improve the survival of the population, this includes enhancing access to nutrients, adapting to the host environment and defending against competitor organisms (Williams, 2007). Interestingly, cross talk between different genera has been observed as some species of different genera have been found to produce and respond to the same signal molecules (Williams, 2007).

The process through which bacteria communicate is known as quorum sensing (QS) which represents a change in gene expression in response to the release and accumulation of a diffusible signal molecule within the environment. This increase in signal molecule concentration is dependent on the cell population density, so QS results in population dependent gene expression. However, the concentration of signal molecule depends on additional factors and as a result QS has also been referred to as diffusion, compartment or

efficiency sensing, as the signals provide information on the local environment and spatial distribution of cells, in addition to population density (Atkinson and Williams, 2009). There are several chemically distinct types of signalling molecules including modified peptides, alkylquinolones and furanones (Yates, Philipp, Buckley, *et al*., 2002) and QS systems are ubiquitous in Gram positive and negative bacteria. It was suggested that there may be a conserved QS system in the form of LuxS and the signalling molecule autoinducer-2 (AI-2) (Xavier and Bassler, 2003; X. Chen, Schauder, Potier, *et al*., 2002). Although *Yersinia* spp. possess a *luxS* gene, there is little evidence that it acts as a QS synthase in these bacteria, and as LuxS is a key metabolic enzyme, phenotypes attributed to the mutation of *luxS* may be a consequence of disrupted *S*-adenosylmethionine (SAM) recycling (Winzer, Hardie, Burgess, *et al*., 2002).

The most widely studied class of signal molecules are the *N*-acylhomoserine lactones (AHLs) which are used by many different Gram-negative species. AHLs are synthesised from precursors of fatty acid and amino acid metabolism and there are many different variations. The basic structure consists of a homoserine lactone ring that is *N*-acylated with a fatty acyl group at the α-position and unsubstituted in the β and γ positions (Chhabra, Philipp, Eberl, *et al*., 2005). AHLs exhibit various saturation levels, oxidation states and acyl chain lengths however most have acyl chains that belong to either *N*-acyl, *N*-(3-oxyacyl) or *N*-(3-hydroxyacyl) classes, which are shown in Figure 1.3 (Williams, 2007). AHLs are usually but not always synthesised by an AHL synthase belonging to the LuxI family of proteins. A single LuxI homologue is often capable of producing a large number of different AHLs and many bacteria contain more than one AHL synthase.

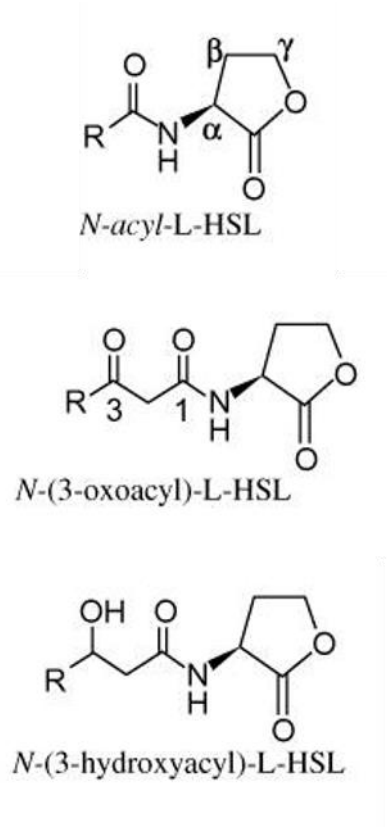

Figure 1.3 The structures of common AHL signal molecules.

Most have acyl chains belong to either *N*-acyl, *N*-(3-oxyacyl) or *N*-(3-hydroxyacyl) classes. Figure adapted from (Atkinson and Williams, 2009)

AHL-mediated QS requires both a synthase and a signal transduction mechanism, represented in Figure 1.4. Depending on the length of the acyl chain, AHL molecules diffuse out or are pumped out of the cell, where they accumulate in the extracellular environment (Pearson, Van Delden, and Iglewski, 1999). Upon reaching a threshold concentration, AHLs exert their effect by binding to members of the LuxR family of transcriptional regulators, which repress or activate target genes.

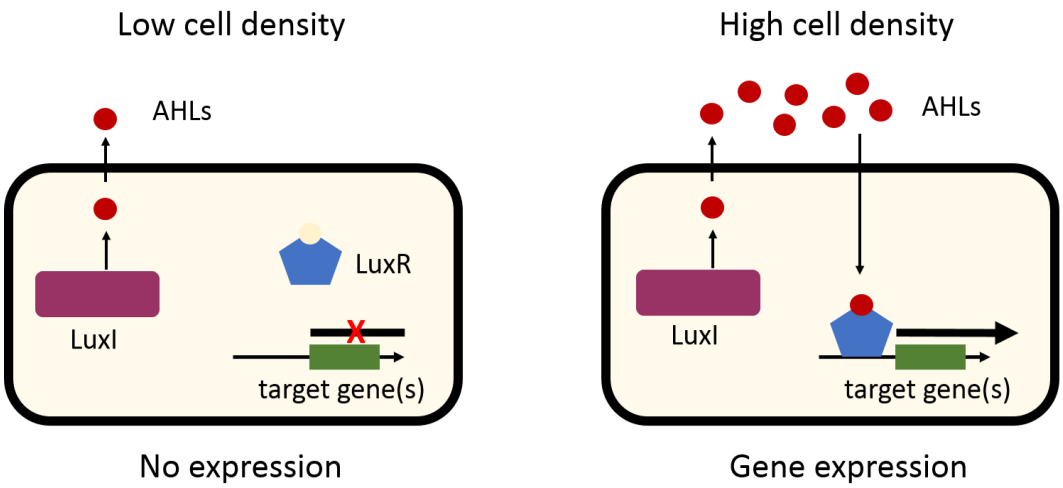

Figure 1.4 Quorum sensing schematic.

Quorum sensing involves the production of *N*-acylhomoserine lactone (AHL) signal molecules by members of the LuxI family of synthases. AHLs bind to members of the LuxR family of response regulators, which can then activate target genes.

In *Y. pseudotuberculosis*, two QS systems homologous to LuxR/I have been identified, known as YpsR/I and YtbR/I (Atkinson, Throup, Stewart, and Williams, 1999). *Y. pseudotuberculosis* is capable of producing 24 different AHLs with acyl chain lengths ranging from C4 to C15. The most abundant AHLs were found to be those with 3-oxo-substituted C6, C7 and C8 as well as the unsubstituted C6 and C8 compounds (Ortori, Atkinson, Chhabra, *et al*., 2007b). Interestingly, not all AHLs are produced by both systems. YtbI is able to produce all 24 AHLs whereas YpsI is only able to synthesise 3-oxo-C6-HSL, C8-HSL and 3-oxo-C7-HSL (Ortori *et al*., 2007b). In *Y. pseudotuberculosis* the four QS genes are present at two loci and are convergent and overlapping. YpsR/I activates itself and the YtbR/I system whereas the YtbI/R activates expression of *ytbI* and has no effect on *ypsI/R*, as shown in Figure 1.5 (Atkinson, Chang, Patrick, et al., 2008).

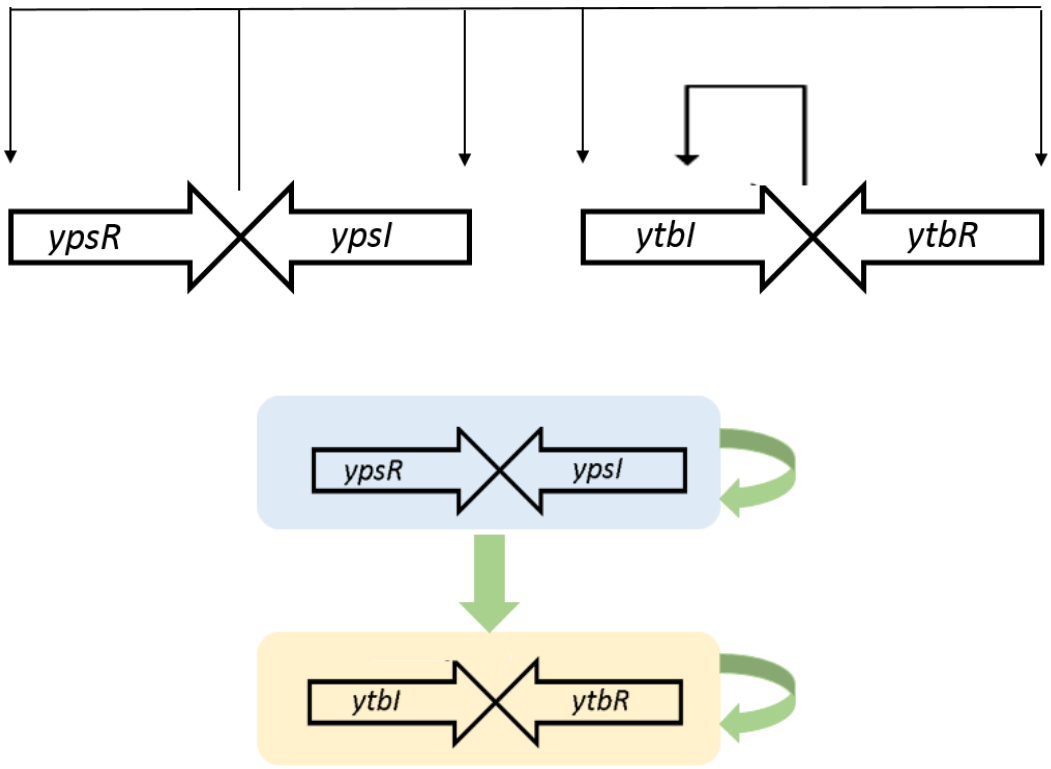

Figure 1.5 A model showing the convergent, overlapping organisation of the quorum sensing *luxRI* homologues in *Y. pseudotuberculosis*

The four quorum sensing genes are arranged in an overlapping organisation. YpsR/I activates both its own expression and the expression of *ytbR/I.* YtbR/I positively regulates its own expression Lines ending in ▼ indicate activation. Adapted from (Atkinson et al., 2008; Slater, 2017).

Y. pestis contain two QS loci, termed *ypeR/I* and *yepR/I* (Isherwood, 2001.; Swift, Isherwood, Atkinson, Oystom, and Stewart, 1999). *yepI* is a homologue of *ytbI* and *ypeI* a homologue of the *ypsI* synthase gene of *Y. pseudotuberculosis* (Atkinson *et al*., 1999). YepI is known to produce 3-oxo-C8-HSL and 3-oxo-C6-HSL primarily, as well as 3-oxo-C10-HLS, C6-HSL and C8-HSL (Kirwan, Gould, Schweizer, *et al*., 2006) but the full AHL profile of YpeI is still unclear.

1.5 Quorum Sensing Regulated Phenotypes

QS systems are known to regulate a number of behaviours and phenotypes including swarming, antibiotic synthesis, plasmid transfer, biofilm development and virulence and in *Y. pseudotuberculosis* these include swimming motility, biofilm formation and aggregation.

1.5.1 Flagellar-Mediated Motility

Flagella-mediated motility is a tightly regulated system that involves structural and regulatory genes arranged in a hierarchy consisting of three gene clusters, I, II and III. Class I consists of *flhDC*, the master regulator operon that is required for the expression of all other flagellar genes. Class II includes the genes coding for the structural proteins needed for basal body and hook component assembly as well as the flagellar specific sigma factor, FilA, and its regulator FlgM. Class III genes are transcribed from FilA dependent promoters and encode proteins needed for the final maturation of the flagellum (MacNab, 1996).

In Y. pseudotuberculosis the motility is in part regulated by QS, through regulation of *flhDC* and *fliA* expression (Atkinson *et al*., 2008). In swim agar plate and liquid media assays *ypsR* and *ypsI* mutants were found to be hypermotile when compared to the parent at 22^{o}C (Atkinson *et al*., 1999) although the hypermotile phenotype was not observed in *ytbI, ytbR, ypsI/ytbI* and *ypsR/ytbR* mutants. This suggests that YpsR in association with YpsI-derived AHLs represses motility whereas the YtbR/I system has a role in activating the system. (Atkinson *et al*., 2008). Despite possessing one full and a second partial set of flagella genes and regulators, *Y. pestis* is non-motile due to a single base-pair mutation in the *flhD* regulator (Parkhill *et al*., 2001; Isherwood, 2001.).

1.5.2 Biofilm Formation

A biofilm is a community of bacteria surrounded by a self-produced matrix of extracellular polymeric substances (Costerton, Lewandowski, Caldwell, Korber, and Lappin-Scott, 1995). Cells in biofilms are physiologically distinct from their planktonic counterparts and are provided with protection in harsh environments, including challenge from antibiotics,

bacteriophages, antibodies, and phagocytes. Biofilms are formed by a number of pathogenic bacteria and they are of significant interest as they reduce the effectiveness of antimicrobial therapies. Antibiotics are less effective because the matrix makes the bacterial cells harder to reach and the bacteria in biofilms are often in a state of slow growth (Costerton, Stewart, and Greenberg, 1999).

The substances making up the matrix include proteins, nucleic acids, polysaccharides and lipids (Flemming and Wingender, 2010). The major component of *Yersinia* spp. biofilms is poly β-1,6-*N*-acetyl-D-glucosamine (GlcNAc), which is produced through the activities of the *hmsHFRS* operon (Hinnebusch and Erickson, 2008; Bobrov, Kirillina, Forman, Mack, and Perry, 2008). The operons *nagE-nagBACD* and *glmUS* are also involved in GlcNAc degradation and production respectively.The NagC repressor controls the expression of *nagE-nagBACD* involved in the uptake and degradation of GlcNAc. The *glmUS* operon encodes proteins necessary for the synthesis of UDP-GlcNAc and is also regulated by NagC (Plumbridge, 1995; Zhou and Yang, 2011).

Biofilms are of specific interest in *Yersinia* research as they form a crucial part of the model for *Y. pestis* transmission by fleas. Within the flea vector, *Y. pestis* uses biofilms to attach to the surface of the spines that line the inside of the proventriculus. The proventriculus separates the insect foregut and midgut, and contains a series of teeth-like denticles capable of grinding up food particles to pass to the midgut (Hinnebusch and Erickson, 2008). Heavy proliferation of bacteria blocks the gut, meaning no blood can pass into the midgut and the flea begins to starve (Hinnebusch, Perry, Schwan, *et al*., 1996; Hinnebusch and Erickson, 2008). This results in repeated attempts to feed, causing distension of the oesophagus but no blood movement. As starvation continues, eventually the flea relaxes its pharyngeal muscles, causing blood to be forced from the flea into the feeding site, taking *Y. pestis* into a new host (Darby, 2008; Bacot and Martin, 1915). Figure 1.4 shows a typical flea infected and blocked with *Y. pestis*.

Figure 1.4 A flea infected and blocked with *Y. pestis.*

Fresh blood can be seen in the esophagus whilst the midgut only contains dark digestion products of previous meals. Image from (B J Hinnebusch *et al*., 1996)**.**

In addition to forming biofilms in the flea gut, *Y. pestis* also forms biofilms on the head and mouth region of the nematode worm *Caenorhabditis elegans*, as the matrix attaches directly to the nematode cuticle (Darby, Hsu, Ghori, and Falkow, 2002; Joshua, Karlyshev, Smith, *et al*., 2003; Tan and Darby, 2004). *C. elegans* is therefore a good model system for *Yersinia* biofilm production. Production of biofilms on *C. elegans* by *Y. pseudotuberculosis* is strain specific and the majority of strains do not form biofilms on nematodes (Joshua *et al*., 2003). However, a small number of strains do produce biofilms due to the inactivation of one or more inhibitory factors. This includes the widely used laboratory strain YPIII, which has a biofilm^{+} phenotype due to the inactivation of PhoP, a member of the PhoP/PhoQ two-component regulatory system (Sun, Koumoutsi, and Darby, 2009). Despite a biofilm^{+} phenotype, none of these *Y. pseudotuberculosis* strains are able to form biofilms in and colonise fleas. Another insect vector linked to *Y. pestis* transmission is *Pediculus corporis,* the human body louse, as studies have shown that *P. corporis* are capable of transmitting *Y. pestis* in rabbits, with as little as 10 lice needed for infection (Houhamdi, Lepidi, Drancourt, and Raoult, 2006). However, little is known about the mechanism of transmission and whether biofilm formation is involved.

It has been shown that the biofilm formation by *Y. pseudotuberculosis* on *C.elegans* is promoted by the QS system as double mutants in AHL synthase (*ypsI/ytbI)* and response regulator (*ypsR/ytbR)* genes showed a reduction in biofilm formation (Atkinson et al., 2011). This study also found that AHLs were detected in biofilms formed on *C. elegans*. Interestingly, deleting key genes involved in flagellar mediated motility, including *flhDC* and *fliA* which are regulated by the QS system, also resulted in loss of biofilm formation yet this is not because flagellar are required as mutants of the flagellin protein FliC form normal biofilms (Atkinson *et al*., 2011). This study also found that curing the pYV virulence plasmid restored biofilm formation in the *flhDC* and *ypsI/ytbI* mutants, suggesting that expression of the T3S system attenuates biofilm formation and that this is reciprocally regulated with motility, through the QS system (Atkinson *et al*., 2011). Similarly, a triple mutant of *Y. pestis* with mutated *ypeR/I, yepR/I* and *luxS* systems showed a mild reduction of biofilm formation *in vitro* (Bobrov, Bearden, Fetherston, *et al*., 2007).

1.5.3 Aggregation

In suspended cultures, many bacteria adhere together to form multi-cellular communities, in a process which in this thesis will be referred to as auto-aggregation. Auto-aggregation is often used by bacteria to adapt to and survive adverse conditions, and in this way may be thought of a suspended biofilm, offering similar levels of protection. In *Campylobacter jejuni* for example, Joshua *et al.* (Joshua, Guthrie-Irons, Karlyshev, and Wren, 2006) identified aggregates encased in an extracellular matrix that provided similar advantages to forming surface biofilms.

Aggregation of *Y. pseudotuberculosis* and *Y. enterocolitica* when grown at 37^{o}C was first reported in the 1980's (Laird and Cavanaugh, 1980). Later transposon mutagenesis identified the role of P1 protein, encoded on pYV, in auto-aggregation in *Y. enterocolitica* (Balligand, Laroche, and Cornelis, 1985). P1 was later reported to be the adhesin protein, YadA, and it was proposed that auto-aggregation was due to hydrophobic interactions mediated by YadA (Paerregaard, Espersen, and Skurnik, 1991). However, other studies

have suggested that P1 and YadA are not the same protein as P1 is 52.5 kDa and YadA is a homotrimer of 45 kDa subunits (Skurnik, Bölin, Heikkinen, Piha, and Wolf-Watz, 1984). Additionally, in *Y. pestis yadA* is non-functional, yet certain strains still auto-aggregate when grown in liquid medium at either 28^{o}C or 37^{o}C (Wessman and Miller, 1966; Rosqvist, Skurnik, and Wolf-Watz, 1988a; Felek, Tsang, and Krukonis, 2010; Laird and Cavanaugh, 1980). Deletion of *ompX,* an *ail* homologue, in *Y. pestis* was shown to reduce aggregation significantly (Kolodziejek, *et al*., 2007). These findings suggest that auto-aggregation in *Yersinia* is not always *yadA* dependent.

The presence of the virulence plasmid is essential for auto-aggregation in *Y. pseudotuberculosis* (Wiechmann, 2015). Analysis of the pYV encoded T3S system demonstrated *via* a series of deletion mutants that the needle tip protein, LcrV, is essential for auto-aggregation (Barratt, 2018). QS has also been identified as having an inhibitory role in auto-aggregation, as a mutant with both AHL synthase genes deleted (*ypsI/ytbI)* exhibits greater aggregation (Barratt, 2018). This T3S- and QS- mediated aggregation is distinct from the YadA-mediated aggregation, as these results were replicated when *yadA* was mutated (Barratt, 2018).

1.5.4 Iron Use and Regulation

The correct concentration and supply of intracellular transition metals is essential for the survival of bacteria as iron, zinc, copper and manganese are essential for many functions. However, in excess these metals can be extremely toxic through the production of reactive hydroxyl radicals and disruption of redox potentials (Hobman and Crossman, 2015). As they are so crucial, host defences often restrict their availability as an early line of defence, which is particularly true for iron acquisition and as a result, much of the research on*Yersinia* has focused on iron uptake (Cassat and Skaar, 2013; S. Chen, Thompson, and Francis, 2016). With a lack of oxygen, iron is present in a soluble ferrous form (Fe^{2+}) and in the presence of oxygen it is found in the insoluble ferric form (Fe^{3+}). To maximise uptake, *Yersinia* has developed mechanisms to utilise both.

Analysis has shown that there is a high degree of similarity between the iron transport systems in both *Y. pestis* and the enteropathogenic *Yersinia* (Forman, Paulley, Fetherston, Cheng, and Perry, 2010). The major system present in all three human pathogenic *Yersinia* for the uptake of ferric iron is the yersiniabactin (Ybt) siderophore-based system. All the genes needed for the synthesis and regulation of Ybt are encoded on a mobile genetic element, the High Pathogenicity Island (Forman *et al*., 2010). However, some virulent *Yersinia* contain truncated or deleted Ybt operons, and instead rely on alternative uptake systems in the presence of oxygen. Alternative siderophore systems include the pseudochelin (Ynp) system, the yersiniachelin (Ysu) system and the aerobactin (Luc) system (Alexander Rakin, Schneider, and Podladchikova, 2012; Forman *et al*., 2010). In anoxic conditions, or in the presence of reducing agents, two systems seem to be the most common, Yfe and Feo, with some redundancy seen between them (Perry, Mier, and Fetherston, 2007). As an additional source of iron when in a mammalian host, *Yersinia* have the ability to use haem due to two transport systems, the Hmu ABC transporter and the Has haemophore system (Forman *et al*., 2010; Hornung, Jones, and Perry, 1996; Rossi, Fetherston, Létoffé, *et al*., 2001). Though in *Yersinia* no links between iron-uptake and QS have been reported, siderophores in *Pseudomonas aeruginosa* are known to act as signal molecules and regulate genes outside of iron acquisition (Lamont, Beare, Ochsner, Vasil, and Vasil, 2002). QS has also been linked to iron chelation in *Erwinia carotovora*, a member of the *Enterobacteriaceae*, as a mutant that does not produce AHLs was found to also not produce siderophores (Rasch, Andersen, Nielsen, *et al*., 2005).

1.6 Iron Sulfur Cluster Regulator

One of the many uses of cellular iron is in the formation of Fe-S proteins which are almost ubiquitous in nature and have a range of cellular functions. In order to avoid toxic accumulation of Fe_2 and S_2, their assembly involves a number of protein factors. These assembly factors are highly conserved, consisting of IscR, IscS, IscU, IscA, Hsc66, Hsc20

and ferredoxin, often found in the operon *iscRSUA* (Schwartz, Giel, Patschkowski, *et al*., 2001).

IscR belongs to the Rrf2 family of winged helix-turn-helix transcription factors, and is best understood for its role in regulating the formation of Fe-S proteins. IscR is itself an Fe-S protein, as it coordinates an iron-sulfur cluster [2Fe-2S] via 3 cysteine and 1 histidine residues. It is capable of binding to two types of DNA motifs, 1 (ATASYYGACTRwwwYAGTCRRSTAT) and 2 (AWARCCCYTSnGTTTGMnGKKKTKWA), depending on its Fe-S state (Giel, Rodionov, Liu, Blattner, and Kiley, 2006b). Clusterless (apo) IscR only recognises type 2, whereas holo IscR can bind to both. Holo IscR represses the *iscRSUA* operon, decreasing the amount of Fe-S protein assembly, therefore forming part of an autoregulatory loop (Schwartz *et al*., 2001; Santos, Pereira, and Macedo-Ribeiro, 2015). The holo/apo ratio is affected by environmental cues such as iron starvation, oxidative stress and oxygen limitation, allowing these factors to effect gene expression via IscR (Giel, Rodionov, Liu, Blattner, and Kiley, 2006a).

In addition to Fe-S cluster homeostasis, recent evidence has shown that IscR regulates the expression of many other genes with an array of functions and phenotypic traits. In *V. vulnificus* an *iscR* mutant showed significant reduction in motility, adhesion to host cells and survival under oxidative stress (Lim and Choi, 2014). IscR is also essential for virulence of *V. vulnificus* and together this evidence suggests IscR is a global regulator of gene expression (Lim and Choi, 2014). Similarly, in *Pseudomonas,* IscR protects against oxidative stress and is essential for full pathogenicity (Somprasong, Jittawuttipoka, Duang-nkern, *et al*., 2012; Romsang, Duang-Nkern, Leesukon, *et al*., 2014; Kim, Lee, Lau, and Cho, 2009). In *E. coli*, IscR regulates iron-dependent biofilm formation, through controlling the expression of type I fimbriae involved in cell attachment (Wu and Outten, 2009).

Recently, a study has shown that IscR controls the T3S system in *Y. pseudotuberculosis* and that T3S is reduced in an *iscR* mutant (Miller *et al*., 2014). This is achieved through

binding to a promoter upstream of *lcrF* and regulating its expression. This study also observed a significant reduction in the colonisation of Peyer's patches and mesenteric lymph nodes in a mouse model by an *iscR* mutant, suggesting it is essential for virulence. An Fe-S clusterless, apo-locked IscR also resulted in both a growth and swimming motility defect (Miller *et al*., 2014).

Transcriptome analysis identified IscR as a global regulator of gene expression in *Y. pseudotuberculosis*, repressing over 100 different genes and activating 92 (Miller *et al*., 2014). This includes genes linked to biofilm formation, auto-aggregation, iron transport and QS. Several *nag* genes involved in the degredation of key biofilm component GlcNAc, including the key regulator *nagC*, were found to be up-regulated in an *iscR* mutant, suggesting IscR represses this system. The *luxS* gene was also found to be up-regulated in the mutant, as was the attachment invasion locus protein *ail* which has been linked to auto-aggregation. Many genes involved in T3S are activated by IscR and consequently expression was reduced in the mutant, as were several genes comprising the Hmu haemin transport system, involved in the uptake of iron (Miller *et al*., 2014). However, the role of IscR in these pheonotypes remains to be determined.

1.7 Aims of this study

Yersinia possess a number of key virulence associated phenotypes that form part of a complex and interrelated network which includes T3S, motility, biofilm formation, auto-aggregation, and QS. Although it is know that IscR regulates T3S in *Y. pseudotuberculosis* (Miller *et al*., 2014) it is unclear whether it is an integral part of this network, and its role in *Y. pestis* remains wholly uncharacterised. The aims of this study were therefore to:

- Characterise *iscR* mutant phenotypes in parent and QS mutant backgrounds in *Y. pseudotuberculosis* and *Y. pestis* by studying:
    - Type Three Secretion

    - Production of AHL signalling molecules
    - Biofilm formation
    - Auto-aggregation
    - Iron uptake
- Develop a model for studying biofilm formation in *P. corporis*
- Investigate the effect of IscR on expression of T3S transcriptional regulators, *lcrF* and *ymoA*
- Investigate the effect of IscR on expression of QS system genes, *ypsR/I* and *ytbR/I*

2 Materials and Methods

2.1 Culture Conditions

Unless otherwise stated *E. coli* were grown at 37°C in LB-Miller (10 g/L tryptone [Oxoid™], 10 g/L NaCl, 5 g/L yeast extract [Oxoid™]) (Bertani, 1951). *Y. pseudotuberculosis* was grown at 30°C in low-salt LB-Lennox (YLB) (10 g/L tryptone [Oxoid™], 5 g/L NaCl, 5 g/L yeast extract [Oxoid™]) (Lennox, 1955). *Y. pestis* was grown at 30°C in brain heart infusion (BHI) broth (Oxoid™) in 50 ml centrifuge tubes with vented caps (Corning). All strains were cultured aerobically with shaking at 200 rpm. When necessary, maintenance of a stable pH 6.8 was achieved with a final concentration of 50 mM 3-(*N*-morpholino) propanesulfonic acid (MOPS). For maintenance of strains on solid media, 15 g/L of agar (Oxoid™) was added to the appropriate growth medium. For selective culture of *Y. pestis*, *Yersinia* selective agar (YSA) (Sigma-Aldrich) was used.

To test for the presence of the pYV/pCD1 virulence plasmid strains were grown on Congo Red magnesium oxalate (CR-MOX) plates comprising 40 g/L tryptic soy agar (Sigma-Aldrich) supplemented with 0.02 M sodium oxalate, 0.02 M $MgCl_2$, 0.2% galactose and 0.005% Congo red (Riley and Toma, 1989). Congo red uptake parallels hemin uptake, indicating that the ability to bind Congo red reflects a plasmid determined system for assimilating iron. pYV^+ cells were identified as dark red pinprick colonies whilst large white colonies represented pYV^- cells.

For assays requiring *Y. pseudotuberculosis* growth in a defined media, *Yersinia* defined minimal medium (YDMM) was used. (1x M9 minimal salts (Gibco™), 0.4% glucose, 0.4% casamino acids, 10 mM $MgCl_2$, 5 mM K_2SO_4 and 10 µg/ml thiamine) (Lavander, Ericsson, Bröms, and Forsberg, 2006).

Semi-solid agar was used to observe swimming motility ((10 g/L tryptone, 5 g/l NaCl, 3 g/l agar (Difco-Bacto™)) (Atkinson *et al.*, 1999).

C. elegans were maintained on nematode growth medium (NGM) containing 2.5 g/L peptone (Difco-Bacto^{TM}), 3 g/L NaCl and 17 g/L agar in 1 L of dH_2O. After autoclaving this was supplemented with 2 ml cholesterol (5 mg/ml), 1 ml $CaCl_2$ (1 M), 1 ml $MgSO_4$ (1 M) and 25 ml KH_2PO_4 (1 M, pH 6) (Epstein and Shakes, 1995).

Appropriate antibiotics were added to media for selection when required at the following concentrations: ampicillin (Ap) at 100 µg/ml, tetracycline (Tc) at 10 µg/ml, gentamicin (Gm) at 10 µg/ml, kanamycin (Km) at 50 µg/ml, chloramphenicol (Cm) at 10 µg/ml and erythromycin (Em) at 25 µg/ml, nalidixic acid (Nal) at 15 µg/ml and streptomycin (Sm) at 100 µg/ml. For blue-white screening, 5-bromo-4-chloro-3-indolyl (X-Gal) was used at a concentration of 20 µg/ml. A list of strains used in this study and their antibiotic resistances is shown in Table 2.1.

2.1.1 Strains

Table 2.1 Bacterial strains used in this study and their antibiotic resistances

Strain	Description	Reference
Escherichia coli		
Top10	Laboratory cloning strain. (Sm^R)	Thermo Fisher Scientific
OP50	A uracil auxotroph nutrient source for *C. elegans* (Tc^R)	(Hall, 1995)
S17.1	λ *–pir.* Permissive host capable of transferring suicide plasmids requiring the Pir protein by conjugation to recipient cells (Sm^R)	(Simon, Priefer, and Pühler, 1983)
S17.1 pDM4	S17.1 λ-*pir* containing suicide vector pDM4 (Cm^R)	(Milton, O'Toole, Horstedt, and Wolf-Watz, 1996)
S17.1 pDM4::*iscR*:Gm	S17.1 containing the construct for the deletion/insertion mutation of *iscR* in *Y. pseudotuberculosis* on pDM4 (Cm^RGm^R)	This study
S17.1 pDM4::*iscR*:Tc	S17.1 containing the construct for the deletion/insertion mutation of *iscR* in *Y. pseudotuberculosis* on pDM4 (Cm^RTc^R)	This study
S17.1 pDM4::*iscR(pestis)*: Gm	S17.1 containing the construct for the deletion/insertion mutation of *iscR* in *Y. pestis* on pDM4 (Cm^RGm^R)	This study
S17.1 pDM4.2::P_{ymoA}::*lux*	S17.1 containing a *lux* fusion of the *ymoA* promoter of *Y. pseudotuberculosis* on pDM4.2 (Gm^R)	Joanne Purves (unpublished)

S17.1 pDM4.2::P_{lcrF}::*lux*	S17.1 containing a *lux* fusion of the *lcrF* promoter of *Y. pseudotuberculosis* on pDM4.2 (Gm^R)	Joanne Purves (unpublished)
S17.1 pDM4.2::P_{yscW}::*lux*	S17.1 containing a *lux* fusion of the *yscW* promoter of *Y. pseudotuberculosis* on pDM4.2 (Gm^R)	(Slater, 2017)
S17.1 pKNG10::P_{ypsR}::lux	S17.1 containing a *lux* fusion of the ypsR promoter of *Y. pseudotuberculosis* on pKNG10 (Sm^R)	(Atkinson *et al*., 2008)
S17.1 pKNG10::P_{ypsI}::lux	S17.1 containing a *lux* fusion of the *ypsI* promoter of *Y. pseudotuberculosis* on pKNG10 (Sm^R)	(Atkinson *et al*., 2008)
S17.1 pKNG10::P_{ytbR}::lux	S17.1 containing a lux fusion of the *ytbR* promoter of *Y. pseudotuberculosis* on pKNG10 (Sm^R)	(Atkinson *et al*., 2008)
S17.1 pKNG10::P_{ytbI}::lux	S17.1 containing a lux fusion of the *ytbI* promoter of *Y. pseudotuberculosis* on pKNG10 (Sm^R)	(Atkinson *et al*., 2008)
S17.1 pDM4::P_{nagC}::lux	S17.1 containing a lux fusion of the *nagC* promoter of *Y. pseudotuberculosis* on pDM4 (Cm^R)	Anja Wiechmann (unpublished)
DH5α pEX18Cm::pPCP1replicon	DH5α containing the replicon of YPCO92 pPCP1 on pEX18Cm (Cm^R)	Vanina Garcia, unpublished
DH5α pEX18Gm::pPCP1replicon	DH5α containing the replicon of YPCO92 pPCP1 on pEX18Gm (Gm^R)	Vanina Garcia, unpublished
Yersinia pseudotuberculosis		
YPIII Parent	Parent strain of *Y. pseudotuberculosis* harbouring the virulence plasmid pYV. Serotype O:III (Nal^R)	(Rosqvist, Skurnik, and Wolf-Watz, 1988b)
YPIII Parent pYV-	*Y. pseudotuberculosis* parent cured of the virulence plasmid pYV (Nal^R)	(Wiechmann, 2015)
YPIII Δ*iscR*	YPIII lacking the iron-sulfur cluster regulator *iscR* (Gm^R)	This study
YPIII Δ*iscR* comp	YPIII lacking the iron-sulfur cluster regulator *iscR* complemented with pHG327::*iscR* (Gm^R Ap^R)	This study
YPIII Δ*iscR* + pHG327	YPIII lacking the iron-sulfur cluster regulator *iscR* harbouring empty pHG327 (Gm^R Ap^R)	This study
YPIII Δ*iscR* (Tc^R)	YPIII lacking the iron-sulfur cluster regulator *iscR* (Tc^R)	This study
YPIII Δ*ypsR*	YPIII lacking the quorum sensing response regulator *ypsR* (Km^R)	(Atkinson *et al*., 1999)
YPIII Δ*ypsI*	YPIII lacking the AHL synthase *ypsI* (Km^R)	(Atkinson *et al*., 1999)
YPIII Δ*ytbR*	YPIII lacking the quorum sensing response regulator *ytbR* (Cm^R)	(Atkinson *et al*., 1999)
YPIII Δ*ytbI*	YPIII lacking the AHL synthase *ytbI* (Cm^R)	(Atkinson *et al*., 1999)
YPIII Δ*ypsR/ytbR*	YPIII lacking the quorum sensing response regulators *ypsR* and *ytbR* (Km^R Cm^R)	(Atkinson *et al*., 1999)

YPIII Δ*ypsI/ytbI*	YPIII lacking the AHL synthases *ypsI* and *ytbI* (Km^R Cm^R)	(Atkinson *et al*., 1999)
YPIII Δ*ypsR/ytbR/iscR*	YPIII lacking the quorum sensing response regulators *ypsR* and *ytbR* and the iron-sulfur cluster regulator *iscR* (Km^R Cm^R Gm^R)	This study
YPIII Δ*ypsI/ytbI/iscR*	YPIII lacking the AHL synthases *ypsI* and *ytbI* and the iron-sulfur cluster regulator *iscR* (Km^R Cm^R Gm^R)	This study
YPIII Δ*ypsR/iscR*	YPIII lacking quorum sensing response regulator *ypsR* and the iron-sulfur cluster regulator *iscR* (Km^R Gm^R)	This study
YPIII Δ*ytbR/iscR*	YPIII lacking quorum sensing response regulator *ytbR* and the iron-sulfur cluster regulator *iscR* (Cm^R Gm^R)	This study
YPIII Δ*lcrF*	YPIII lacking the virulence regulator *lcrF* (Km^R)	Atkinson *et al* (unpublished data)
YPIII Δ*nagC*	YPIII lacking the repressor of the GlcNAc-operon NagC (Km^R)	(Wiechmann, 2015)
YPIII parent GFP	YPIII harbouring the GFP plasmid pXYLAP (Ap^R)	(Wiechmann, 2015)
YPIII Δ*iscR* GFP	YPIII Δ*iscR* harbouring the GFP plasmid pXYLAP (Gm^R Ap^R)	This study
YPIII Δ*iscR* comp GFP	YPIII Δ*iscR* complemented harbouring the GFP plasmid pXYLAP (Gm^R Ap^R)	This study
YPIII P_{lcrF}*::lux*	*lux* fusion of the *lcrF* promoter of YPIII integrated into YPIII by pDM4.2 (Gm^R)	(Slater, 2017)
YPIII P_{yscW}*::lux*	*lux* fusion of the *yscW* promoter of YPIII integrated into YPIII by pDM4.2 (Gm^R)	(Slater, 2017)
YPIII P_{ymoA}*::lux*	*lux* fusion of the *ymoA* promoter of YPIII integrated into YPIII by pDM4.2 (Gm^R)	(Slater, 2017)
YPIII P_{ypsR}*::lux*	*lux* fusion of the *ypsR* promoter of YPIII integrated into YPIII by pKNG10 (Sm^R)	(Atkinson *et al*., 2008)
YPIII P_{ypsI}*::lux*	*lux* fusion of the *ypsI* promoter of YPIII integrated into YPIII by pKNG10 (Sm^R)	(Atkinson *et al*., 2008)
YPIII P_{ytbR}*::lux*	*lux* fusion of the *ytbR* promoter of YPIII integrated into YPIII by pKNG10 (Sm^R)	(Atkinson *et al*., 2008)
YPIII P_{ytbI}*::lux*	*lux* fusion of the *ytbI* promoter of YPIII integrated into YPIII by pKNG10 (Sm^R)	(Atkinson *et al*., 2008)
YPIII P_{nagC}*::lux*	*lux* fusion of the *nagC* promoter of YPIII integrated into YPIII by pDM4 (Cm^R)	(Wiechmann, 2015)
YPIII Δ*iscR* P_{lcrF}*::lux*	*lux* fusion of the *lcrF* promoter of YPIII integrated into YPIII Δ*iscR* (Tc^R) by pDM4.2 (Gm^R)	This study
YPIII Δ*iscR* P_{yscW}*::lux*	*lux* fusion of the *yscW* promoter of YPIII integrated into YPIII Δ*iscR* (Tc^R) by pDM4.2 (Gm^R)	This study
YPIII Δ*iscR* P_{ymoA}*::lux*	*lux* fusion of the *ymoA* promoter of YPIII integrated into YPIII Δ*iscR* (Tc^R) by pDM4.2 (Gm^R)	This study
YPIII Δ*iscR* P_{ypsR}*::lux*	*lux* fusion of the *ypsR* promoter of YPIII integrated into YPIII Δ*iscR* by pKNG10 (Gm^R Sm^R)	This study
YPIII Δ*iscR* P_{ypsI}*::lux*	*lux* fusion of the *ypsI* promoter of YPIII	This study

	integrated into YPIII Δ*iscR* by pKNG10 (Gm^R Sm^R)	
YPIII Δ*iscR* P_{ytbR}*::lux*	*lux* fusion of the *ytbR* promoter of YPIII integrated into YPIII Δ*iscR* by pKNG10 (Gm^R Sm^R)	This study
YPIII Δ*iscR* P_{ytbI}*::lux*	*lux* fusion of the *ytbI* promoter of YPIII integrated into YPIII Δ*iscR* by pKNG10 (Gm^R Sm^R)	This study
YPIII Δ*iscR* P_{nagC}*::lux*	*lux* fusion of the *nagC* promoter of YPIII integrated into YPIII Δ*iscR* by pDM4 (Gm^R Cm^R)	This study
YPIII Δ*iscR* P_{lcrF}*::lux* comp	*lux* fusion of the *lcrF* promoter of YPIII integrated into YPIII Δ*iscR* (Tc^R) by pDM4.2 (Gm^R) complemented with pHG327::*iscR* (Ap^R)	This study
YPIII Δ*iscR* P_{yscW}*::lux* comp	*lux* fusion of the *yscW* promoter of YPIII integrated into YPIII Δ*iscR* (Tc^R) by pDM4.2 (Gm^R) complemented with pHG327::*iscR* (Ap^R)	This study
YPIII Δ*iscR* P_{ypsR}*::lux* comp	*lux* fusion of the *ypsR* promoter of YPIII integrated into YPIII Δ*iscR* by pKNG10 (Gm^R Sm^R) complemented with pHG327::*iscR* (Ap^R)	This study
YPIII Δ*iscR* P_{ypsI}*::lux* comp	*lux* fusion of the *ypsI* promoter of YPIII integrated into YPIII Δ*iscR* by pKNG10 (Gm^R Sm^R) complemented with pHG327::*iscR* (Ap^R)	This study
YPIII Δ*iscR* P_{ytbR}*::lux* comp	*lux* fusion of the *ytbR* promoter of YPIII integrated into YPIII Δ*iscR* by pKNG10 (Gm^R Sm^R) complemented with pHG327::*iscR* (Ap^R)	This study
YPIII Δ*iscR* P_{ytbI}*::lux* comp	*lux* fusion of the *ytbI* promoter of YPIII integrated into YPIII Δ*iscR* by pKNG10 (Gm^R Sm^R) complemented with pHG327::*iscR* (Ap^R)	This study
YPIII Δ*iscR* P_{nagC}*::lux* comp	*lux* fusion of the *nagC* promoter of YPIII integrated into YPIII Δ*iscR* by pDM4 (Gm^R Cm^R) complemented with pHG327::*iscR* (Ap^R)	This study
Yersinia pestis		
YPCO92	Parent strain. pPCP1 pCD1 pMT1 *pgm*+ (Em^R)	(Doll, Zeitz, Ettestad, *et al*., 1994) Gifted by Professor Petra Oyston, DSTL
YPCO92 Δ*iscR*	YPCO92 lacking the iron-sulfur cluster regulator, *iscR*. (Em^R Gm^R)	This study
YPCO92 Δ*iscR* comp	YPCO92 Δ*iscR* complemented with pHG327::*iscR* (Em^R Gm^R Ap^R)	This study
YPCO92 Δ*iscR* + pHG327	YPCO92 Δ*iscR* containing empty pHG327 (Em^R Gm^R Ap^R)	This study
YPCO92 Δ*nagC*	YPCO92 lacking the GlcNAc-operon repressor NagC, (Em^R, Gm^R)	(Elton, 2018)

2.2 Cloning

2.2.1 Polymerase Chain Reactions (PCR)

PCRs were performed in a programmable thermocycler using either GoTaq® G2 DNA polymerase (Promega) or Q5® High-Fidelity DNA polymerase (NEB) according to the manufacturer's guidelines.

A typical GoTaq® G2 DNA polymerase reaction mixture contained 1.25 U DNA polymerase, 1x GoTaq® flexi buffer, 2.5 mM $MgCl_2$, 0.2 µM of each primer, 200 µM of each deoxynucleotide triphosphate (dNTP), ~1ng template DNA and sterile H_2O to a final volume of 50 µl.

A typical Q5® High-Fidelity DNA polymerase reaction was carried out at a final volume of 50 µl, containing 0.5 µl Q5® High-Fidelity DNA Polymerase (New England Biolabs), 1x Q5 reaction buffer (NEB), 0.2 mM dNTPs, 0.2 µM of each forward and reverse primer, ~1 ng template DNA and sterile H_2O.

Prior to ligation into pGEM®-T Easy, PCR products amplified with Q5® High-Fidelity DNA polymerase were subject to A-tailing using Go Taq® DNA polymerase (Promega). This added 3' adenine overhangs to the otherwise blunt ended fragments for insertion into linearised pGEM®-T Easy which has 3' terminal thymine overhangs. The reaction was carried out in a final volume of 50 µl containing <1 µg purified PCR fragment, 0.2 mM dATP, 1x GoTaq® flexi buffer, 2.5 mM $MgCl_2$ and 1U DNA polymerase. This was incubated at 72^{o}C for 20 min.

2.2.1.1 Primers

Oligonucleotide primers were synthesised by Sigma-Aldrich (Sigma-Aldrich) or Eurofins Genomics (Eurofins Scientific Group) and are listed in Table 2.2. Any introduced restriction endonuclease recognition sites are shown in bold.

Table 2.2 Oligonucleotide Primers

Name	Sequence (5'-3')	Restriction Sites	Source
M13_F	TGTAAAACGACGGCCAGT		(Norrander, Kempe, and Messing, 1983)
M13_R	CAGGAAACAGCTATGACC		(Norrander *et al*., 1983)
pDM4_F	TAGCGGAGTGTATATCAAGC		Jo Purves (unpublished)
pDM4_R	GGATGTAACGCACTGAGAAG		Jo Purves (unpublished)
*iscR*_Up_F_*XhoI*	CC**CTCGAG**AAGAAGAGGAAGAGGCACC	*XhoI*	This study
*iscR*_Up_R_*XbaI_XmaI*	AT**CCCGGG**AC**TCTAGA**TAAAGTTACCTGTTGGTG	*XbaI, XmaI*	This study
*iscR*_Dw_F_*XhoI_XmaI*	CC**CTCGAG**AA**CCCGGG**ATTAACGTCAATCTGC	*XhoI, XmaI*	This study
*iscR*_Dw_R_*SpeI*	CC**ACTAGT**GCTCCAATTGGCGACAGCTATC	*SpeI*	This study
Tet_F_*XbaI*	AT**TCTAGA**CGCAGTCAGGCACCG	*XbaI*	This study
Tet_R_*XmaI*	AA**CCCGGG**GAGTGGTGAATCCGTTAG	*XmaI*	This study
Gm_F_*XbaI*	CG**TCTAGA**GTCGATGTTAGTTGTTATG	*XbaI*	Jo Purves (unpublished)
Gm_R_*XmaI*	AC**CCCGGG**TTAGGTGGCGGTACTTG	*XmaI*	Jo Purves (unpublished)
IscR_Screen_F	TTGCCGGATGTAGTTTGGT		This study
IscR_Screen_R	GTGCTTCAATACGAATACG		This study
*iscR*_Comp_F_*XbaI*	**TCTAGA**TGATACTATCGAGCG	*XbaI*	This study
*iscR*_Comp_R_*HindIII*	**AAGCTT**CCGCAAATTCTGCTTA	*HindIII*	This study
Lux_R	CTACAACATCATAAAGGCC		Jo Purves (unpublished)
IscR_promoter_F_*XhoI*	**CTCGAG**TTATATCAATTGGTTATAATTAATTC	*XhoI*	This study
IscR_promoter_R_*XmaI_SpeI*	AACGG**ACTAGTCCCGGG**AATGTAATGCCA	*XmaI, SpeI*	This study

2.2.2 Gel Electrophoresis

DNA gel electrophoresis was typically performed using 1% (w/v) agarose gels (1% agarose, 1x Tris-acetate-EDTA [TAE] buffer [50 x Stock: 2 M Tris-acetate pH 8, 0.05 M ethylene-diamine-tetraacetic acid]). 5 µl - 20 µl of each sample were loaded in 6 x loading dye (Promega) and 1 x SYBR® Safe DNA Gel Stain (ThermoFisher Scientific) to visualise DNA. Samples were electrophoresed for 45 min at 85 V in 1 x TAE buffer. An appropriate DNA ladder (usually 1 kb DNA ladder, Promega) was used as a size marker.

2.2.3 DNA Extraction and Clean up

PCR products, DNA fragments excised from agarose gels and digested vectors were purified and cleaned using the Wizard® SV Gel and PCR Clean up System (Promega), according to manufacturer's instructions, and stored at -20^{o}C unless otherwise stated.

Sigma GenElute^{TM} Plasmid Miniprep Kit was used to extract plasmids, which were eluted in H_2O.

Genomic DNA (gDNA) was extracted using the GenElute^{TM} Bacterial Genomic DNA Kit (Sigma Aldrich) according to manufacturer's instructions, then eluted in H_2O and stored at 4^{o}C.

2.2.4 Restriction Digests

Restriction enzymes (Promega and NEB) and their corresponding buffers were used according to the supplier's instructions. Reactions were incubated at 37^{o}C for 1-4 h.

2.2.4.1 Plasmids

All plasmids used in this study are listed in **Table 2.3**.

Table 2.3 Plasmids used in this study and their antibiotic resistances

Plasmid	Description	Source
pGEM®T Easy	High copy number cloning vector (Ap^R)	Promega, UK
pDM4	Suicide vector. *mob*RK2, *ori*R6K (*pir* requiring), *sacBR* of *Bacillus subtilis* (Cm^R)	(Milton *et al*., 1996)

pDM4::*iscR*:Gm	Suicide vector containing the construct for the deletion/insertion mutation of *iscR* in *Y. pseudotuberculosis,* replacing *iscR* with a Gm cassette (Cm^RGm^R)	This study
pDM4::*iscR*:Tc	Suicide vector containing the construct for the deletion/insertion mutation of *iscR* in *Y. pseudotuberculosis*, replacing *iscR* with a Tc cassette (Cm^RTc^R)	This study
pDM4::*iscR(pestis)*:Gm	Suicide vector containing the construct for the deletion/insertion mutation of *iscR* in *Y. pestis,* replacing *iscR* with a Gm cassette (Cm^RGm^R)	This study
pHG327	Low copy number complementation vector. (Ap^R)	(Stewart, Libinsky-Mink, Jackson, Cassel, and Kuhn, 1986)
pHG327::*iscR*	pHG327 carrying a functional copy of *iscR* (Ap^R)	This study
pxylAp	Vector carrying GFP (Ap^R)	Stephan Heeb
pEX18Gm	Source of Gm resistance cassette. oriT+, sacB+, gene replacement vector, MCS from pUC18 (Gm^R)	(Hoang, Karkhoff-Schweizer, Kutchma, and Schweizer, 1998)
pBlueTet	Source of Tc resistance cassette. pBluescript II KS+ encoding *tetA* gene from pBR322. (Ap^R, Tet^R)	(Atkinson *et al*., 2008)
pBlue*lux*	pBluescript II KS+ Vector containing the *luxCDABE* operon (Ap^R)	(Atkinson *et al*., 2008)
pKNG101::P_{ypsI}::*lux*	Suicide vector containing a promoter::*lux* fusion of *ypsI* (Sm^R)	(Atkinson *et al*., 2008)
pKNG101::P_{ypsR}::*lux*	Suicide vector containing a promoter::*lux* fusion of *ypsR* (Sm^R)	(Atkinson *et al*., 2008)
pKNG101::P_{ytbI}::*lux*	Suicide vector containing a promoter::*lux* fusion of *ytbI* (Sm^R)	(Atkinson *et al*., 2008)
pKNG101::P_{ytbR}::*lux*	Suicide vector containing a promoter::*lux* fusion of *ytbR* (Sm^R)	(Atkinson *et al*., 2008)
pDM4.2::P_{nagC}::*lux*	Suicide vector containing a promoter::*lux* fusion of *nagC* (Cm^R)	(Wiechmann, 2015)
pDM4.2::P_{ymoA}::*lux*	Suicide vector containing a promoter::*lux* fusion of *ymoA* (Gm^R)	Joanne Purves (unpublished)
pDM4.2::P_{lcrF}::*lux*	Suicide vector containing a promoter::*lux* fusion of *lcrF* (Gm^R)	Joanne Purves (unpublished)
pDM4.2::P_{yscW}::*lux*	Suicide vector containing a promoter::*lux* fusion of *yscW* (Gm^R)	(Slater, 2017)
pEX18Cm::pPCP1replicon	pEX18Cm carrying the YPCO92 pPCP1 origin of replication (Cm^R)	Vanina Garcia, unpublished
pEX18Gm::pPCP1replicon	pEX18Gm carrying the YPCO92 pPCP1 origin of replication (Gm^R)	Vanina Garcia, unpublished

2.2.5 Ligations

Ligations of insert into vector were incubated overnight on a 30ºC (30 s) and 10ºC (30 s) cycle in a thermocycler. Reactions were carried out in a final volume of 20 µl consisting of 1 unit of T4 DNA Ligase (Promega), 1x T4 ligation buffer (Promega), purified insert and vector at a 3:1 molar ratio, and H_2O.

2.2.6 Transformation of DNA into Competent Cells

2.2.6.1 Electro-Competent Cells

To make electro-competent cells, overnight cultures of *Y. pseudotuberculosis* or *E. coli* were diluted to an OD_{600} of 0.1 in 100 mls YLB/LB and grown until early exponential phase (OD_{600} = 0.6-0.8). Cells were pelleted by centrifugation (5000 x g, 4ºC, 8 min) and re-suspended and washed with H_2O. This step was then repeated twice with 40 ml and 4 ml of 10% glycerol. Finally, cells were re-suspended in 500 µl of 10% glycerol and stored in 50 µl aliquots at -80 ºC.

DNA was dialysed using 0.025 µm pore Millipore® filters (Fisher Scientific) in H_2O for 20 min. The sample was then added to competent cells, on ice, and the mixture transferred to a 1 mm electroporation cuvette. Cells were electroporated using a Gene Pulsar (BioRad) set to 2.5 kV,200 Ω,25 µF before being recovered in 500 µl YLB/LB. Cells were then incubated for 1 h at 30ºC/37ºC before plating onto LB containing the appropriate antibiotic.

2.2.6.2 Chemical-Competent Cells

Y. pestis was grown overnight in medium A (YLB broth supplemented with 10 mM $MgSO_4.7H_2O$ and 0.2 % glucose) (Nishimura, Morita, Nishimura, and Sugino, 1990) and diluted 1/10 for further incubation in medium A until early exponential phase (OD_{600} = 0.5-0.9) was reached. Cells were harvested by centrifugation at 13,000 x g for 1 min and washed in medium A. Centrifugation was repeated and the pellet suspended in 50 µl media A and 250 µl medium B (YLB broth supplemented with 36% (v/v) glycerol, 12% polyethene glycol (PEG) (MW7500) and 12 mM $MgSO_4.7H_2O$). Cells were stored in 50 µl aliquots at -80ºC.

For heat shock transformations, 1 ng DNA was added to thawed chemically-competent cells and incubated on ice for 20 min. Cells were then heat shocked at 37ºC for 1 min before being recovered on ice for 5 min and plating onto BHI medium containing the appropriate antibiotics.

2.2.7 DNA Sequencing and Analysis

A Nano Drop® 1000 spectrophotometer (Fisher Scientific) was used to asses DNA purity and quantity. Sanger sequencing was carried out by Source Bioscience, Science Park, Nottingham, UK. Illumina sequencing (Shen, Fan, Campbell, *et al*., 2005) was carried out by MicrobesNG, University of Birmingham, and samples compared to *Y. pseudotuberculosis* YPIII NCBI reference sequence NC_010465.1 or *Y. pestis* CO92 NCBI reference sequence NC_003143.1. Variant analysis was carried out by MicrobesNG. Snapgene® Viewer 4.2.6 (GSL Biotech LLC) and Artemis Release 16.0.0 (Wellcome Trust, Sanger Institute, Pathogen Genomics Group) were used to analyse sequence data and to design virtual cloning strategies.

2.2.8 Mutagenesis of *iscR*

An in-frame deletion mutant was created by removing 442 base pairs from the *iscR* gene and inserting in its place either a tetracycline (Tc) or gentamicin (Gm) cassette, using the protocol previously described in (Atkinson *et al*., 2008). Using primers with engineered restriction sites (Table 2.2), upstream and downstream regions of *iscR* were amplified using *Y. pseudotuberculosis* YPIII or *Y. pestis* YPCO92 as a template. Tetracycline (Tc^R) and gentamicin (Gm^R) resistance cassettes were cloned from pBR322 and pEX18Gm respectively. PCR products were first ligated into pGEM®-T Easy and transformed in to *E. coli* Top10. Using the engineered restriction sites, Tc^R/Gm^R fragments were excised and ligated into the vector containing the upstream *iscR* fragment. The Up-Tc^R/Gm^R fragment was then excised and ligated into the downstream containing vector, resulting in an upstream – Tc^R/Gm^R – downstream insert. This insert was then digested and ligated into the suicide vector pDM4, which was propagated in *E. coli* S17-1.

Conjugations were carried our as described in (Milton *et al*., 1996). Overnight cultures of *E. coli* S17-1 containing the vector and YPIII parent, *ΔypsR/ytbR* or *ΔypsI/ytbI* were mixed in 1:1, 3:1 or 9:1 ratios before being pelleted at 16000 x g for 2 minutes. Pellets were washed twice with BHI before being re-suspended in 30 µl in BHI and spotted onto a non-selective BHI plate. Plates were incubated at 30^{o}C for 5 or 24 h before the bacteria were re-suspended in 200 µl BHI and plated onto appropriate antibiotics. Plates were incubated at 30^{o}C until colonies appeared. Colonies were then patched onto various selective plates. Colonies that grew on 12% (w/v) sucrose and tetracycline or gentamicin were screened by PCR.

2.2.8.1 Genetic complementation

Primers with engineered restriction sites were used to amplify the *iscR* gene of *Y. pseudotuberculosis* or *Y. pestis*, including the promoter sequence. This fragment was ligated into pGEM®T-Easy and propagated in *E. coli* TOP10 before being excised and ligated into the low copy number vector pHG327, described in (Stewart *et al*., 1986).

2.3 Phenotypic Assays

2.3.1 *Yersinia* Outer Protein Expression and Extraction

2.3.1.1 Induction of Type Three Secretion

Cultures were grown overnight at 22^{o}C in BHI and diluted to an OD_{600} of 0.1 in BHI or BHI with 20 mM sodium oxalate (NaOx), 20 mM magnesium chloride ($MgCl_2$) and 0.2% (w/v) glucose. Cultures were incubated at 22^{o}C for 2 h before being shifted to 37^{o}C for 3 h to induce Yop expression. OD's were standardised before the supernatant was filtered through a 0.2 µM filter. For *Y. pestis*, supernatants were filtered twice.

2.3.1.2 Trichoracetic Acid Precipitation

Trichloracetic acid (TCA) at a final concentration of 10% was added to the supernatants on ice for 30 min, before centrifugation for 10 min, 10000 x g at 4ºC. Pellets were resuspended in 10% (w/v) sodium dodecyl sulphate (SDS) and 1 ml of ice cold acetone. Proteins were pelleted at 16 000 x g, 4ºC for 30 min and washed twice in ice cold acetone before being air dried. Finally, pellets were resuspended in 30 µl phosphate buffered saline (PBS).

2.3.1.3 Sodium Dodecyl Sulfate Polyacrylamide Gel Electrophoresis (SDS-PAGE)

2x SDS loading buffer ((100 mM Tris-Cl, 4% (w/v) SDS, 20% (v/v) glycerol, 200 mM dithiothreitol (DTT) and 0.2% (w/v) bromophenol blue)) was added to the protein samples. Prior to loading samples were boiled at 98ºC for 2 min. Samples were analysed using 12% SDS-PAGE gels alongside ColorPlus™ Prestained Protein Ladder size markers (NEB) for 80 minutes at 200 V. Proteins were stained using Coomassie Blue.

2.3.2 *C. elegans* Maintenance and Biofilm Assays

C. elegans were maintained at 22ºC on nematode growth medium (NGM) seeded with *E. coli* OP50, a uracil auxotroph and food source for the nematodes. *C. elegans* were reseeded every 2-3 days onto a fresh plate by transfer of a 1 cm square patch of agar. Biofilm assays were carried out as previously described (Atkinson *et al*., 2011). 2 ml of an overnight culture of *Y. pseudotuberculosis* was diluted to an OD_{600} of 1.0 and spread onto a fresh NGM plate. For *Y. pestis*, OD_{600} 0.4 was used. After drying the plate, 30 young adult *C. elegans* were aseptically picked over from the stock plate. After incubation for 24 h at 22ºC, biofilms were scored from 0 – 3 and an infection index was calculated using the following equation:

$$Infection\ Index = \frac{SUM\ (N\ x\ Score)}{N\ x\ Highest\ Score}\ x\ 100$$

0 = No biofilm, 1 = A small biofilm around the head region 2 = Larger amount around head region 3 = Large biofilm on head that has extended to other areas of the body. (Atkinson *et al.*, 2011).

2.3.3 Biofilm Formation on an Abiotic Surface

Strains were grown in 10 ml *Yersinia* defined minimal medium (YDMM) at 30ºC overnight. Cultures were washed and equalised to an OD_{600} of 0.5 in freshly prepared YDMM. 1 ml volumes were added to a 24-well glass bottomed microtitre plate (Greiner, BioOne). Plates were sealed and incubated statically at 22ºC or 37ºC for 24 h. Growth medium was then removed and wells were washed twice with PBS to remove loosely associated bacteria and then air dried at 37ºC. Cells were stained with 300 µl of 5 µg/ml Fluorescein conjugated Wheat Germ Agglutinin (WGA) (Vector Laboratories). Plates were incubated for 2 h at 4ºC in the dark. After staining wells were washed twice in PBS and air dried at 37ºC. Quantitative analysis of biofilm levels was performed by measuring fluorescence (484 nm absorption, 512 nm emission) with a Tecan SPARK® plate reader. A 15 x 15 circular scan was performed, emitting the outer 2000 µm.

2.3.4 *P. corporis* Maintenance and Colonisation Assay

2.3.4.1 Insect Handling and Maintenance

P. corporis colonies were obtained from Dr Carola Kuhn and the Umweltbundesamt, Berlin, Germany.

Before feeding, lice were maintained in modified 60 ml Sterilin polystyrene containers, with a voile mesh lid to allow air flow. A piece of corduroy (500 mm x 200 mm) was placed into the containers to allow the lice to hide. Temperature was controlled in Genlab Limited incubators (model INC/50/DIG) and humidity was maintained using plastic trays filled with water.

Lice were carefully moved between containers using a forceps. Fluon® (BioQuip Products Inc.) was used on the edge of work areas to prevent insects from escaping.

2.3.4.2 Blood Reservoir Preparation

The Hemotek® 5W1 (Hemotek Ltd.) system was used to artificially feed lice. To prepare the feeding chambers, 1 ml (195 mm^2) reservoirs covered with Hemotek's collagen feeding membrane were used to contain the blood. The membrane was stretched over the feeding chamber and secured with an O-ring, so there were no creases and the membrane was taut. The meal reservoirs were filled by carefully pipetting blood and bacteria into the chamber which was closed with polystyrene plugs. Usually, 200 µl of overnight bacterial (OD_{600} 0.1, approximately 2 x 10^8) culture was added to 1 ml of human blood, alongside 2 µl rhodamine labelled wheat-germ agglutinin (WGA) to stain poly-GlcNAc.

2.3.4.3 *P. corporis* Feeding and Biofilm Assay

P. corporis (usually 20) were transferred to 3 x 3 cm cardboard tubes (Crayford Tubes Ltd.) which had been previously been prepared with mesh glued to the one end to prevent escape and enable air flow. The tubes fit snugly to the Hemotek meal reservoirs on one end, allowing insects direct contact with the membrane and ensuring they cannot escape,

The assembled reservoir and feeding house were placed onto the Hemotek feeding arm and insects were allowed to feed for 1 hour in the dark with the blood maintained at 37°C. A typical feeding experimental set up is shown in Figure 2.1. The unit was then transferred to an incubator at 30°C and 75% relative humidity for various incubation times.

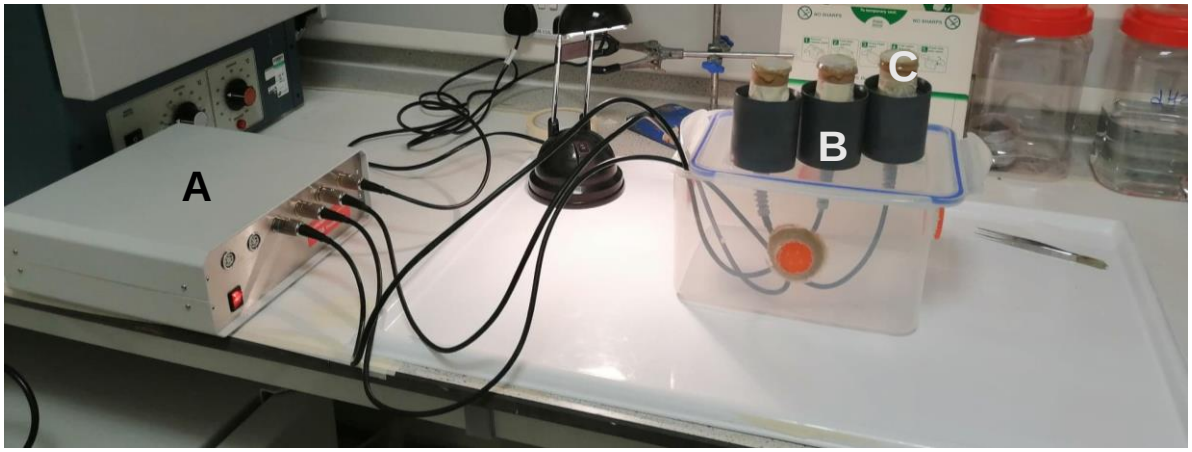

Figure 2.1 Experimental set up for feeding *P. corporis* in CL2

Photo shows the Hemotek artificial feeding system set up in the insect laboratory. (A) shows the Hemotek unit (B) shows the feeding arms and (C) cardboard tubes used for housing feeding insects.

To kill lice for imaging they were placed at -80^{o}C for 15 min and then submerged in 200 µl 4% paraformaldehyde (PFA) for 20 min to kill surface bacteria. Insects were washed twice in distilled H_2O and mounted in FluoroGel mounting medium (GeneTex Inc.).

Once used, the reservoirs were cleaned with 5% Distel HLD4L (MediMark Scientific Ltd.) and rinsed thoroughly. Reservoirs used in CL3 were autoclaved prior to removal from the suite and further disinfecting.

2.3.4.4 Human Blood

An ethical licence (Number: A051016SA-Steve Atkinson), obtained from the School of Life Sciences Ethical Committee, was used to collect blood from human volunteers. 10 ml of blood was taken from the antecubital vein and deposited into a Sterilin tube. This was defibrinated by swirling approximately 5 glass beads (5 mm) in the blood for 5-10 min until a blood clot forms around them, a method modified from (Rodda, 1996). The liquid portion of blood was then stored in a fresh Sterilin tube for up to a week before being discarded, in accordance with the ethical licence guidelines.

2.3.5 Swimming Motility Plates

1 µl of overnight culture was pipetted directly into the centre of swim agar (10 g/L tryptone, 5 g/L NaCl, 3 g/L agar (Difco-Bacto™)) and incubated statically at 22°C for up to 48 h. (Atkinson *et al*., 1999)

2.3.6 Chrome Azurol S Assay

This method was adapted from (Schwyn and Neilands, 1987). Initially, $FeCl_3$ was diluted to 1 mM in 10 mM HCL. 375 µl of this was mixed with 1.875 ml of 2 mM Chrome azurol S (CAS), 12.5 ml of 438 mg/l hexadecyltrimethyl ammonium bromide (CTAB), 9.2 ml of 117.25 g/l piperazine pH 5.6, 1.05 ml dH_2O and 500 µl 0.2 M 5-sulfosalicyclic acid. Care was taken to ensure reagents were added in order. The solution was filtered through a 0.2 µm filter before 500 µl of solution was added to 500 µl of bacterial supernatant. The reaction was allowed to equilibrate for 15 min at room temperature before the OD_{630} was measured, using dH_2O as a blank. M9 medium was used as a reference sample and the iron chelation unit was calculated using the following equation:

$$Iron\ Chelation\ Unit = \frac{(ODreference - ODsample)}{ODreference}\ x\ 100$$

For blue agar CAS plate assays, the protocol described in (Louden, Haarmann, and Lynne, 2011) was followed.

2.3.7 Haem Uptake Plate Assay

Yersinia strains of interest were grown until stationary phase in YDMM and diluted to OD_{600} 0.1. 100 µl of culture was then vortexed into 5 ml molten semi-solid agar (0.8% w/v) containing 125 µM EDDA before the agar was poured on top of a solidified LB-agar plate. Whatman paper disks (6 mm diameter) were carefully placed onto the agar and spotted

with 10 µl of metal free water, 10 mM haemin hydrochloride or 10 mM $FeCl_3$. Plates were incubated for up to 48 h at 22ºC or 37ºC and growth around the disks assessed.

2.3.8 Cellular Aggregation

2.3.8.1 Cuvette Assays

The settling of *Y. pseudotuberculosis* autoaggregates under gravity was assayed in plastic cuvettes (Sarstedt, Germany). Cells were grown for 16 h in YLB at 37ºC, cultures were diluted to standardise the OD_{600} values within each assay and 1 ml transferred to a cuvette. Cultures were incubated statically at 22ºC for up to 60 min. The settling of *Y. pestis* aggregates under gravity in cuvettes was carried out in BHI broth and cuvettes incubated statically at 22ºC for up to 120 min.

2.3.8.2 Imaging of Cellular Aggregates

Cuvettes were photographed using a Nikon D40 camera to look for suspended auto-aggregates and settlement at the bottom. Aliquots (10 µl) of the cuvette sample were mounted onto glass slides with a coverslip and examined under an optical microscope at 40 x magnification (Nikon Eclipse 50i).

2.3.9 Promoter Fusions

The putative promoter region of *iscR* was amplified using PCR with primer pair: *iscR*_promoter_F and *iscR*_promoter_R (Table 2.2) and ligated upstream of the *luxCDABE* operon of *P. luminescens* in pGEM®-T Easy. The construct was then sub-cloned into suicide vector pDM4 using the engineered restriction sites *XhoI* and *SpeI*. *E. coli* S17.1 cells containing the donor suicide vector and *Y. pseudotuberculosis* strain of interest were mixed in ratios of 1:1, 3:1, 9:1 (donor:recipient) in a total volume of 1 ml. Cells were washed twice before resuspending in 30 µl YLB and spotting onto LB agar for incubation at 37ºC for 24 hours. Cells were then re-suspended in YLB, spread onto YLB agar plates containing the appropriate antibiotics and incubated at 30ºC until colonies appeared. Colonies containing the fusion were identified using photon detecting imaging software

Wasabi® and the photon detection imaging camera (Hamamatsu Photonics Germany GmbH). The primer *iscR*_promoter_F was used with *lux_R* to confirm positive colonies via PCR. A similar strategy was used to transfer previously constructed promoter fusions (P_{ypsI}::*lux,* P_{ypsR}::*lux,* P_{ytbI}::*lux,* P_{ytbR}::*lux,* P_{nagC}::*lux,* P_{ymoA}::*lux,* P_{lcrF}::*lux,* P_{yscW}::*lux*)(Table 2.3) in an *iscR* mutant background.

2.3.9.1 Recording and Analysis of Promoter Activity

Strains containing the promoter-*lux* fusion of interest were grown overnight at 30ºC and sub-cultured to OD_{600} of 0.01. Cultures were grown at 30ºC until exponential phase was reached. 1 ml of culture was washed twice in YLB before diluting to an OD_{600} of 0.006 in YLB-MOPS pH 6.8. Samples were plated in triplicate in a 96-well microtiter plate (Greiner Chimney black, GreinerBioOne). A Tecan Infinite®, Infinite Pro® or Genius Pro® luminometer/spectrophotometer was used to record optical density (OD_{600}) and luminescence every 30 min for 15 h, with an integration time of 4500 ms.

2.3.10 AHL Extraction and Analysis

The production of AHL molecules was analysed using a protocol adapted from (Ortori, Atkinson, Chhabra, *et al*., 2007a). Cultures of *Y. pseudotuberculosis* were grown in 10 ml YLB-MOPs to early log, late log and stationary phase at 22ºC and 37ºC. Cultures of *Y. pestis* were grown in 10 ml YLB-MOPs to stationary phase at 22ºC and 37ºC.

3 ml of cell free supernatant was mixed with an internal standard (d9-C5-AHL) at a final concentration of 10 µM. The deuterium component of the internal standard allows differentiation from C5-AHL by mass spec and allows the resulting concentration to be used as a control marker. 1.5 ml 100% acidified ethyl acetate was added to the supernatant before the sample was vortexed for 30 s and centrifuged at 3000 x g for 10 min. The upper organic layer containing solubilised AHLs was pooled in a fresh tube and the process repeated twice more on the lower inorganic layer. The pooled sample was then dried using a centrifugal evaporator and resuspended in 10 µl acetonitrile.

The relative molar ratios of AHLs were calculated using the liquid chromatography-mass spectrometry (LC-MS/MS) technique described in (Ortori *et al*., 2007a), carried out by Nigel Halliday, Experimental Officer, School of Life Sciences, Centre for Biomolecular Sciences, University of Nottingham.

2.3.11 Microscopy

2.3.11.1 Dissection Microscope

To analyse bacterial colony morphology, biofilm formation on *C. elegans* or to transfer *C. elegans* between plates, a dissecting microscope (Nikon SMZ100, Nikon) was used. To examine *Y. pestis* biofilm formation on *C. elegans* under CL3 conditions, the AMG Evos®xl core digital microscope was used.

2.3.11.2 Confocal Microscopy

Confocal microscopy was undertaken using a Zeiss LSM700 confocal microscope for *C. elegans* and abiotic biofilm imaging and a Zeizz Elyra PS.1 super resolution microscope for louse imaging.

2.3.11.3 Environmental Scanning Electron Microscopy

All Environmental Scanning Electron Microscopy (ESEM) work was done with the help of Nicola Weston, from the Nanoscale and Microscale Research Centre (nmRC), University of Nottingham. To study biofilm on glass, overnight cultures were standardised to OD 0.5 in YDMM and incubated on 10 mm diameter glass coverslips for 24 h at 37^{o}C. Coverslips were then washed twice in PBS before being fixed in 10% formal saline overnight. Samples were washed well in dH_2O prior to imaging on FEI Quanta 650 ESEM, using a Peltier stage to control temperature and relative humidity.

2.3.12 Statistical Analysis

All analysis was performed using GraphPad Prism 7.0 (GraphPad Software). Unless otherwise stated, results are expressed as mean ± standard deviation. Students (unpaired) T-tests were used to determine significance between conditions One-way analysis of

variance (one-way ANOVA) followed by Tukeys multiple comparison test was used to determine significance when more than two groups were compared to each other.

2.4 Containment Level 3 Methods

Special measures were taken and protocols were adapted for work with *Y. pestis*. Extensive training was necessary before being signed off as competent to work in the containment level 3 (CL3) laboratory. All CL3 level work was undertaken in a Class I MSC. All protocols from the CL2 laboratory were adapted where necessary and approved for CL3 work, which included the addition of mandatory disinfection steps for all equipment and consumables with 2% Distel (Star Lab Group) alongside additional disposal measures. In order to remove sterile material for analysis in CL2 conditions, such as supernatants or PCR reaction mixtures, comprehensive sterility testing was carried out by plating onto BHI agar and incubating at 30^{o}C for up to 48 h.

3 Exploring the Relationship Between Type Three Secretion, Quorum Sensing and the Iron Sulfur Cluster Regulator, IscR.

3.1 Introduction

All three human pathogenic *Yersinia* possess a 70 kb plasmid harbouring the T3S system and its associated effector proteins, known as Yops (Cornelis *et al*., 1998; Cornelis, 2006). T3S systems function as injectisomes, injecting effector proteins directly into the cytosol of host cells. Yops act to inhibit phagocytosis, reduce inflammatory responses, induce apoptosis and prevent autophagy (Reviewed in (Trosky *et al*., 2008)). T3S system expression also imposes a high metabolic burden, leading to growth arrest (R R Brubaker, 1987), therefore expression of T3S systems is under tight regulatory control, largely due to two transcriptional regulators, LcrF and YmoA. T3S expression is dependent on environmental conditions, specifically temperature and Ca^{2+} levels, due to the biphasic nature of *Yersinia* spp.

The stringent pYV-based regulation of the T3S system is far from a stand alone system, as it is also impacted by QS. QS is a method of bacterial communication and represents a coordinated change in gene expression in response to the release and accumulation of a diffusible signal molecule within the environment. This increase in signal molecule concentration is dependent on the cell population density, so QS results in population dependent gene expression, allowing a collective change in behaviour in response to environmental signals (Williams, 2007; Atkinson and Williams, 2009). Behaviours known to be under QS control in *Yersinia* spp. include T3S, biofilm formation, aggregation and swimming motility (Atkinson *et al*., 2008; 2011).

Yersinia spp. are able to form biofilms on a number of biotic and abiotic surfaces. *Y. pestis* transmission via the flea vector depends on its ability to form biofilms to block the proventriculus (Reviewed in (Hinnebusch and Erickson, 2008)). Whilst fleas have been the primary model for the study for *Y. pestis* transmission, several studies have demonstrated

that human body lice are also capable of transmitting *Y. pestis* (Drali, Shako, Davoust, Diatta, and Raoult, 2015; Houhamdi *et al*., 2006). Recent work has shown that the biofilm regulator NagC plays a role in the colonisation of the louse gut by *Y. pseudotuberculosis* (Elton, 2018). *Y. pestis* and several strains of *Y. pseudotuberculosis*, including YPIII, are able to form biofilms on the mouth and body of *C. elegans*, blocking feeding when severe (Joshua *et al*., 2003). Both species are also able to form biofilms on a number of abiotic surfaces, including polystyrene and glass, which provide a more adaptable model for studying biofilm formation in different conditions (Joshua *et al*., 2003; Barratt, 2018; Slater, 2017).

QS coordination of biofilm formation allows a population wide approach of when to settle, synthesise biofilm components or migrate to new sites (Atkinson et al., 2006). Atkinson *et al*. (Atkinson *et al*., 2011) reported that biofilm formation on *C. elegans* by *Y. pseudotuberculosis* is mediated by QS, as AHLs were found in the biofilm matrix and strains with mutations in the QS systems, either AHL synthases or response regulator genes, show attenuation of biofilm production. Mutation of QS systems in *Y. pestis* also results in attenuation of biofilm production (Bobrov *et al*., 2007). In *Y. pseudotuberculosis*, QS regulation of biofilm production is proposed to be T3S system mediated, through inappropriate assembly of the injectisome in QS mutants (Atkinson *et al*., 2011). It was observed that biofilm formation was attenuated in strains carrying mutations in the QS-controlled motility regulator genes, *flhDC* and *fliA,* and the flagellin export gene, *flhA.* These strains all shared an upregulation of Yop virulon proteins in a temperature and calcium independent manner. Similar observations were found for the QS mutants, which also show attenuated biofilm production. This suggested that the Yop virulon is repressed by QS via the master motility regulator flhDC. By curing the pYV plasmid from QS mutants, growing YPIII under conditions permissive for T3S needle formation but not Yop secretion, and by mutating T3S gene, *yscJ*, biofilm formation is restored in *flhDC* and QS mutants.

This data shows that T3S blocks biofilm formation and is reciprocally regulated with motility via QS (Atkinson et al., 2011).

QS has been further linked to T3S through auto-aggregation. Whilst not fully understood, in *Y. pseudotuberculosis*, aggregation only happens at 37^{o}C and is lost in the absence of the virulence plasmid, suggesting that it is T3S system dependent (Swift *et al*., 1999; Wiechmann, 2015). This was further confirmed by mutation of other genes on the plasmid, namely structural components of the T3S system, leading to ceased aggregation (Wiechmann, 2015; Barratt, 2018). QS has been shown to be a repressor of auto-aggregation as a double AHL synthase mutant shows greater aggregation (Wiechmann, 2015; Barratt, 2018). *Y. pestis* does not aggregate at 37^{o}C, due to expression of Caf1, an adhesin that is absent in *Y. pseudotuberculosis*, but it has been shown to aggregate after growth at 28^{o}C (Felek *et al*., 2010).

Another recently identified regulator of T3S is the iron sulfur cluster regulator, IscR. Miller *et al*., (2014) suggested that IscR may control the activity of the T3S system by acting upon LcrF, and T3S is reduced in an *iscR* mutant. A transposon screen also identified many genes as regulated by IscR that are also under QS control, including those linked to biofilm formation and aggregation.

No further work has been published on IscR in *Yersinia*, and considering the well-known links between T3S, QS systems and QS coordinated behaviours, it would be interesting to determine if QS plays a role in the regulation of T3S *via* IscR. In addition to this, little is known about other roles of IscR in *Yersinia*, and indeed it is completely uncharacterised in *Y. pestis*. This chapter aims to characterise the *iscR* mutant phenotype, particularly in regard to behaviours under the control of QS.

3.1.1 Aims of this Chapter

To date the only studies focusing on IscR in *Yersinia* have looked at IscR in *Y. pseudotuberculosis* strain IP2666, and have uncovered a role for IscR in regulating T3S.

To confirm these findings in *Y. pseudotuberculosis* YPIII and to expand the observations to *Y. pestis* this chapter describes the construction of *iscR* mutants in both strains which were subsequently used to investigate the role of IscR in regulating T3S in *Y. pseudotuberculosis* YPIII and determine whether this regulation is conserved in *Y. pestis* by:

- Analysing the levels of secreted Yop effectors
- Looking at the effect of *iscR* mutation on T3S associated growth arrest

To determine whether QS is implicated in IscR-dependent regulation of T3S, triple mutants will be used to:

- Analyse levels of secreted Yop effectors in *iscR* and QS mutant backgrounds

Y. pseudotuberculosis and *Y. pestis* mutants will be characterised in a series of phenotypic assays to see if there is a role for IscR in:

- Colony morphology
- Growth Rate
- Flagellar mediated motility
- Biofilm formation on abiotic and biotic surfaces
- T3S dependent autoaggregation
- Iron uptake
- Production of AHL signalling molecules

If IscR is seen to affect any of these phenotypes, they will also be studied in a QS deficient background to establish any links to QS.

3.2 Results

3.2.1 Mutagenesis of *iscR*

3.2.1.1 Construction of an *iscR* mutant in *Y. pseudotuberculosis* and *Y. pestis*

In order to explore the role of IscR in *Yersinia* spp., in-frame deletion mutants were constructed. Despite *Y. pseudotuberculosis* and *Y. pestis iscR* being 100% identical, the cloning strategy included the up- and down-stream intergenic regions in which 1 and 2 bases differ respectively. The *iscR* locus is shown in Figure 3.1. Therefore, separate constructs were made for each species and in order to have a more flexibility in the number of compatible strains available for future experiments, a second *Y. pseudotuberculosis iscR* mutant was made following the same strategy using a tetracycline resistance cassette instead of gentamicin. Details of the cloning strategy can be seen in Figure 3.2.

The most widely studied strains of *Y. pestis* are KIM (Kurdistan Iran man) 10+, isolated from a clinical case in 1968 (Finegold, Petery, Berendt, and Adams, 1968; Deng, Burland, Plunkett, *et al*., 2002) and CO92 (Colorado 1992) isolated from a fatal case of pneumonic plague contracted from a domestic cat in the USA (Doll *et al*., 1994). However, most of the research conducted on *Y. pestis* is carried out on modified, avirulent variants of the KIM strain, which lack the pCD1 virulence plasmid (W. Sun, Six, Kuang, *et al*., 2011). When studying T3S it is beneficial to have a strain with all three plasmids present, so a fully virulent strain of CO92 was used harbouring all three virulence plasmids.

Primers (Table 2.2) used for *Y. pseudotuberculosis* and *Y. pestis iscR* mutagenesis were IscR_Up_F and IscR_Up_R to amplify a 432 bp upstream fragment of *iscR* and IscR_Dw_F and IscR_Dw_R to amplify a 452 bp downstream fragment. For the antibiotic cassettes, which both lacked promoter and terminator sequences, Gm_F and Gm_R amplified a 570 bp gentamicin cassette and Tc_F and Tc_R were used to amplify a 1260 bp tetracycline cassette. Engineered restriction sites (XhoI and SpeI) were used to clone these fragments stepwise into pGEM®-T (Table 2.3), and the resulting fragment was then

cloned into the pDM4.1 suicide vector (Table 2.3) as a XhoI/SpeI fragment. Once confirmed by PCR the mutated *iscR* constructs were conjugated into the appropriate strains of *Y. pseudotuberculosis* and *Y. pestis* and screened using sucrose selection. PCR (using primers IscR_Screen_F and IscR_Screen_R) (Figure 3.3 A) and Sanger sequencing were used to check that the mutants were correct (data not shown).

To validate the mutations, complemented strains were constructed by adding a functional copy of *IscR* (amplified using primers IscR_Comp_F and IscR_Comp_R) via the low copy number vector pHG327 (Table 2.3) (Stewart *et al*., 1986) (Figure 3.3 B).

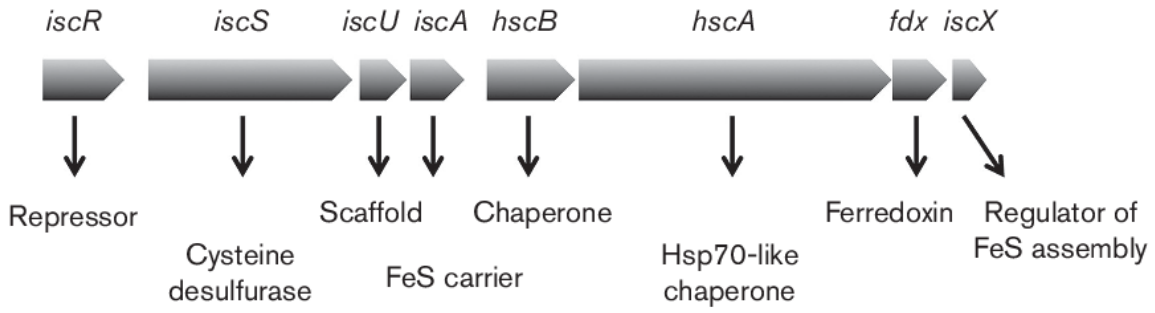

Figure 3.1 Schematic representation of the isc locus and function of the gene products. The isc operon of *E. coli* is shown. The proposed or demonstrated functions of the gene products are indicated below each gene. Figure from (Jaroschinsky, Pinske, and Sawers, 2017)

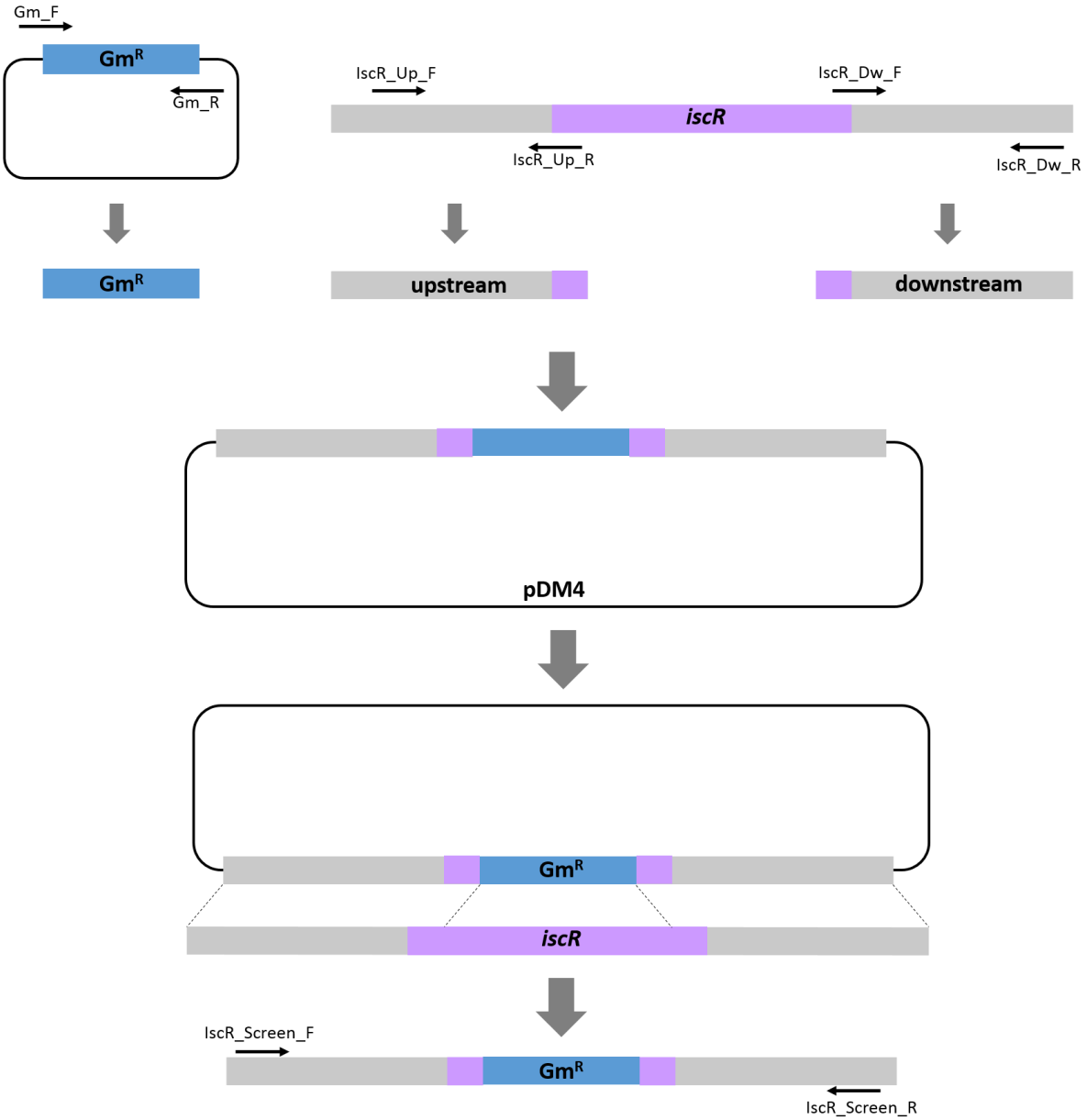

Figure 3.2 Schematic of the construction of the *iscR* mutants in *Yersinia* by substitution of 459 bp of iscR with a gentamicin resistance cassette using the suicide plasmid system pDM4.

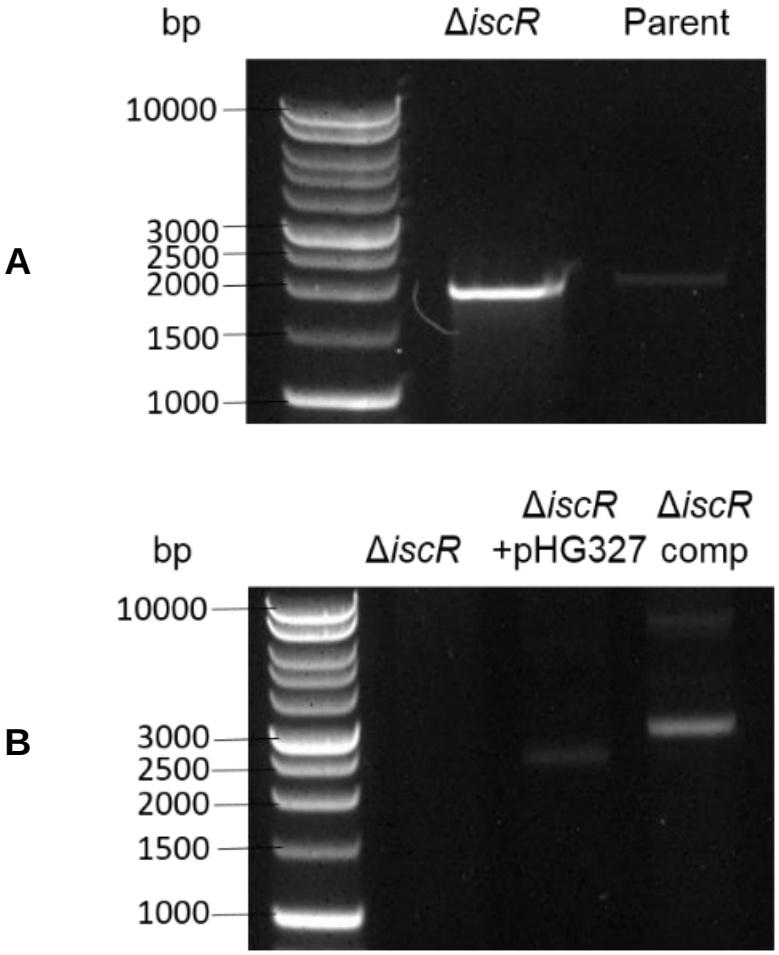

Figure 3.3 Confirmation of *iscR* mutagenesis and complementation

A) PCR amplification of the *iscR* region shows that the product of the *iscR* insertion-deletion mutant is smaller. Parent product = 2034 bp, Δ*iscR* product = 1969 bp. B) Minipreps show no plasmid in Δ*iscR*, empty pHG327 vector in Δ*iscR* +pHG327 and pHG327::iscR (+631 bp) in Δ*iscR* comp. The figure is representative of both YPIII and YPCO92 Δ*iscR* mutants.

3.2.1.2 Whole-genome sequencing of *iscR* mutants

True complementation is often difficult to achieve, due to the complex nature of regulatory networks and factors such as differences in plasmid copy number, as a result the Δ*iscR* mutants of both *Y. pseudotuberculosis* and *Y. pestis* were subjected to whole-genome analysis via illumina sequencing, to identify any additional mutations or rearrangements that could explain any observed phenotypes in the mutant strains.

3.2.1.2.1 Whole genome sequencing of *Y. pseudotuberculosis* strains

The parent *Y. pseudotuberculosis* used in this study had been recently sequenced by Atkinson *et al.* (Slater, 2017) and variant calling and single-nucleotide polymorphism (SNP) analysis was carried out against the reference sequence for YPIII. This data was used as a comparison for the *iscR* mutant, to determine where the *iscR* mutant differed from the parent strain and omit any differences shared by both strains compared the reference sequence. A summary of the SNP's identified in the chromosome of the *Y. pseudotuberculosis iscR* mutant are shown in Figure 3.4.

A total of 7 SNPs were identified in non-coding regions of the genome, and 14 SNPs within coding regions resulted in synonymous SNPs (sSNP), where single base changes still resulted in the same amino acid being coded. These polymorphisms are less likely than others to have a phenotypic effect on the organism, however it cannot be assumed that they will all be silent, especially as the importance of non-coding regions of the bacterial genome for gene regulation becomes increasingly evident (Gil and Latorre, 2012).

Non-synonymous SNPs (nSNP), are more likely to have a significant effect. They include missense polymorphisms, where a single base change in a coding region results in a different amino acid, the effect of which will depend on how much the amino acids differ in properties, and where on the protein, such as in an active site, the amino acid is located (Choi, Sims, Murphy, Miller, and Chan, 2012). A second type of nSNP are nonsense

polymorphisms, where a change in nucleotide leads to the introduction of a stop codon, the effect of which is likely to be strong. Variant analysis identified 4 missense SNPs and one nonsense SNP in the *iscR* mutant.

The insertion or deletion of a number of nucleotides that is not divisible by three leads to a frameshift, where the reading frame of the DNA is altered. If a frameshift mutation occurs in a coding region, it can lead to a completely different translational product, so the effect of these mutations can be great. Variant analysis found one frameshift mutation in the *iscR* mutant.

However, when considering variant calling results, it is necessary to consider the chance of obtaining false positives or negatives during analysis. For all SNPs listed at least 10% of the reads have that variant, suggesting that this is a true reflection of all true SNPs that are present. However, it is likely that some of these calls will be false positives and when discussing the impact of SNPs it is often taken that 95% of reads having the variant is the cut off for biological statistical significance (Olson, Lund, Colman, *et al*., 2015). Taking this into account, there is only one polymorphism that meets this cut off, highlighted in bold in Figure 3.4. This is an insertion/deletion in an intergenic region. As discussed above, whilst this is unlikely to have a major impact given that it is not in a coding region, any potential impact on regulatory regions must still be considered when analysing future results.

In addition to variant calling, a simple assembly was performed and no large insertions, deletions or rearrangements were identified.

Due to time constraints, variant analysis was not carried out on pYV, and this must be considered when analysing future results.

Nucleotide Position	Base Change	Codon Change	Mutation Type	Amino Acid Substitution	Gene	Max Frequency %
174181	T - C	gtT/gtC	Silent	-	*invC*	*10.64*
174542	G - A	Gtc/Atc	Missense	V1283I	*invC*	*11.32*
174877	A - G	acA/acG	Silent	-	*invC*	*11.71*
175189	G - C	gcG/gcC	Silent	-	*invC*	*10*
175549	G - A	gcG/gcA	Silent	-	*invC*	*11.48*
176384	A - G	Aac/Gac	Missense	N1897D	*invC*	*10.57*
177611	G - A	Gac/Aac	Missense	D2306N	*invC*	*11.11*
177625	T - G	gcT/gcG	Silent	-	*invC*	*10.43*
182095	A - G	acA/acG	Silent	-	*invC*	*12.36*
1292586	G - T	-	-	-	Non-coding	16.67
1442555	C - G	gcC/gcG	Silent	-	*invD*	*11.84*
1444439	G - A	ccG/ccA	Silent	-	*invD*	*11.11*
1587830	A - T	-	-	-	Non-coding	13.04
1587835	A - T	-	-	-	Non-coding	14.06
1587838	T - C	-	-	-	Non-coding	11.76
1587850	G - T	-	-	-	Non-coding	11.27
1650233	C - A	acC/acA	Silent	-	*vgrG*	*10.71*
1650284	G - A	gaG/gaA	Silent	-	*vgrG*	*14.71*
1650323	C - A	acC/acA	Silent	-	*vgrG*	*28.57*
1650716	G - A	gaG/gaA	Silent	-	*vgrG*	*13.79*
1732042	C - G	taC/taG	Nonsense	Y715*	*nuoG*	*35.53*
2540730	G - A	acG/acA	Silent	-	YPK_2291	10.45
3486208	**TCATTC - T**	**-**	**-**	**-**	**Non-coding**	**100**
3628536	C - G	aCc/aGc	Missense	T1742S	YPK_3312	10.42
3628829	T - C	acT/acC	Silent	-	YPK_3312	12.7
3998138	G - GCAGT	-	-	-	Non-coding	40.52
4411742	AAGAAGCCC – A	ggggcttct/	Frameshift	-	*pldA*	*94.38*

Figure 3.4 SNPs in the genome of a *Y. pseudotuberculosis iscR* mutant compared to the parent identified by Illumina sequencing.

Nucleotide positions refer to NCBI reference sequence NC_010465.1. SNPs with frequency >95% are shown in bold.

3.2.1.2.2 Whole genome sequencing of *Y. pestis* strains

Our parent *Y. pestis* CO92 strain was sequenced and analysed against the reference CO92 genome (Appendix 7.1) and the results were then compared to the variant calling of the *iscR* mutant, and any differences are shown in Figure 3.5.

A number of sSNPs, nSNPs and frameshifts were identified and although the majority did not make the 95% cut-off three were biological significant (Figure 3.5, highlighted in bold), although all were in non-coding regions so unlikely to have a phenotypic effect.

Variant analysis was also conducted on the three plasmids harboured by *Y. pestis*. The results of the plasmids in the parent strain vs the reference sequences are shown in appendix 7.1. No further differences were identified on any of the plasmids between the *iscR* mutant and the parent.

Nucleotide Position	Base Change	Codon Change	Mutation Type	Amino Acid Substitution	Gene	Max Frequency %
82	**C - A**	**-**	**-**	**-**	**Non-coding**	**100**
633753	T - G	gAa/gCa	Missense	E599A	YPO0587	11.9
1047292	TC - T	-	-	-	Non-coding	17.86
1221220	**T - C**	**-**	**-**	**-**	**Non-coding**	**100**
1925703	C - A	-	-	-	Non-coding	18.75
3058062	C - A	acC/acA	Silent	-	YPO2725	16.36
3058182	A - G	ccA/ccG	Silent	-	YPO2725	35
3058275	G - A	gaG/gaA	Silent	-	YPO2725	18.18
3058308	G - A	ccG/ccA	Silent	-	YPO2725	17.07
3058348	A - C	Aca/Cca	Missense	T849P	YPO2725	12.5
3058362	G - A	ccG/ccA	Silent	-	YPO2725	10.64
3058398	G - A	ccG/ccA	Silent	-	YPO2725	12.24
3058434	G - A	ccG/ccA	Silent	-	YPO2725	17.24
3081533	C - CGCTTATTG	-	-	-	Non-coding	25
3081582	A - G	-	-	-	Non-coding	41.07
3240727	**C - A**	**-**	**-**	**-**	**Non-coding**	**100**
3471434	TG - T	-	-	-	ascB	17.54
3955329	A - G	-	-	-	Non-coding	12.5
4065224	A - G	gcT/gcC	Silent	-	cspa2	13.79

Figure 3.5 SNPs in the genome of a *Y. pestis iscR* mutant compared to the parent identified by Illumina sequencing.

Nucleotide positions refer to NCBI reference sequence NZ_CP009973.1. SNPs with frequency >95% are shown in bold.

3.2.2 Analysis of IscR, QS on T3S using SDS-PAGE

3.2.2.1 T3S is reduced in a *Y. pseudotuberculosis iscR* mutant

IscR was first implicated in the regulation of *Yersinia* type three secretion by (Miller *et al*., 2014), when looking for genes important for T3S function via a transposon screen. This study demonstrated that deletion of *iscR* led to a decrease in the secretion of T3S system effectors relative to the parent strain. To show that the *Y. pseudotuberculosis iscR* mutant made in this study possesses this previously reported phenotype, supernatant protein assays in Yop-inducing conditions were carried out.

Figure 3.6 shows that mutation of *iscR* leads to the production of less Yops, suggesting a defective T3S system, and this was partially restored by complementation with plasmid-encoded *iscR*. The difference in secretion between mutant and parent in this study is not as severe as previously reported, as Yops are still visibly produced by the *iscR* mutant, and the secreted levels of different Yops were not equally affected by the deletion of IscR.

Previously, mass spectrometry was used to identify which bands corresponded to secreted Yops and Yops M, B, D and E were easily identifiable as single bands (Wiechmann, 2015). The distinct bands shown in Figure 3.6 were subject to similar densitometry analysis and their densities calculated relative to the parent which revealed that mutation of *iscR* severely reduces the levels of Yops B, D and E up to 10-fold whereas YopM secretion only undergoes a 2-fold reduction. This is particularly interesting when comparing YopM and YopE as both of these are secreted effector proteins so an overall T3S reduction would be expected to affect both equally.

A

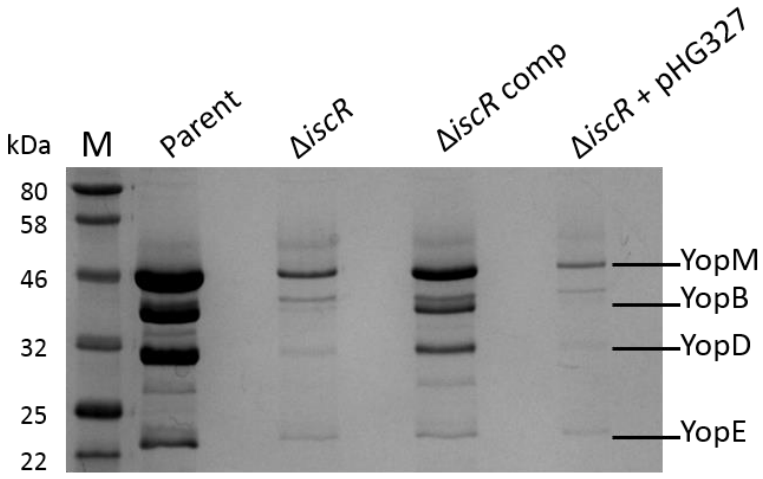

B

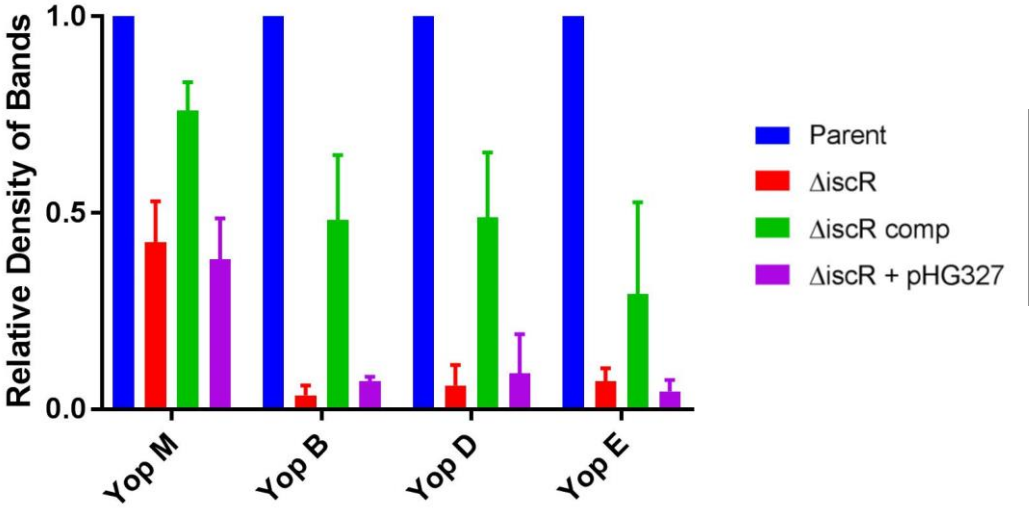

Figure 3.6 **Analysis of Yop profiles of *Y. pseudotuberculosis iscR* mutant**

Strains were grown in conditions to induce T3S system expression (37ºC, low Ca^{2+}) and supernatant proteins were analysed by SDS-PAGE. The *iscR* mutant had reduced secretion of Yops and this was partially restored by complementation (A). Bands corresponding to each Yop were then subject to densitometry analysis and the density calculated relative to in the parent. Mutation of *iscR* severely reduces the levels of Yops B, D and E whereas Yop M secretion is less affected (B). Results are representative of three independent experiments.

3.2.2.2 Studying T3S secretion in a *Y. pestis iscR* mutant

Because IscR is functionally analogous in *Y. pseudotuberculosis* and *E. coli*, and given the similarities between *Y. pseudotuberculosis* and *Y. pestis* it was hypothesised that IscR would have a similar role in T3S regulation in *Y. pestis* (Bölin, Forsberg, Norlander, Skurnik, and Wolf-Watz, 1988; Schwiesow, Lam, Dersch, and Auerbuch, 2016). Whilst working with *Y. pestis* harbouring all three plasmids necessary for virulence provides more biologically relevant results, it posed problems when attempting to study T3S *in vitro*, and as such the assays used to study T3S in *Y. pseudotuberculosis* could not be utilised.

Published T3S profiles in *Y. pestis* are performed in strains which lack the pPst plasmid because *in vitro* the plasminogen activator protease Pla which is located on pPst, degrades Yops when they are secreted into culture supernatants (Sample, Fowler, and Brubaker, 1987b). This is shown in Figure 3.7, which compares the parent strain to an *lcrV* mutant (Natalie Barratt, Unpublished). LcrV is the needle tip protein and has shown to be essential for the secretion of Yop effectors (Dewoody *et al*., 2013). As there is no difference in protein profiles between the strains, this suggests that none of the visible bands correspond to secreted T3S proteins, and this method of studying T3S *in vitro* is unreliable in *Y. pestis.* Despite published protein profiles lacking Pla, this finding wasn't taken into account until extensive optimisation of the T3S assay had been carried out in an attempt to replicate the protein profiles observed in *Y. pseudotuberculosis*.

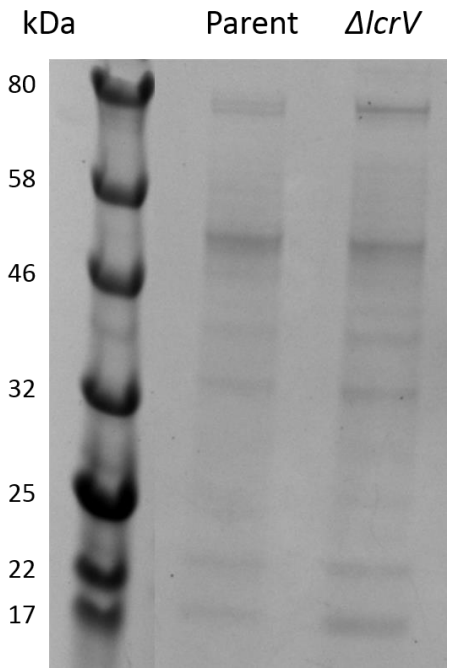

Figure 3.7 *Y. pestis* Yop secretion assay.

Parent and *lcrV* mutant strains show identical protein profiles when grown in low calcium media at 37°C and ran on SDS-PAGE. Results are indicative of three independent repeats. (Natalie Barratt, unpublished)

For continuity between experiments it would be ideal to use a strain with all three plasmids present, so initially an inhibitor of Pla was added to cultures to try and prevent its activity. Pla is part of the Omptin family of proteases (Suomalainen, Haiko, Kukkonen, *et al*., 2007), which combine features of both serine and aspartate proteases, so the inhibitor aprotinin was chosen, as this has been shown to inhibit Pla activity *in vitro* (Brannon, Burk, Leclerc, *et al*., 2015). However, as shown in Figure 3.8 the addition of aprotinin during induction of T3S did not prevent degradation of Yops. This may be because a higher concentration would be needed for complete inhibition, but a higher concentration than the 20µM used severely inhibited growth. It may also be that the half-life of inhibition by Aprotinin is too short to last the duration of Yop secretion and action of Pla.

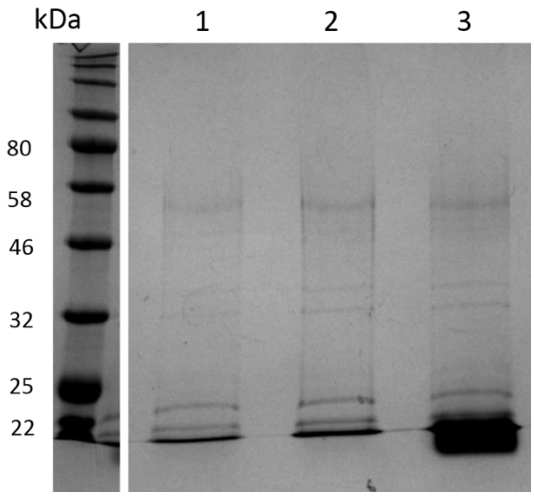

***Figure 3.8 Y. pestis* Yop secretion assay with protease inhibitor**

Parent (1) and *iscR* mutant (2) strains show identical protein profiles when grown in MOPs calcium chelated medium at 37°C and ran on SDS-PAGE. The addition of protease inhibitor aprotinin did not result in visible Yop production by the parent (3). Results indicative of three independent repeats.

The decision was made to remove pPst from *Y. pestis* parent and mutant strains following the strategy outlined in (Ni, Du, Guo, Zhang, and Yang, 2008). This method is based on plasmid incompatibility as the pPst replicon is cloned onto plasmid pEX18Gm, which also contains a counter-selectable *sacB* gene. This was transformed via electroporation into *Y. pestis* and antibiotic selection used to select for strains carrying this recombinant plasmid in place of pPst, as the cells are unable to replicate both. Once the loss of pPst is confimed via PCR, the pEX18Gm plasmid can be cured using sucrose selection. A modified plasmid was made containing a chloramphenicol resistance cassette instead of gentamicin (Vanina Garcia, unpublished) to keep within limits on antibiotic resistance cassettes and to be compatible with the current library of *Y. pestis* mutants. However, due to time constraints this strategy could not be completed as only the initial rounds of conjugation screening were carried out.

3.2.2.3 Growth arrest is still observed during T3S in the absence of IscR

An alternative method to observe T3S *in vitro* is to measure growth rate over time in the presence of chelated calcium and at 37°C. These conditions induce T3S expression, resulting in growth arrest in *Yersinia* spp. in a process known as the low calcium response (Mehigh *et al*., 1989). Figure 3.9 shows that in accordance with the literature, when grown at 37°C in the presence of the calcium chelator MOX, the *Y. pseudotuberculosis* parent shows severe growth restriction when compared to growth in BHI medium alone. Despite an *iscR* mutant secreting less Yops than the parent, Figure 3.9 shows that in *Y. pseudotuberculosis*, an *iscR* mutant still exhibits growth arrest in T3S inducing conditions. This is likely to be because the growth arrest is due to the expression of the complete T3S system, and not just the later stage secretion of Yops.

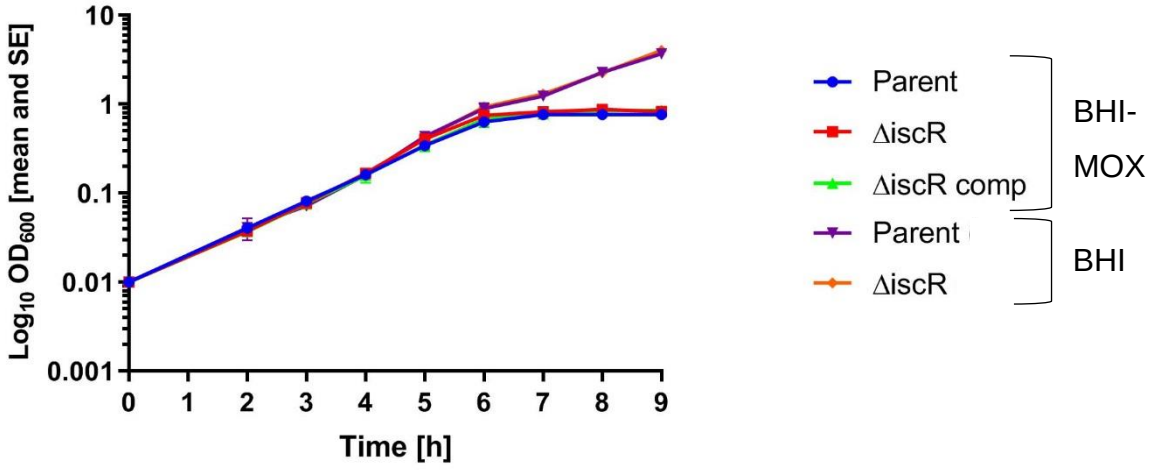

Figure 3.9 Growth arrest is observed in T3S-inducing conditions in the *Y. pseudotuberculosis* parent and *iscR* mutant strains

Cultures were grown in BHI-MOX (low calcium) or BHI (high calcium) medium at 30°C for 5 h before switching to 37°C to induce T3S expression in those with low calcium media. Growth (OD_{600}) was measured every hour. Results show three independent repeats.

Due to constraints of CL3 laboratory work a modified experiment was used to study growth arrest in *Y. pestis*. Growth was analysed at a single time point, 5 h after growth at 37^{o}C in either BHI-MOX or BHI. Figure 3.10 shows that the parent strain grew less in BHI-MOX when compared to BHI alone. Interestingly, the *iscR* mutant did not exhibit growth arrest, although this change was only partially restored by complementation by a plasmid borne *iscR*. Despite being unable to confirm by analysis of protein profiles, the significant reduction in growth arrest suggests that T3S may be reduced or absent in the *iscR* mutant.

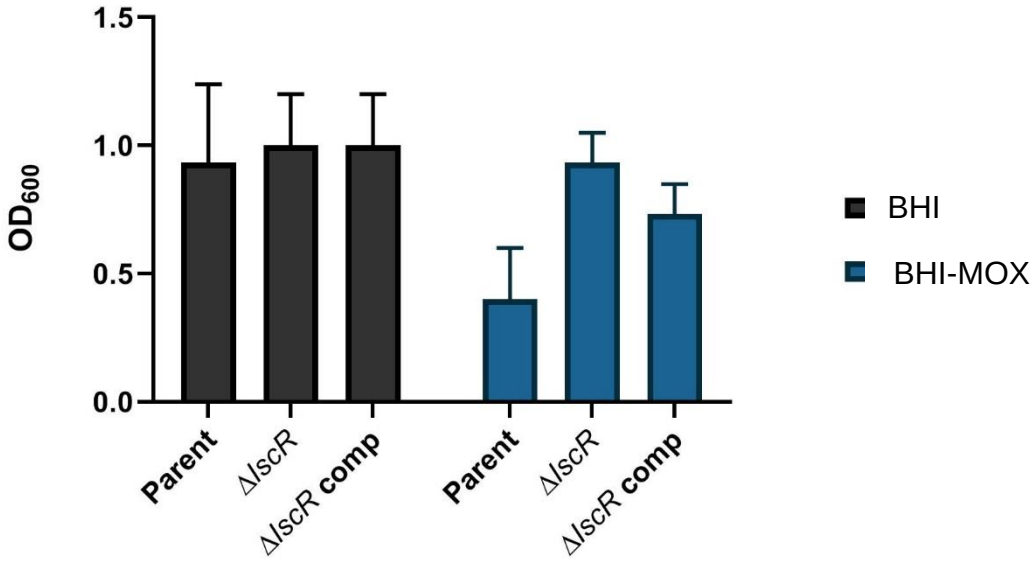

Figure 3.10 **Growth arrest is observed in *Y. pestis* parent but not *iscR* mutant in T3S inducing conditions.**

Cultures were grown in BHI-MOX (low calcium) or BHI (high calcium) at 30^{o}C for 2 h before switching to 37^{o}C to induce T3S expression in low calcium cultures. Growth (OD_{600}) was measured after 5 h. Results show three independent repeats.

3.2.2.4 The impact of QS and IscR on T3S in *Y. pseudotuberculosis*

Previous phenotypic analysis has demonstrated a regulatory link between T3S and QS, as T3S has been shown to affect biofilm formation, aggregation and swimming motility

(Atkinson *et al*., 2006; 2008), which are phenotypes mediated by the QS system. Studies have shown that QS affects T3S via its activation of the master motility regulator FlhDC, which in turn represses T3S through LcrF (Atkinson *et al*., 2011; Slater, 2017). Given the links between T3S and IscR, it would be interesting to determine whether QS also plays a role in how IscR regulates T3S.

3.2.2.4.1 Triple mutant construction

To determine whether there are any links between IscR and QS, *iscR* knock out mutants were made in two QS mutant backgrounds, one in which both AHL synthase genes had been deleted (*dI)* and one in which the response regulator genes had been deleted (*dR),* following the strategy detailed in section 3.2.1.

3.2.2.4.2 Identifying a link between IscR and QS through T3S assays

The *dR* and *dI* YPIII mutants showed a reduction in Yop secretion similar to that seen by (Wiechmann, 2015). However this is opposite to the reported phenotype in (Atkinson et al., 2011). Figure 3.11 shows that when *iscR* is mutated in an AHL synthase negative background (*dI/iscR)*, the severe defect in Yop production is still observed. Interestingly, when *iscR* is mutated in a background lacking both regulators (*dR/iscR)*, this defect is not seen. This suggests that a fully functional QS system is necessary for IscR to regulate T3S, and that this regulation may be direct through either one or both of the response regulators, YpsR and YtbR.

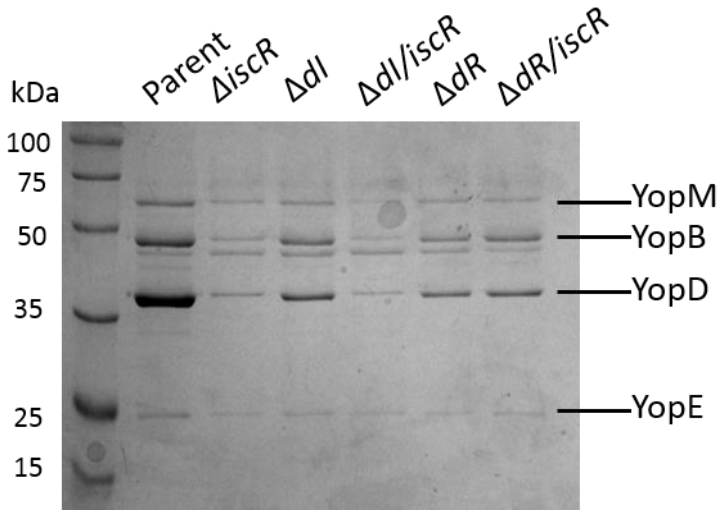

Figure 3.11 Analysis of Yop profiles of *Y. pseudotuberculosis iscR,* QS and *iscR*/QS mutants. Strains were grown in conditions to induce T3S system expression (37ºC, low Ca^{2+}) and supernatant proteins were analysed by SDS-PAGE. ΔdI and ΔdR showed reduced Yop secretion. Additionally, mutation of *iscR* in the ΔdI background led to a further reduction in secretion, but not in the ΔdR background. Results are representative of three independent experiments.

The next step was to determine if one or both of the response regulator genes are necessary for *iscR* to regulate T3S, and so *iscR* knockouts were made in both of these backgrounds and Yop secretion assays carried out. Figure 3.12 shows that the Yop secretion defect due to the *iscR* mutation is still observed in the absence of YpsR or YtbR and this is restored by complementation. This suggests that one QS response regulator is enough for IscR to regulate T3S, and suggests that one may be able to compensate for the loss of the other during this regulation.

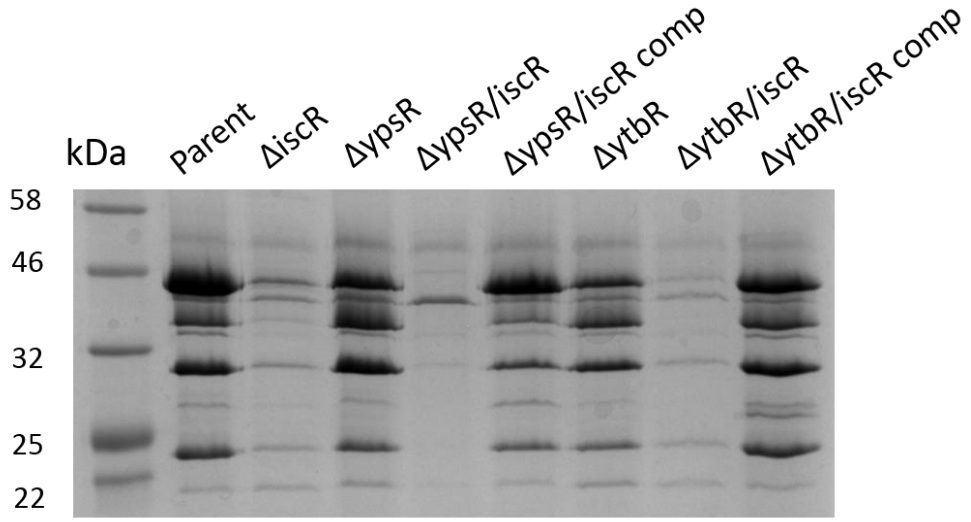

Figure 3.12 Analysis of Yop profiles of *Y. pseudotuberculosis iscR*, QS response regulators and *iscR*/response regulator mutants.

Strains were grown in conditions to induce T3S system expression (37ºC, low Ca^{2+}) and supernatant proteins were analysed by SDS-PAGE. A further reduction in Yop secretion is observed in Δ*ypsR* and Δ*ytbR* backgrounds when *iscR* is knocked out. Results are representative of three independent experiments.

3.2.2.5 Does iscR *affect the production of QS signalling molecules*

To determine whether iscR affected the levels of secreted AHL signalling molecules, and if perhaps this could be why T3S is affected differently in QS mutant backgrounds, AHL extraction and ananlysis was performed from *Y. pseudotuberculosis* parent, *iscR* mutant and complemented strains. Growth curves were carried out at 22ºC and 37ºC in YLB Mops to see if *iscR* affected growth rate and to allow for the correct identification of early logarithmic, late logarithmic and stationary phases to carry out the extractions (Figure 3.13). As no difference in growth was observed, samples were taken for AHL extraction at the same time as previous studies to allow comparison (Slater, 2017), early log (OD_{600} 0.02), late log (OD_{600} 1.0) and stationary phase (OD_{600} 2).

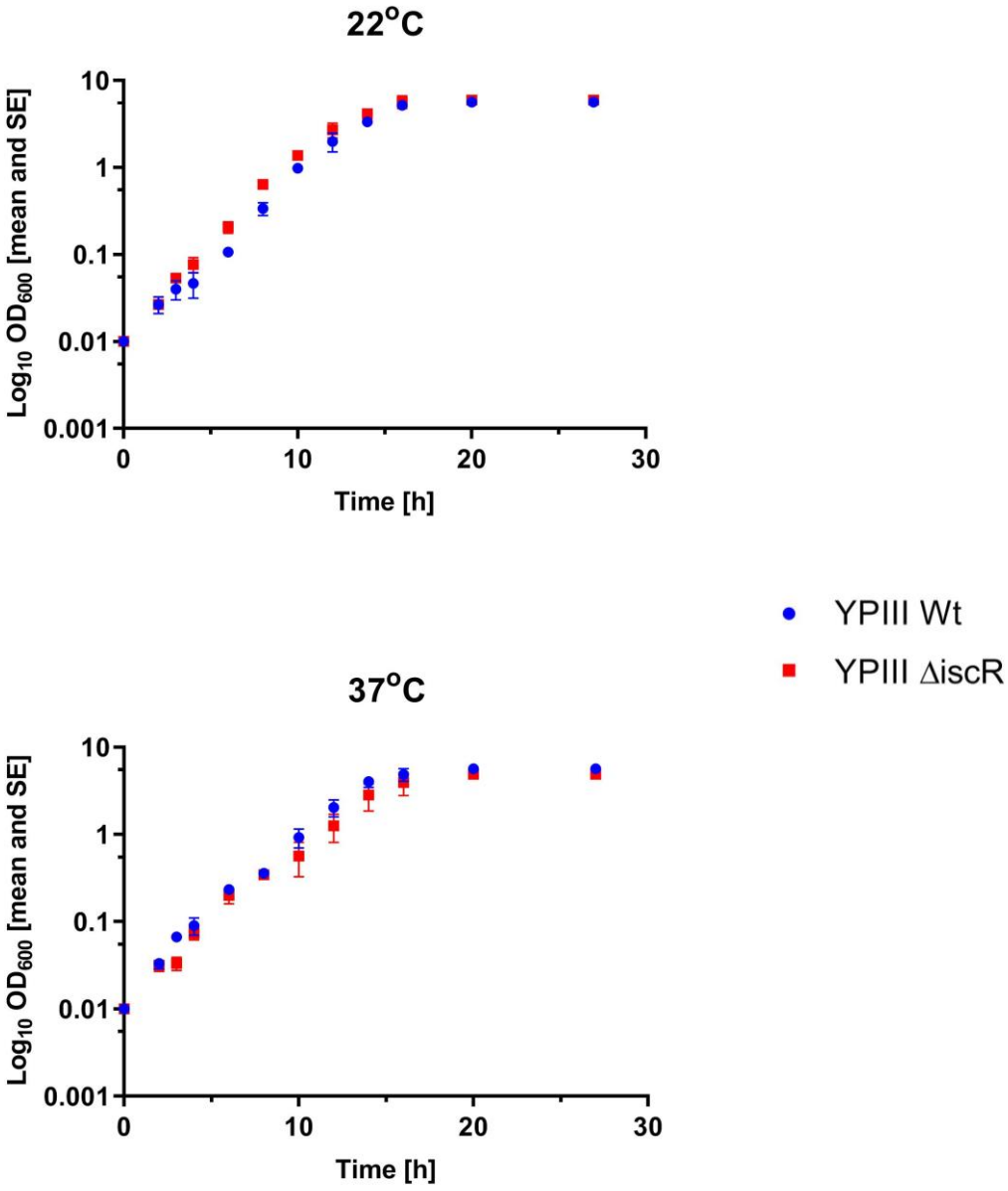

Figure 3.13 Growth curves of *Y. pseudotuberculosis* parent and *iscR* mutant in YLB Mops at 22°C and 37°C

Strains were grown in YLB Mops at 22°C and 37°C and Growth (OD_{600}) measured every hour.There is no difference in growth rate between the two strains present. Results show three independent repeats.

To determine the consistency of the extractions and the validity of any data generated, the concentration of an internal standard extracted as the same time as AHLs was studied.The concentration of internal standard deuterated *N*-pentylhomoserine lactone (d9-C5-AHL)

was within 2 standard deviations of the mean in only 83% of the samples (Figure 3.14). As the standard was co-extracted alongside the AHLs, this low level of reproducibility suggests the extraction of AHLs was unsuccessful and subsequent analysis is unreliable. For this reason, it would be best to repeat AHL extractions before coming to any conclusions.

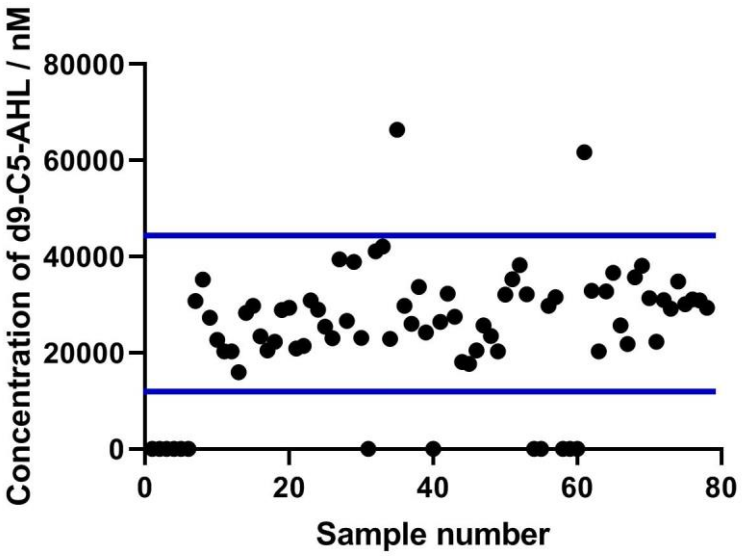

Figure 3.14 AHL extraction consistency.

The concentration of synthetically produced d9-C5-AHL extracted from each sample during LCMS is plotted against sample number. +/- 2 standard deviations are marked with blue lines, within which 83% of the data fall.

3.2.3 Further phenotypic analysis of the *iscR* mutants

3.2.3.1 Colony Morphology

In order to establish any links between IscR and QS it is necessary to know which phenotypes are regulated by each system. Whilst this has been well established for QS mutants there are no details relating to the *iscR* mutant, so a number of phenotypic assays were conducted to characterise the respective mutant in *Y. pseudotuberculosis* and *Y. pestis*. Under normal growth in liquid media no growth defect or advantage was identified for the *iscR* mutant (Figure 3.13) and when growth was observed on solid media no

differences were observed in colony morphology between mutant and parent for *Y. pseudotuberculosis* or *Y. pestis* (Figure 3.15).

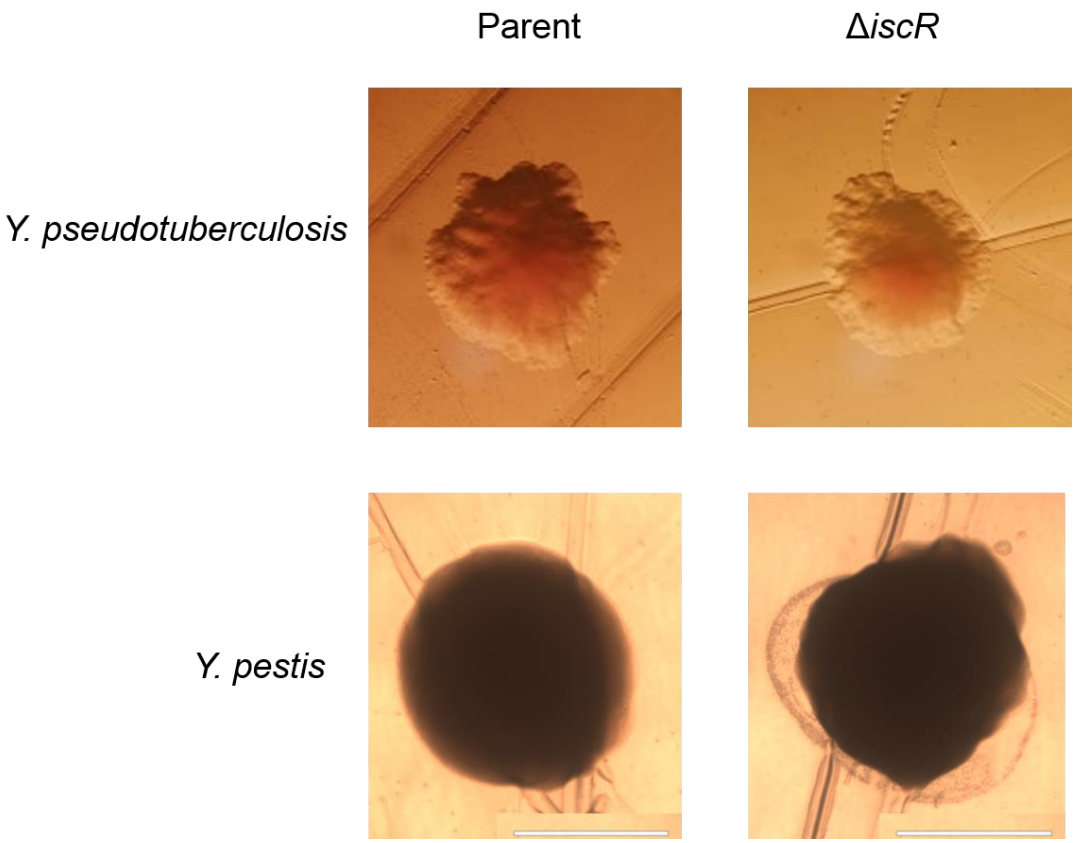

Figure 3.15 Colony morphology of *iscR* mutant on Congo red agar.

Colonies were streated onto agar plates and visualised under light microscopy (x4). No difference in morphology is seen between *iscR* mutant and the parent in *Y. pseudotuberculosis* or *Y. pestis*. Results representative of three independent repeats.

3.2.3.2 Swimming Motility

Goldstone (2012) reported that flagellar-mediated motility in *Y. pseudotuberculosis* is linked to T3S, since a *yscJ* mutant showed increased swimming motility. This hyper-motility has also been linked to QS as this increased motility was lost in a QS negative background. The QS mutant *ypsR* was also found to be hypermotile, as revealed when liquid cultures were viewed down a microscope and by the production a large, translucent circles when grown on swimming agar. The parent strain was previously shown to be non-motile under these conditions (Wiechmann, 2015) so the parent and *ypsR* mutant were used as controls

to determine if mutating *iscR* affected motility. Figure 3.16 shows that motility is not upregulated in the *iscR* mutant strain under these conditions.

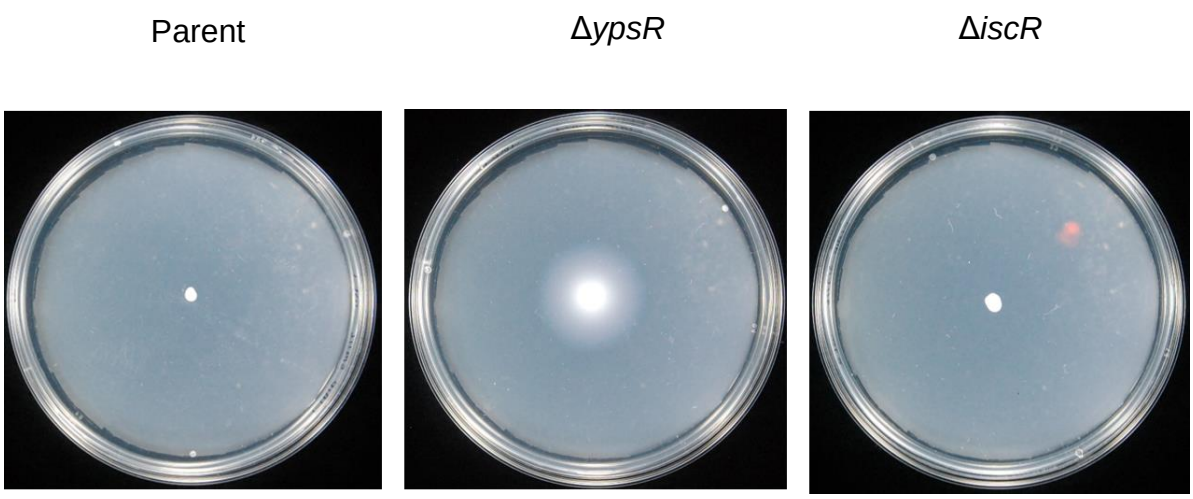

Figure 3.16 Mutation of *Y. pseudotuberculosis iscR* does not result in motility.

Strains were spotted into swimming agar and incubated at 22ºC for 24 h. Δ*ypsR* is shown as a hypermotile control and swimming motility is shown as a halo. Like the parent strain the *iscR* mutant is non-motile under these conditions. Pictures represent 3 independent repeats.

3.2.3.3 The effect of IscR on Biofilm Formation

One of the phenotypes under the control of QS is biofilm formation. Having identified a relationship between QS and IscR in section 3.2.2 and as IscR is known to regulate biofilm formation in other species (Wu and Outten, 2009) and that several *nag* genes are up-regulated in an *iscR Y. pseudotuberculosis* mutant (Miller *et al*., 2014), biofilm assays were conducted to investigate the effect of IscR on biofilm formation.

3.2.3.3.1 Biofilm formation on C. elegans

A useful model for *Yersinia* biofilm formation on a biotic surface is *C. elegans*, as *both Y. pseudotuberculosis* and *Y. pestis* form biofilms on the head and block nematode feeding (Joshua *et al*., 2003; Tan and Darby, 2004). Biofilm formation on nematodes has been proposed to offer protection from protozoan grazing (Atkinson *et al*., 2011; Matz and

Kjelleberg, 2005). In environmental temperatures, QS, T3S and biofilm formation are linked, as both *dR* and *dI* QS mutants show reduced biofilm formation on *C. elegans*, which is further reduced if the virulence plasmid is present (Atkinson *et al*., 2011). Biofilm formation by the *Y. pseudotuberculosis* parent, *iscR* mutant and QS mutant strains on *C. elegans* was examined. As the *nagC* mutant produces a significantly reduced biofilm, it was used as a negative control strain (Wiechmann, 2015).

There was a slight increase in biofilm from parent to *iscR* mutant, however this was not significant (Figure 3.17). The results support the finding that QS regulates biofilm formation, as both *dR* and *dI* mutants showed a reduction in biofilm formation, as previously reported (Atkinson *et al*., 2011). Upon further mutation of *iscR* in these backgrounds, the levels of biofilm increased to similar levels to the single *iscR* mutant and in both strains biofilm levels were partially restored by complementation with plasmid borne *iscR*.

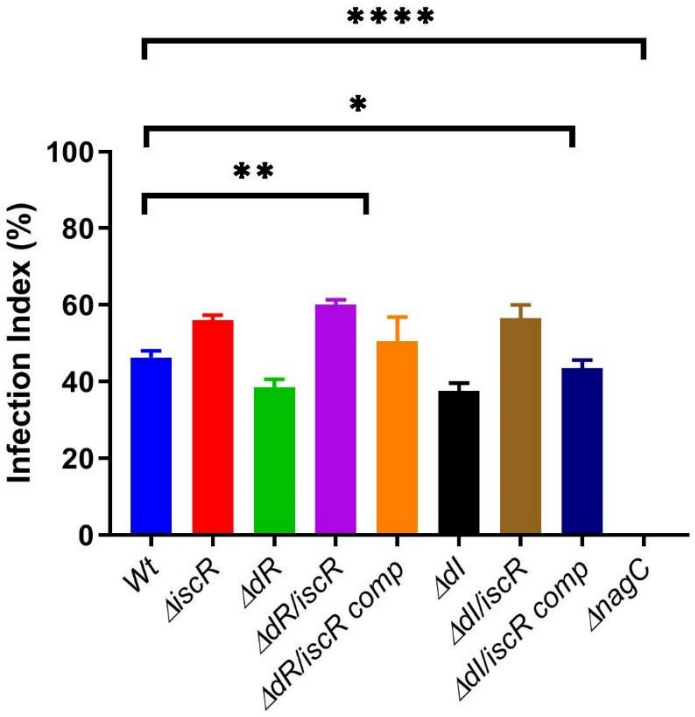

Figure 3.17 Biofilm formation on *C. elegans* in the parent, Δ*iscR,* Δ*dR,* ΔdR/*iscR,* Δ*dl,* Δdl/*iscR* and complemented *Y. pseudotuberculosis* strains.

Nematodes were fed parent or mutant *Y. pseudotuberculosis* strains for 24 h before biofilms were visually inspected and given a severity rating (Infection index %). Reduced biofilm formation was observed for both Δ*dR and* Δ*dl* backgrounds. A slight increase is seen when iscR is knocked out both as a single mutant and triple in both QS backgrounds, though this was not significant. Negative control Δ*nagC* did not produce any biofilm. Results representative of three independent repeats. The data was analysed by one-way ANOVA column analysis where stars indicate results that differ significantly from the parent where * (P<0.1), **(P<0.01) and **(P<0.0001).**

Previously, some strains have been found to have different distributions of biofilm when examined under a microscope (Goldstone, 2012; Wiechmann, 2015). Therefore *C. elegans* biofilms of parent and *iscR* mutant strains were examined using confocal microscopy, with fluorescently tagged WGA used to stain the poly(GlcNac) biofilm. There was no difference

in biofilm distribution between the strains, with most biofilm concentrated around the head region with occasional pockets along the body in severe cases (Figure 3.18).

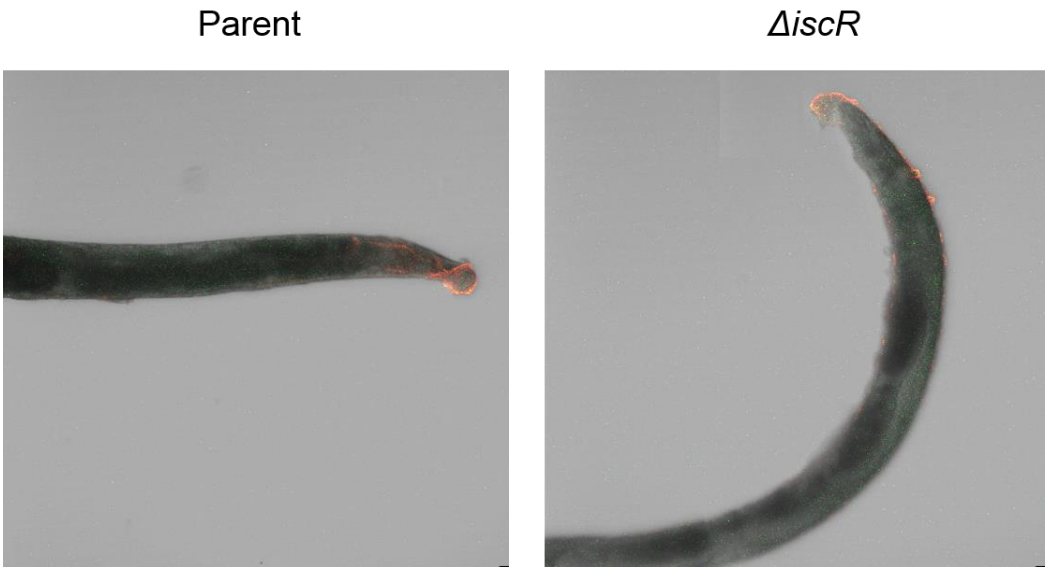

Figure 3.18 Confocal microscopy images of biofilm formation on *C. elegans* in *Y. pseudotuberculosis*.

Nematodes were fed parent or *iscR* mutant *Y. pseudotuberculosis* strains for 24 h and poly(GlcNAc) was stained with WGA-F (Red) to visualise biofilm. Both strains mainly formed pockets around the nematode head. Images are representative of experimental triplicates.

The effect of mutating IscR on biofilm formation in *Y. pestis* was also tested using *C. elegans*. The YPCO92 parent strain forms large amounts of biofilm around both the anterior and posterior regions of *C. elegans* and seeding with similar amounts of bacteria to *Y. pseudotuberculosis* resulted in 100% mortality of *C. elegans* in all strains tested (Barratt, 2018). The number of bacteria seeded onto plates was reduced to allow formation of large biofilms without killing the nematodes, so infection severity could be calculated. No significant differences were found between the parent and *iscR* mutant (Figure 3.19).

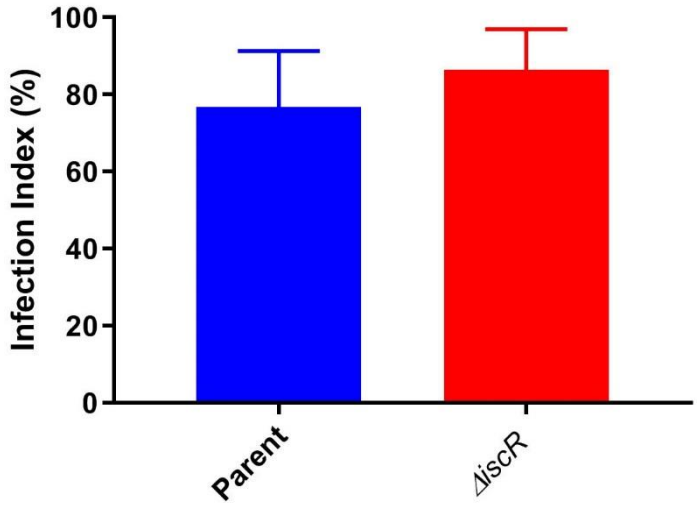

Figure 3.19 Biofilm formation on *C. elegans* in the *Y. pestis* parent and *iscR* mutant.

Nematodes were fed parent or *iscR* mutant *Y. pestis* strains for 24 h before biofilms were visually inspected and given a severity rating (Infection index %). No significant differences were found between biofilm levels formed by either strain. Results show three independent repeats.

3.2.3.3.2 Abiotic Surface

C. elegans assays cannot be carried out at 37ºC as the nematodes are unable to survive at this temperature. Therefore, abiotic surfaces were used to study biofilm formation at a range of temperatures. Previous optimisation of abiotic biofilm assays for *Y. pseudotuberculosis* found that glass provided the most consistent results, so this protocol was used for this study (Slater, 2017; Barratt, 2018). The effect of IscR and QS on biofilm on glass was examined at 22ºC and 37ºC (Figure 3.3). At 22ºC (Figure 3.3A), in the absence of *iscR*, biofilm formation is reduced which is opposite to the trend observed on *C. elegans*. However, complementation did not restore biofilm to levels similar to those seen in the parent. Mutations in the *ypsR* and *ytbR* or *ypsI* and *ytbI* genes also results in reduced biofilm production, and is comparable to the effect of the mutations on biofilm formation on *C. elegans* (Figure 3.17) Mutating *iscR* in these backgrounds did not further impact on

biofilm levels. At 37^{o}C, (Figure 3.2B) no significant difference was observed between the parent and any other *iscR* or QS mutant strain. Although a slight reduction in biofilm formation was observed on the Δ*iscR* strain and this could be complemented back to parental levels when a plasmid-based copy of *iscR* was introduced. These results support previous findings that mutating the QS system alone does not impact on biofilm formation on glass at 37^{o}C, only at 22^{o}C (Slater, 2017; Barratt, 2018).

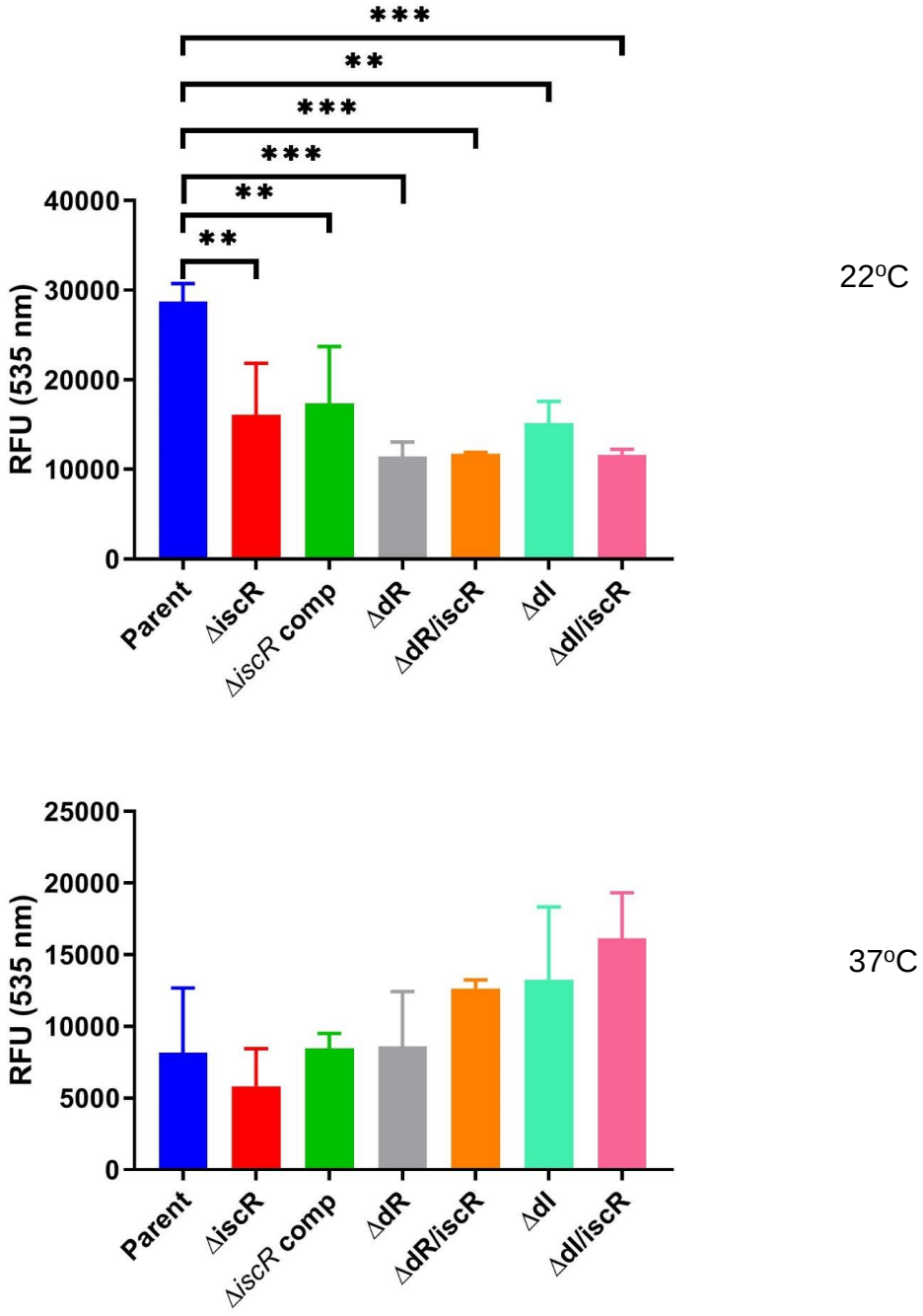

Figure 3.20 Biofilm formation on glass in the parent, Δ*iscR*, Δ*dR*, ΔdR/*iscR*, Δ*dI*, ΔdI/*iscR* and complemented *Y. pseudotuberculosis* strains at 22ºC and 37ºC.

At 22ºC a reduction in biofilm production was observed in Δ*iscR*. Both Δ*dR* and Δ*dI* show attenuated biofilm production which was not affected by further mutation of *iscR* (ΔdR/iscR and ΔdI/*iscR*). At 37ºC no significant differences were observed. Results representative of three experimental triplicates. The data was analysed by one-way ANOVA column analysis

where stars indicate results that differ significantly from the parent where * (P<0.1), **(P<0.01), *(P<0.001) and ****(P<0.0001).**

As there were differences in the levels of biofilm formed by the *iscR* mutant on glass when compared to the parent, the distribution and morphology of cells within biofilms on glass was examined using ESEM to examine the parent, *iscR* mutant and complemented strains (Figure 3.21). All strains formed a multi-layered biofilm with evidence of ECM around cells, although the *iscR* mutant showed far less ECM and a thinner biofilm overall, with only a small number of cells attached in comparison. Parent and complemented strains formed a thick, multicellular biofilm layer with clear dark deposits representing ECM. Evidence of ECM is still visible in the *iscR* mutant but the biofilm is much thinner and appears to be largely a single-cell layer. This is a novel finding and supports the fluorescence data described above in figure 3.2, showing a clear role for IscR in biofilm formation.

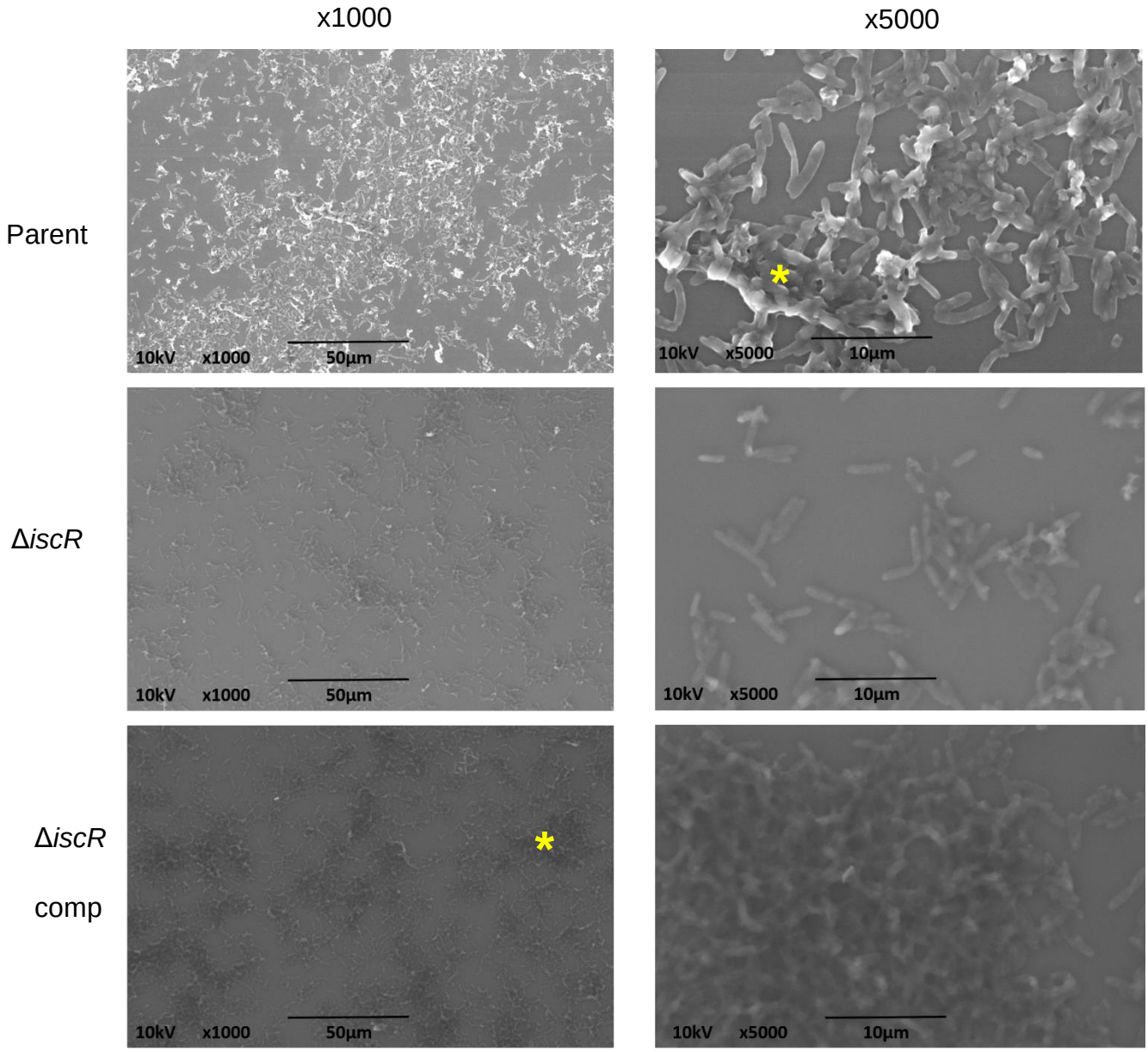

Figure 3.21 ESEM images of biofilms on glass of the *Y. pseudotuberculosis iscR* mutant.

Strains were grown for 24 h on glass coverslips at 37oC before being washed and fixed in formal saline. Samples were then imaged on FEI Quanta 650 ESEM. Dark deposits representing ECM (*).Image representative of three independent experiments.

3.2.3.3.3 Development of louse model for biofilm production

Insects play a crucial role in *Y. pestis* transmission but has been little studied in the human body louse. Due to the differences in biofilm results previously obtained, a third model would be beneficial to see if the differences are due to changes in surface properties. Extensive work was done previously to determine the best practise for louse husbandry and infection assays (Elton, 2018), however optimisation was still needed, particularly before the assays could be conducted in CL3 conditions. Due to issues establishing a breeding lice colony, lice were regularly supplied by Carola Kuhn (Umweltbundesamt, Berlin, Germany) and used immediately for experiments, with no attempt to keep them alive long term. This provided the most successful experiments, with a feeding rate of between 80 – 90% when lice were placed on the feeding pods filled with defibrinated, freshly collected human blood for 1 hour (data not shown). Feeding success was determined by visual examination under a light microscope due to the relative transparency of the lice (Figure 3.22). A small percentage of lice turned red and died very quickly after feeding, which has previously been suggested to be due to epithelial cell rupture within the louse gut and erythrocytes from the fresh blood meal spreading to the haemolymph (Houhamdi, Fournier, Fang, Lepidi, and Raoult, 2002) (Figure 3.22). These lice were counted as ‘fed’ but would need to be discounted in future experiments to determine biofilm formation, as they do not represent a natural feeding model.

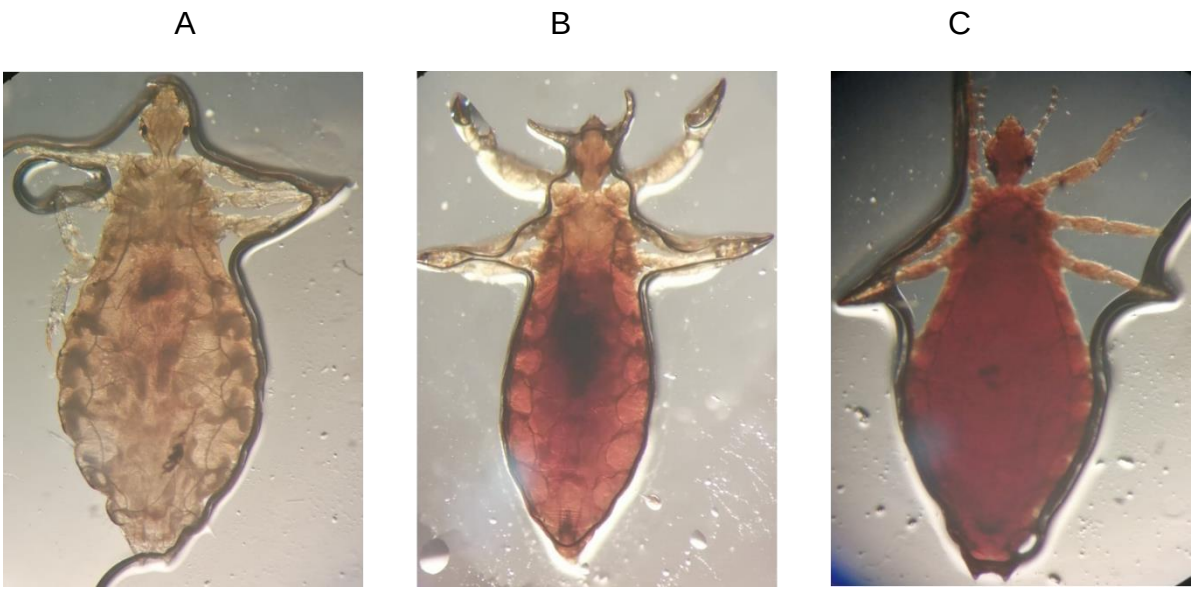

Figure 3.22 Comparison of non-fed and fed *P. corporis.*

(A) Non-fed louse with an empty gut. (B) A fed louse with an abdomen of red blood. (C) An example of haemolytic epithelial cell rupture. Red colouration is observed across the entire abdomen, thorax and legs. Images representative of experimental triplicates.

Once successful feeding and experimental conditions were optimised, the effect of IscR on biofilm formation in lice was investigated using *P. corporis* which had been fed on defibrinated human blood inoculated with the *Y. pseudotuberculosis* parent and *iscR* mutant, as well as uninfected blood as a negative control. Survival was measured by visual observation and the results shown in Figure 3.23. Survival of lice fed uninfected blood was consistent with previousl reports, with all lice dead 60 h post infection (Elton, 2018). Lice fed parental strains died rapidly, with a sharp drop observed after 36 h and complete killing by 48 h. Interestingly, the *iscR* mutant appeared to kill lice faster than the parent strain, with only around a 50% survival rate after 24 h, compared to 80% for the parent.

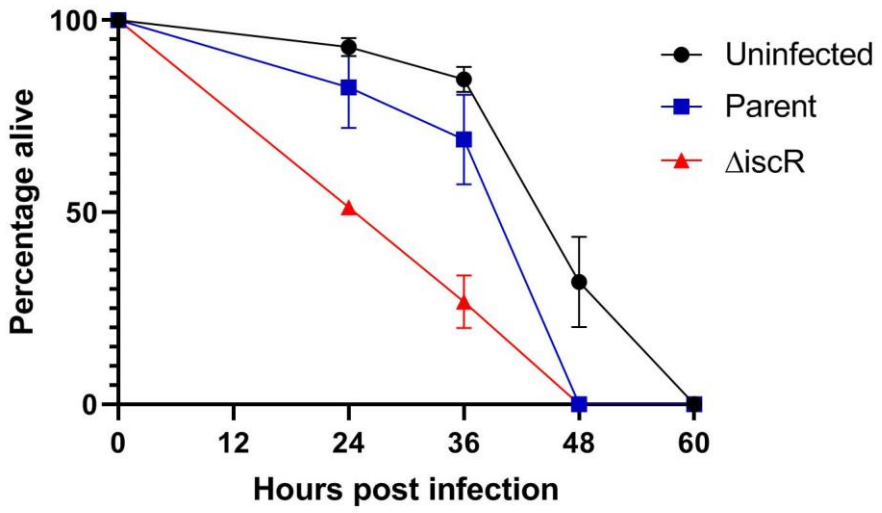

Figure 3.23 *P. corporis* survival rates when fed blood infected with *Y. pseudotuberculosis* parent or *iscR* mutant

Lice were fed blood containing either parent or *iscR* mutant *Y. pseudotuberculosis* strains and the number of live lice visually inspected every 12 hours. The *iscR* mutation negatively affected the survival of lice with the time to death decreasing compared to the parental strains. Uninfected blood is shown as a control. Results show experimental triplicates.

To see the distribution of bacteria and biofilm within the fed lice, insects were imaged using CLSM at 24 h post infection (Figure 3.24). Texas-red conjugated WGA was added to blood meals in an attempt to identify biofilm within the insects, however no biofilm was detectable and instead it was found that the lice auto-fluoresce at this wavelength, so this was exploited during imaging. Lice that had clearly taken a blood meal were imaged. In the lice fed uninfected blood, no GFP was visible. Both the lice fed parent strains and the *iscR* mutant showed diffuse GFP throughout the abdomen. However, this did not appear to be concentrated in the gut as seen in previous studies of this model (Elton, 2018). Slight accumulation is observed for the *iscR* mutant, which could suggest this is the beginning of biofilm formation and colonisation of the gut, and later timepoints should have been analysed.

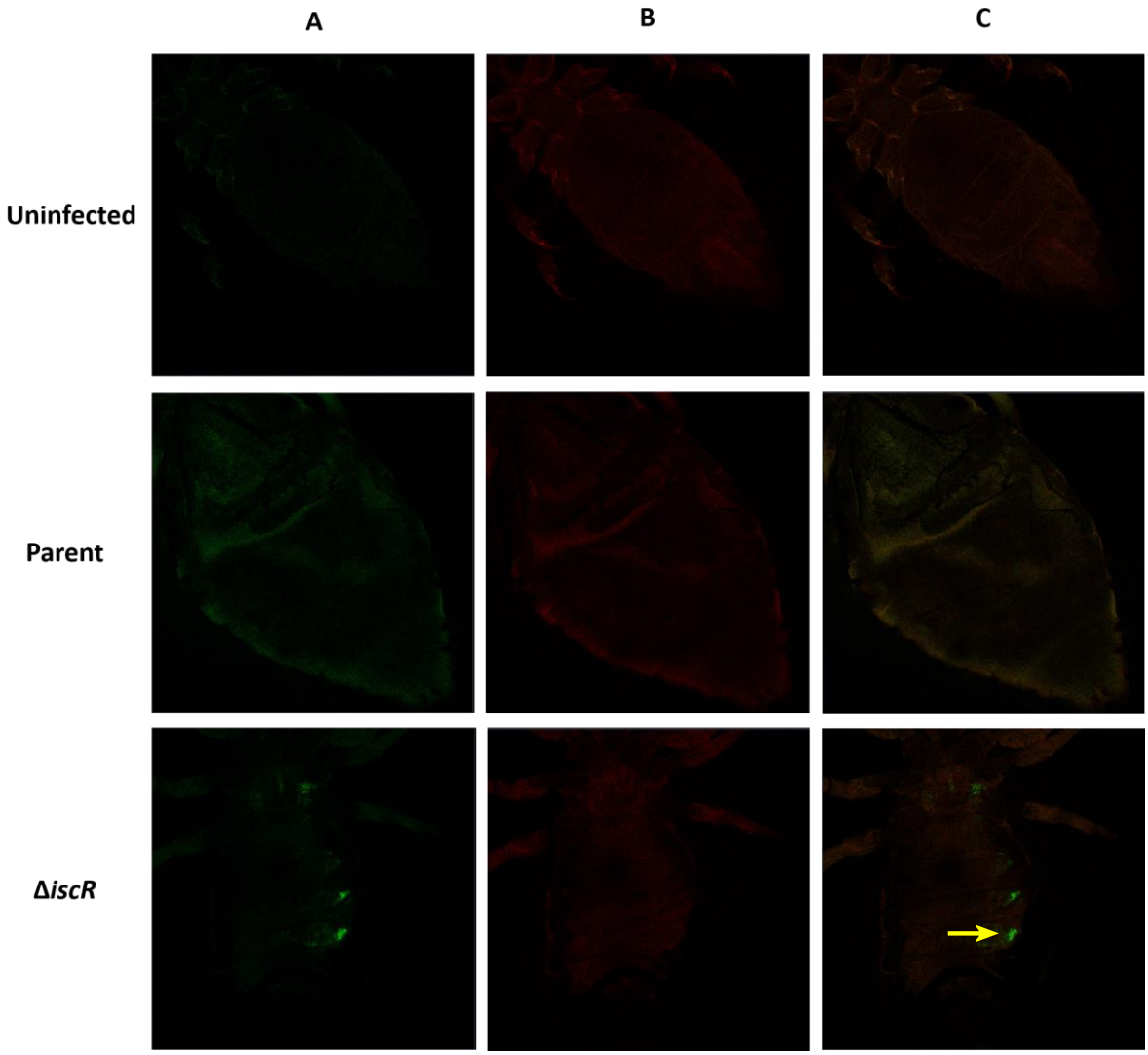

Figure 3.24 Confocal images of *P. corporis* 24 h post infection with *Y. pseudotuberculosis*.

Lice were fed blood containing either parent or *iscR* mutant *Y. pseudotuberculosis* strains and imaged after 24 hours. No GFP (A) can be seen in the negative control insect fed sterile blood. Diffuse green fluorescence is seen in louse fed with parent and *iscR* mutant strains. Autofluorescence is used to provide an outline of the louse body (B). (C) The merged image is shown. Small pockets of GFP can be identified in those fed with *iscR* (→) suggesting colonisation of the gut. Lice were imaged at 5x magnification and images are representative of experimental triplicates.

3.2.3.4 Aggregation

In *Y. pseudotuberculosis* QS mutants show an increase in non-YadA dependent aggregation, which is most pronounced after an overnight culture has been left statically for 45 min in a cuvette. This phenotype is T3S dependent as strains that do not secrete Yops do not aggregate to the same degree as those that are permissive for Yop secretion (Wiechmann, 2015; Barratt, 2018). Given the links between IscR and T3S (Section 3.2.2), auto-aggregation was examined in the *iscR* mutant using cuvette based aggregation assays and microscopy. Figure 3.25 shows that the *iscR* mutant has a defective aggregation phenotype, and that this is restored by complementation. This is likely due to the reduction in YOP secretion observed in section 3.2.2.

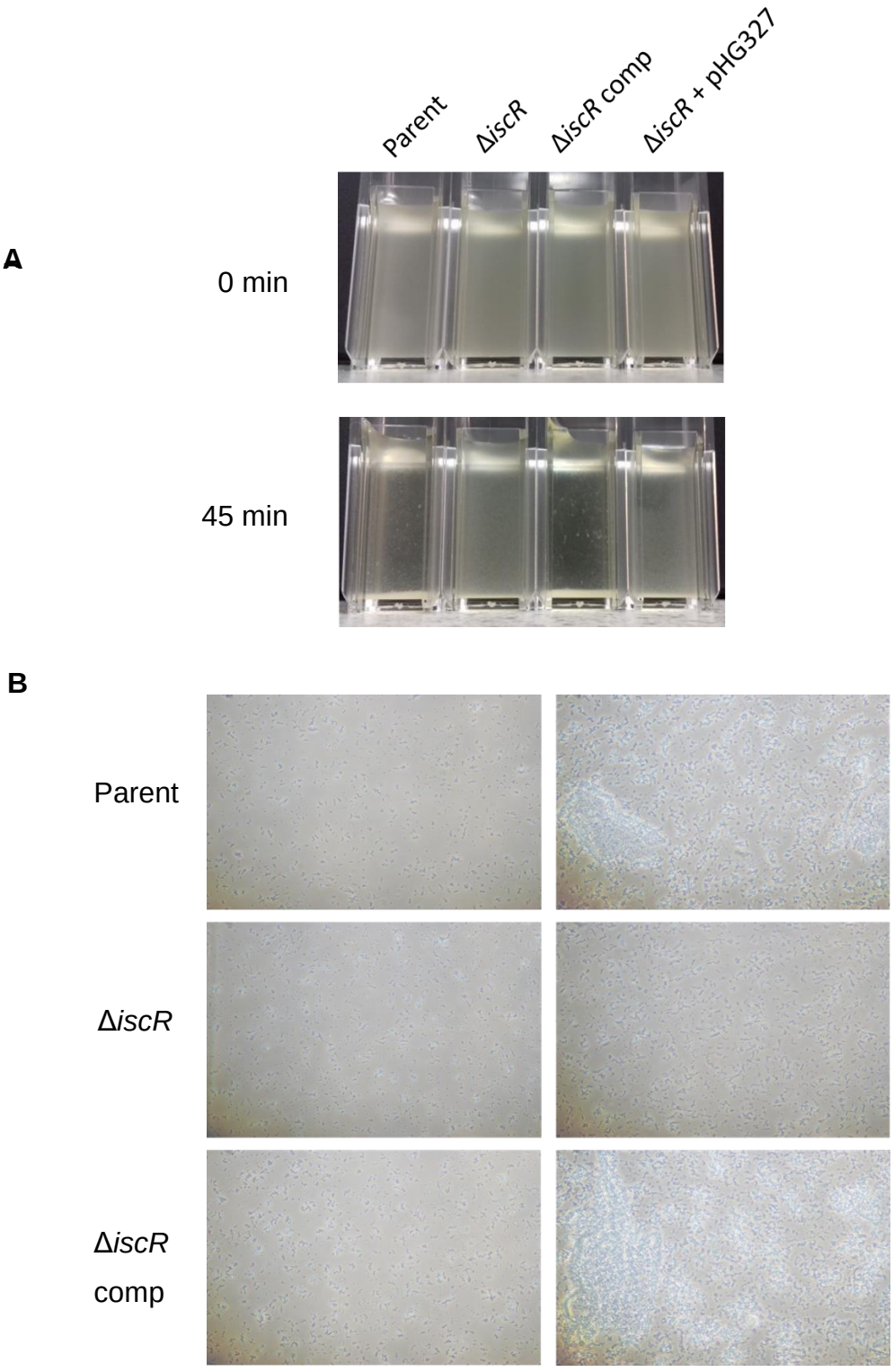

Figure 3.25 A *Y. pseudotuberculosis iscR* mutant shows reduced auto-aggregation.

Strans were grown overnight at 37ºC and incubated at room temperature for 45 minutes, in cuvettes (A) before being mounted onto a glass slide (B). (A) After 45 min less cells accumulate at the bottom of the cuvette and instead remain planktonic in the *iscR* mutant and complementing plasmid vector control. When the cultures from (A) were examined under a light microscope large aggregates were observed for both parent and

complemented *icsR* mutant strains after 45 min but not for the *iscR* mutant (B). Results representative of experimental triplicates.

When QS double mutants were examined, enhanced aggregation was seen in dR and dI mutants, consistent with previous reports. Further mutation of *iscR* in these backgrounds, reduced aggregation levels below that of the parent, and reached similar aggregation levels to those observed for the single *iscR* mutant. Increased aggregation was restored by complementation with plasmid borne IscR (Fig 3.2.3). These results do not correlate with the levels of Yops secreted by these strains (Figure 3.11), as ΔdR/iscR and ΔdI/iscR were found to secrete different levels of Yops. If reduced aggregation in the *iscR* mutant was purely due to less Yops, aggregation levels for ΔdR and ΔdR/iscR would be the same. This suggests that another as yet uncharacterised mechanism is involved in auto-aggregation in addition to T3S, and this may involve regulation by IscR, highlighting a novel potential pathway of regulation.

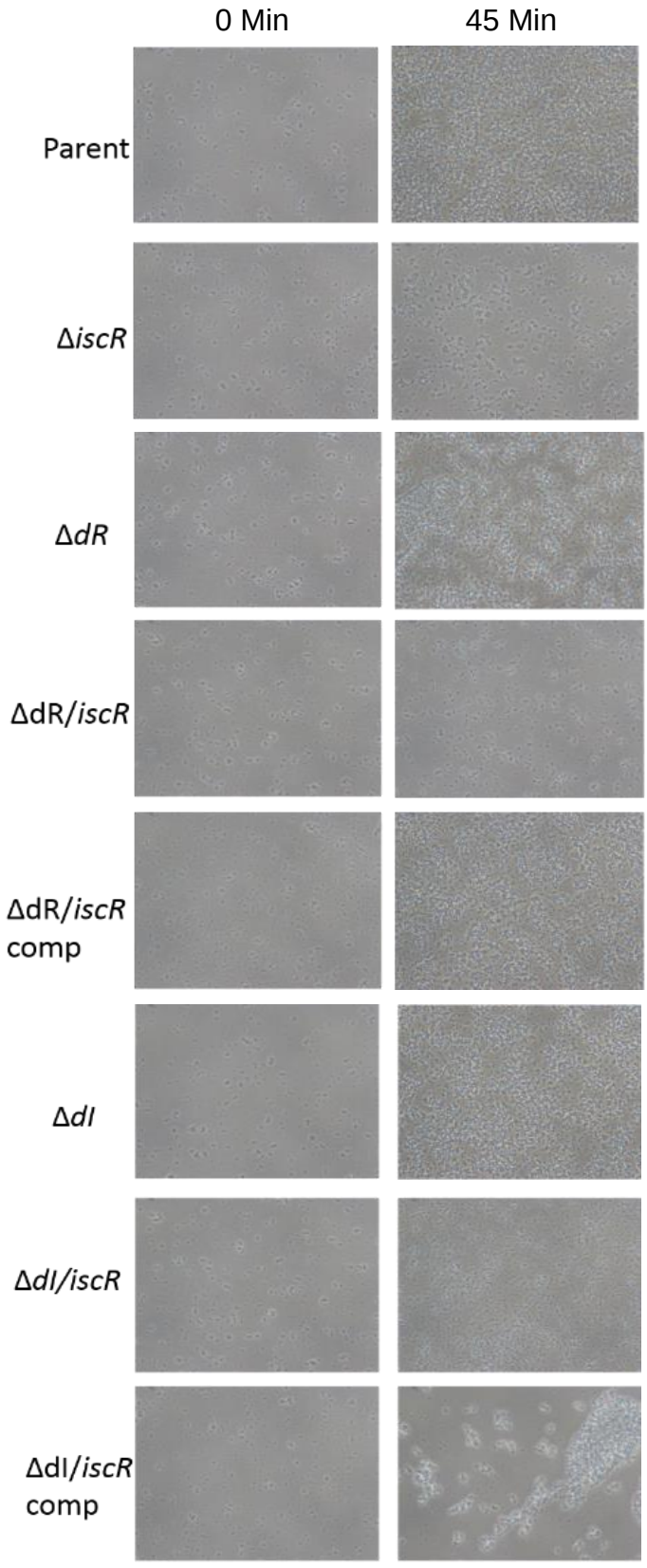

Figure 3.26 A *Y. pseudotuberculosis iscR* mutant shows reduced auto-aggregation in QS mutant backgrounds.

Strans were grown overnight at 37ºC and incubated at room temperature for 45 minutes, in cuvettes before being mounted onto a glass slide. After 45 min smaller aggregates are observed in the *iscR*, dR/*iscR* and dI/*iscR* mutants. The hyper aggregation phenotype of dR and dI strains is restored by complementation with *iscR*. Results represent experimental triplicates.

Y. pestis strains did not show aggregation after incubation at 22ºC or 28ºC (data not shown), consistent with previous findings of our group (Barratt, 2018). Interestingly, although the parent strain did not aggregate at 37ºC, again consistent with previous findings, the *iscR* mutant had settled after 40 min of aggregation, and this could be restored by genetic complementation (Figure 3.27). Unfortunately, due to constraints of CL3 working, time 0 images could not be taken, and so the *iscR* mutant had already began to aggregate at this time. In addition, higher quality pictures or microscopy work were not able to be carried out at this time due to difficulties associated with double containing cultures and use of glass slides or coverslips under CL3.

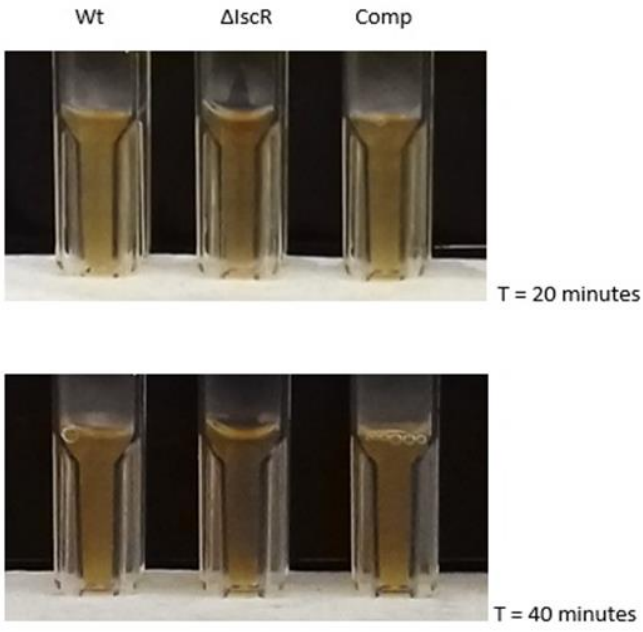

Figure 3.27 A *Y. pestis iscR* mutant shows increased auto-aggregation.

After growth at 37ºC cultures were left to settle at room temperature and settlement of aggregates on the bottom of the cuvette observed. After 45 minutes, settled cells can be observed at the bottom of the *iscR* mutant cuvette. Results represent experimental triplicates.

3.2.3.5 Iron uptake

Iron witholding is a key part of host invasion, as hosts often sequester iron as a form of immune defence and so concentrations in host tissues are very low. Bacteria overcome this defence mechanism by using siderophores, which are able to chelate the iron due to having a higher affinity for iron than the host iron-binding proteins such as transferrin and lactoferrin (Miethke and Marahiel, 2007).

As IscR coordinates an Fe-S cluster, and the presence of the iron cluster dictates what motifs IscR is able to bind (Giel, Rodionov, Liu, Blattner, & Kiley, 2006a), it would be interesting to see if deleting *iscR* regulates siderophore production or has any effect on iron acquisition. To determine this, iron acquisition at 22^{o}C was examined in *Y. pseudotuberculosis* using a liquid CAS assay, as described in (Louden *et al*., 2011; Pérez-Miranda, Cabirol, George-Téllez, Zamudio-Rivera, and Fernández, 2007). As Figure 3.28 shows, no difference was noted in iron chelation between the *iscR* mutant and the parent strains.

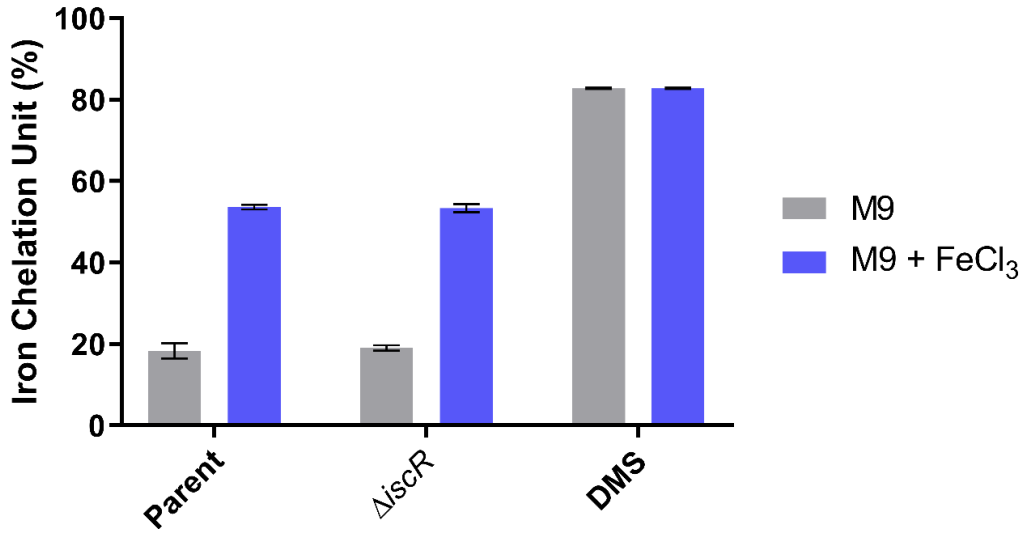

Figure 3.28 . Iron scavenging activity of *Y. pseudotuberculosis* is not affected by IscR.

A chrome azurol S assay was carried out to measure siderophore activity. A colour change of blue to orange is observed as iron is removed from the dye complex, which can be measured spectrophotometrically and used to calculate an Iron Chelation Unit. Assays were carried out in liquid form using bacterial supernatants. Deferoxamine mesylate salt (DMS) was used as a positive control. There was no difference between *iscR* mutant and parental strains.

In addition to the uptake of free iron by siderophores, *Yersinia* are also able to use haem once inside a mammalian host. (Forman *et al*., 2010; Hornung *et al*., 1996; Rossi *et al*., 2001). Several genes involved in the haemin transport system, *hmu*, were identified as being down regulated in an *iscR* mutant (Miller *et al*., 2014), so a haem uptake assay was used to see if this phenotype was affected by the deletion of *iscR*. Iron-starved bacteria were plated and exposed to H_2O, haem or free iron and left to grow at 37^{o}C, corresponding to mammalian body temperature. Equivalent growth was seen around the haem disks in both the *iscR* mutant and the parent (Figure 3.29) suggesting that deletion of *iscR* does not affect haem scavenging ability, perhaps due to the ability of the Has haemophore system to compensate for the potential downregulation of *Hmu*.

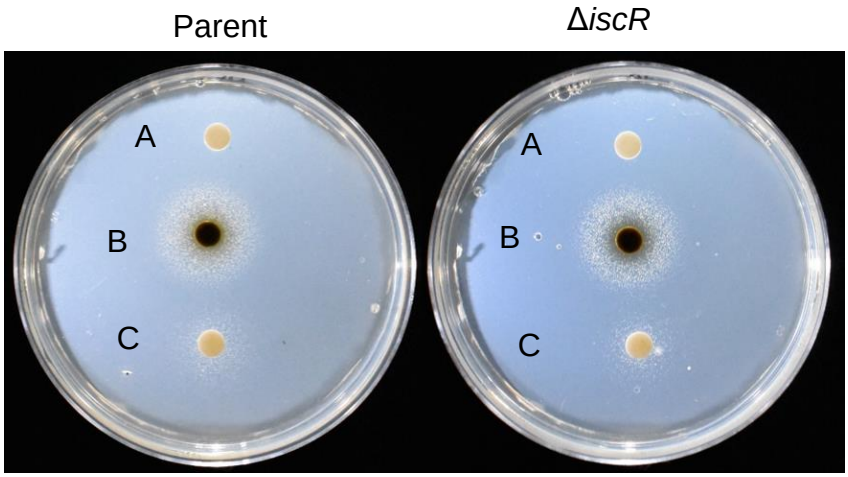

Figure 3.29 Uptake of haem in *Y. pseudotuberculosis iscR* mutant.

Iron starved bacteria were plated and growth observed around either water (A), Haemin hydrochloride (B) or free Fe3+ (C). No growth was observed around the negative control and a small amount around free iron. Both *iscR* mutant and parent strain grew equally when provided with haem (B). Results are representative of 3 independent repeats.

3.3 Discussion

Recently Miller *et al* suggested that IscR is crucial for virulence, and regulates the T3S system in *Y. pseudotuberculosis* (Miller *et al*., 2014). The work described in this chapter aimed to confirm this observation and further characterise the role of IscR in *Y. pseudotuberculosis* and *Y. pestis.* Insertion-deletion mutants were made to remove part of the *iscR* gene and replace with an antibiotic resistance casettes in both organisms. This strategy resulted in in-frame mutants that were confirmed by PCR and DNA sequencing initially, followed by whole-genome illumina sequencing and analysis. Variant analysis and complete confirmation of mutant fidelity was carried out to ensure that any phenotype attributed to the deletion of *iscR* was not a consequence of an unwanted secondary mutation.

Variant analysis of the chromosome of *Y. pseudotuberculosis* Δ*iscR* found only one mutation that met the 95% cut off used to determine that all listed variants are true, and this

was in an intergenic region. This is unlikely to have any phenotypic effect as it is located in a non-coding region, however the possibility of disrupted regulatory regions must be considered. In *Y. pestis* Δ*iscR,* three significant changes were identified, though again these were in non-coding regions. However, following a strict cut off for variant calling frequency means there is a chance of missing variants with less coverage. On further inspection of the variant calling data for *Y. pseudotuberculosis* Δ*iscR*, one additional mutant just missed out on this cut off, at 94.38%. This is a frameshift mutation in the coding region for *pldA*, coding for Phospholipase A1. This is an enzyme present in the outer-membrane linked to pathogenesis by its role in the disruption of membranes during host cell invasion. (Istivan and Coloe, 2006.; Schmiel, Wagar, Karamanou, Weeks, and Miller, 1998). A frameshift in the coding region would likely result in a non-functional protein, the phenotypic effects of which are unknown. The possibility of repairing this mutation through further cloning, or re-making the *iscR* mutant to try and avoid this secondary mutation, was considered. However, when considering time limitiations and the chance of incorporating additional SNPs when manipulating such a large genome it was decided that instead genomic complementation would be used to validate any phenotypic results. Due to time constraints during analysis, the pYV plasmid of *Y. pseudotuberculosis* Δ*iscR* was not subject to variant calling. As T3S is a crucial focus of this study, future work should look to complete this analysis and assure there are not further mutations on pYV.

This study confirmed that mutating *iscR* in *Y. pseudotuberculosis* resulted in reduced secretion of Yops. However, the difference in secretion between the *iscR* mutant and parent was not as severe as reported (Miller *et al*., 2014). A possible explanation is that this study used BHI-MOX, which chelates the calcium from the medium but is otherwise nutrient rich, whereas previous studies used minimal media. The use of minimal media in previous studies may provide additional limiting factors for T3S and secretion of Yops. Repeating Yop secretion assays in a minimal medium, perhaps YDMM, may give a more comparable Yop profile.

Interestingly, the levels of Yops secreted were not equally affected by the deletion of *iscR.* This was most noticeable when analysing YopM and YopE, both of which are secreted effector proteins. It was initially thought that the difference could be because YopM does not require a chaperone protein to be effectively delivered, whereas YopE does, and IscR may regulate levels of this chaperone too (Dewoody *et al*., 2013; Boyd, Lambermont, and Cornelis, 2000). However, published RNA-seq analysis did not find that *iscR* changed the level of SycE, Yop E's chaperone protein, so this is unlikely to be a limiting factor (Miller *et al*., 2014). Effector Yops are in constant competition to be secreted in what is an energetically costly process, and as it is such a finely balanced system, the *iscR* mutation could effect this in a number of ways. However, the phenotypic consequence of having a greater proportion of YopM secreted is not yet known but would be interesting to explore. Due to the high degree of homology between IscR and T3S systems among *Yersinia* spp. it was hypothesised that IscR would also regulate T3S in *Y. pestis*. Unfortunately, due to the activity of Pla this was unable to be tested, as Yops are rapidly degraded *in vitro* upon secretion. A number of strategies were discussed to try and solve this problem, and the possibility of using a Pla inhibitor was explored. However, this did not work as concentrations needed to have any effect also inhibited growth. A strategy was designed to remove pPst in the current strains, however this could not be completed in time. This would be a logical next step, as it would allow comparisons between mutant strains where the only difference is the plasmid, as opposed to remaking the whole mutant library in pPst negative strains and potentially introducing secondary mutations.

Despite a reduction in Yop secretion, *Y. pseudotuberculosis* Δ*iscR* still showed growth arrest in T3S inducing conditions, and although a slight increase in growth rate was observed in the mutant, this was not significant. This is likely because growth arrest is due to expression of the entire T3S and not just late stage secretion of Yops, which may indicate that IscR does not impact these early stages of T3S. Interestingly, *Y. pestis ΔiscR* appeared to show complete relief from T3S system associated growth arrest. However,

due to constraints of working in a CL3 laboratory, namely restrictions on working hours and working around other lab users, this data currently only relies on one time point and would need to be repeated over time before any reliable conclusions can be drawn. However, this result does suggest a possible role for IscR in the regulation of T3S in *Y. pestis*, perhaps more significant than what is seen in *Y. pseudotuberculosis*. The Lcr is reported to be more severe in *Y. pestis* (Brubaker, 1991; Carter, Zahorchak, & Brubaker, 1980) so it may be that any relief from growth arrest due to IscR is amplified. This finding also adds further weight to the need to develop a way of studying T3S in *Y. pestis in vitro.*

As there are known links between T3S and QS, and work outlined in this chapter explored the links between IscR and T3S, it was decided to explore any potential links between QS and IscR in *Y. pseudotuberculosis*. Triple mutants were constructed by using the same strategy as previously described to mutate *iscR* in either a strain lacking both QS response regulators (*ypsR/ytbR)*, or both AHL synthases (*ypsI/ytbI)*. These mutants were confirmed by PCR and DNA sequencing, but were not subject to whole-genome analysis and variant calling. As previously discussed, this is beneficial when doing phenotypic analysis as additional mutations can be unknowingly introduced that could have a phenotypic consequence. This is something that could be done for future experiments, but for now plasmid based genetic complementation was used by introducing a fully functional copy of *iscR*.

When studying QS it is be best to use a strain that is completely QS negative, and has both *ypsR/I* and *ytbR/I* systems mutated. However, previous attemps to construct this quadruple mutant have proved to be difficult, so using the dR and dI backgrounds is currently the only option, neither of which has a fully functional QS system but still has some functional components. For future work, the construction of a quadruple QS mutant would be invaluable.

Similarly, investigating the link between QS and IscR in *Y. pestis* has not been possible at this time due to difficulties during mutagenesis and strict limitations on the number of antibiotic resistances that can be introduced to a single strain. Future plans to use the Flp recombinase system (Hoang *et al*., 1998) to remove resistance casettes at the end stages of mutagenesis should mean that creation of these mutants complying with GMO licencing will soon be possible.

Yop secretion assays confirmed the previously reported defects in secretion in *dR* and *dI* strains (Atkinson *et al*., 2008), but the secretion defects were not as severe as in the *iscR* mutant. In a *dI* mutant background, the severe Yop secretion defect due to the mutation of *iscR* was still observed. However, this was not the case in a *dR* mutant background, and Δ*dR* and *ΔdR/iscR* showed similar levels of Yop secretion. As the severe secretion defect of Δ*iscR* is lost in the absence of both R genes it suggested that *ypsR*, *ytbR* or both are are necessary for IscR-dependent regulation of T3S. Further studies confirmed that only one R gene is necessary for the defect in secretion to occur, suggesting the presence of one R gene is enough for IscRs action on T3S, and this can be either *ypsR* or *ytbR*.

LC-MS analysis of AHL levels was unsuccessful, likely due to experimental error, and due to premature shut down of laboratory research this was unable to be repeated, therefore this remains an interesting area to explore.

After establishing a phenotypic link between IscR, T3S and QS, the IscR mutant phenotype was further characterised in a number of assays that had also previously been reported to be under QS or T3S control. No differences were observed in colony morphology or growth rate in *Y. pseudotuberculosis* or *Y. pestis*, indicating IscR does not regulate these.

The effect on flagellar mediated swimming motility was studied using semi-solid swim agar plates, and it was found that the *iscR* mutant was not hypermotile. However, despite YPIII being previously reported as a motile strain, it is non-motile in these conditions, so if IscR was to negatively affect a swimming motility phenotype, this would be unclear. Additionally,

recent illumina sequence analysis of the *Y. pseudotuberculosis* parent strain found a missense SNP in *fliC,* which is hypothesised to disrupt the interaction of flagellin filaments and explain why the parent strain is now non-motile (Slater, 2017). The repair of this mutation or the introduction of a functional copy of *fliC* is the next step in studying motility. Therefore, further work is needed before conclusions can be drawn on IscR and motility.

This study found that mutating *iscR* had no effect on the formation or distribution of *Y. pseudotuberculosis* biofilm on *C. elegans*. Although overall trends did suggest mutating *iscR* leads to an increase in biofilm formation, this was not significant. No differences was also observed in *Y. pestis*, although distribution was not examined at at this time so this would be interesting to follow up.

To allow the study of biofilm formation at a range of temperatures, biofilm formation by *Y. pseudotuberculosis* on glass was investigated. Biofilm formation was attenuated in an *iscR* mutant at 22^{o}C, although this did not complement back to parent levels, but no difference was noted at 37^{o}C. At 22^{o}C biofilm is reduced in the QS mutants, but this was not affected by mutation of *iscR*. This suggests that iscR- and QS- regulation of biofilm formation on glass is not interdependent. In RNA-seq analysis, mRNA levels of *nagC, nagA, nagB* and *nagE* were up-regulated in an *iscR* mutant, suggesting that IscR represses the *nagE-nagBACD* operon (Miller *et al*., 2014). This operon is responsible for the degradation of GlcNAc, a major component of biofilm. Increased expression would therefore likely lead to a reduction polyGlcNAc and consequentially biofilm formation in the *iscR* mutant, which may explain the phenotype observed here.

This chapter described some of the refinements of a model for *P. corporis* infection, which allowed for successful feeding and infection of lice. In *Y. pseudotuberculosis a*n *iscR* mutant appeared to result in a higher kill rate of lice than the parent strain, however a genetically complemented strain was not analysed during this study. Microscopic imaging of the lice was unable to confirm if the change in survival rate was due to the production of

more biofilm in the gut, as methods to sustain fluorescent staining in the louse gut over time need to be refined. However, current models suggest that biofilm blockage of the louse gut, similar to that reported in the flea vector, enables the transmission of *Y. pestis* (Houhamdi *et al*., 2006) and *Y. pseudotuberculosis* is also capable of forming biofilm in the louse gut (Elton, 2018), so this phenotype may be biofilm mediated. Whilst the original intention was to establish the louse as a model of biofilm formation, at the current stage it is more representative of an infection model, as a clear link between the killing observed and biofilm formation has not yet been established. Following extensive discussions and approvals, adaptation of the feeding model was made to enable safe use in CL3 conditions, and practise runs were successful. This will offer a novel way for studying biofilm formation in *Y. pestis* and shed further light into whether and how *P. corporis* may aid plague transmission.

Before the *iscR* mutants are used in future lice feeding assays, it would be good to study the differential survival of strains in blood, as a recent publication reported that an *iscR* mutant in *Y. pseudotuberculosis* has a survival defect when incubated in whole blood, that is independent of haem uptake, T3S, complement and the ability to replicate intracellularly (Schwiesow, Mettert, Wei, *et al*., 2018). If the *iscR* mutant has a different survival in whole blood then this may affect the results of future lice biofilm work. However, this would not explain the reduced survival of lice fed the *iscR* mutant, indeed the opposite result would be expected.

QS and T3S are also linked to non-YadA dependent aggregation. *Y. pseudotuberculosis* QS mutants exhibit a hyper-aggregation phenotype, which was confirmed in this study, and strains deficient in Yops are also often deficient in aggregation (Barratt, 2018). The *iscR* mutant was found to aggregate much less than parental strains which could be due to the impaired Yop secretion previously discussed. However, the defective aggregation for *iscR* mutants was still observed in both dI and dR mutant backgrounds, which did not correlate with the levels of Yops secreted for these strains (Figure 3.11). This suggests a different

mechanism behind auto-aggregation, separate to the regulation by T3S. The levels of *ail* mRNA is up-regulated in an *iscR* mutant, and it was hypothesised that Ail may regulate auto-aggregation, as OmpX, an *ail* homologue in *Y. pestis* was reported to positively regulate aggregation (Kolodziejek. *et al*., 2007; Miller *et al*., 2014). If this were true, upregulation of *ail* would likely result in increased aggregation, which was not observed here. This suggests that either Ail does not mediate aggregation in *Y. pseudotuberculosis*, or does so in a different way than in *Y. pestis*. It may also highlight a common problem when relying solely on RNAseq data, as transcription levels do not always correlate with translation.

When *iscR* was mutated in *Y. pestis,* a hyper-aggregation phenotype was observed however this contradicts literature that says *Y. pestis* cannot aggregate at 37^{o}C. In addition, no aggregation was seen at 22^{o}C or 28^{o}C which has been reported in *Y. pestis*. However, the presence of Pla must again be considered here, as whilst Yops are translated *in vitro* they are promptly degraded (Mehigh *et al*., 1989). YopH has been identified as key for auto-aggregation in *Y. pseudotuberculosis* (Barratt, 2018) so its absence may explain why aggregation was not observed in this assay. Again this highlights the benefits of constructing a pPst negative strain for future studies.

No change in iron chelation nor haem uptake uptake was observed for the *Y. pseudotuberculosis iscR* mutant. The *hmu* operon is downregulated according to RNA seq data (Miller *et al*., 2014) and IscR has since been shown to be essential for the expression of *hmuSTUV* in the presence of inorganic iron, due to the direct action of IscR on a promoter in the intergenic region between *hmuR* and *hmuS* (Schwiesow *et al*., 2018). As no difference in haem uptake was observed between the *iscR* mutant and parent strain, it suggests that perhaps the Has haemophore is able to compensate for the down-regulation of the *hmu* operon.

4 Exploring the regulation of T3S by IscR using chromosomal promoter::*lux* fusions in *Y. pseudotuberculosis.*

4.1 Introduction

The work described in Chapter 3 demonstrates that IscR is necessary for the regulation of T3S, and Yop secretion is significantly reduced in an *iscR* mutant in *Y. pseudotuberculosis*, in accordance with previous reports (H. K. Miller *et al*., 2014). A phenotypic link between IscR, QS and T3S was also established, as the IscR-dependent suppression of Yop secretion is lost in a QS response regulator mutant background (Figure 3.11). How IscR regulates T3S still remains to be determined, although Miller *et al*., (2014) hypothesised that it may be through regulation of LcrF, and indeed they found that purified IscR bound to an identified *lcrF* promoter, and mRNA levels of *lcrF* and 24 other T3S genes were reduced in *Y. pseudotuberculosis* in the absence of *iscR*.

LcrF is an AraC-like transcriptional activator, encoded on pYV/pCD1, and highly conserved amongst all human pathogenic *Yersinia*. At 37^{o}C LcrF binds as a dimer to promoter sequences of target genes on the virulence plasmid (King, Schesser Bartra, Plano, and Yahr, 2013). *LcrF* expression is subject to thermoregulation, via a short stem loop structure or 'RNA-thermometer' which at environmental temperatures conceals the *lcrF* ribosome binding site and prevents translation. It has been proposed that when temperature increases, hydrogen bonds in the AT-rich thermometer melt, unmasking the RBS and initiating *lcrF* translation (Hoe and Goguen, 1993; Böhme, Steinmann, Kortmann, Seekircher, Heroven, Berger, Pisano, Herbst, *et al*., 2012).

The RNA thermometer is located in an intergenic region between *lcrF* and the T3S system chaperone *yscW*, which lies 123 bp upstream of *lcrF*, in the same operon and under the control of the same promoter (Böhme, Steinmann, Kortmann, Seekircher, Heroven, Berger, Pisano, Herbst, *et al*., 2012). In addition to the translational regulation, this operon is under

the control of the transcriptional repressor, YmoA (*Yersinia* modulator). YmoA is a histone-like protein that is proposed to prevent expression of *lcrF* at low temperatures through influencing DNA topology, such as compaction of chromatin and influence on DNA supercoiling (Cornelis *et al*., 1991; Cornelis, 1993). At 37°C *ymoA* repression is removed and this is the trigger behind the thermo-dependent assembly of the T3S system. This is partly due to ClpXP and Lon mediated proteolysis of YmoA, temperature-induced topological changes of the promoter and conformational changes in the regulatory proteins. (Jackson *et al*., 2004; Ono *et al*., 2005). It has since been proposed that there is another, *lcrF* specific, promoter within the intergenic region of *yscW* and *lcrF* (Slater, 2017).

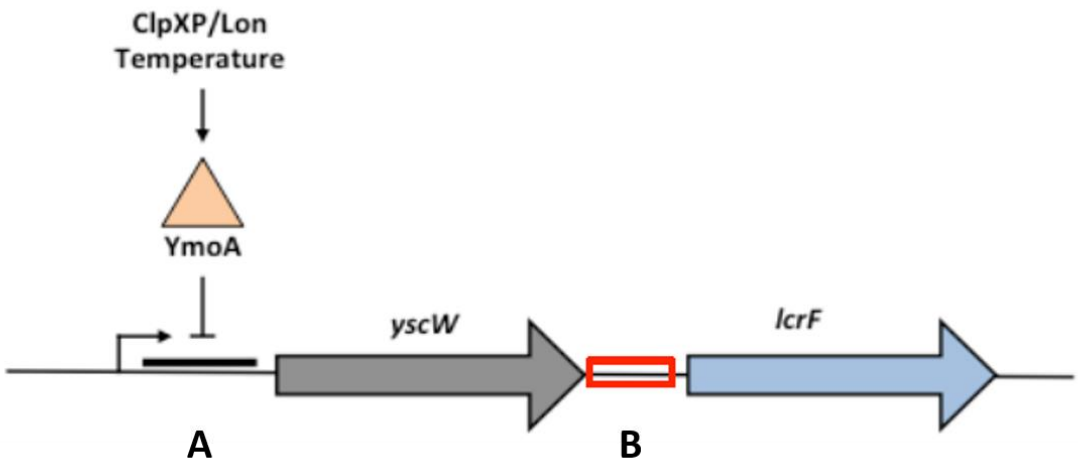

Figure 4.1 *lcrF* expression is under the control of two different promoters

***yscW* and *lcrF* are arranged in an operon under the control of a single promoter (A). A second, weaker promoter was identified in the intergenic region between *yscW* and *lcrF* (B). Adapted from (Böhme, Steinmann, Kortmann, Seekircher, Heroven, Berger, Pisano, Herbst, *et al*., 2012; Slater, 2017)**

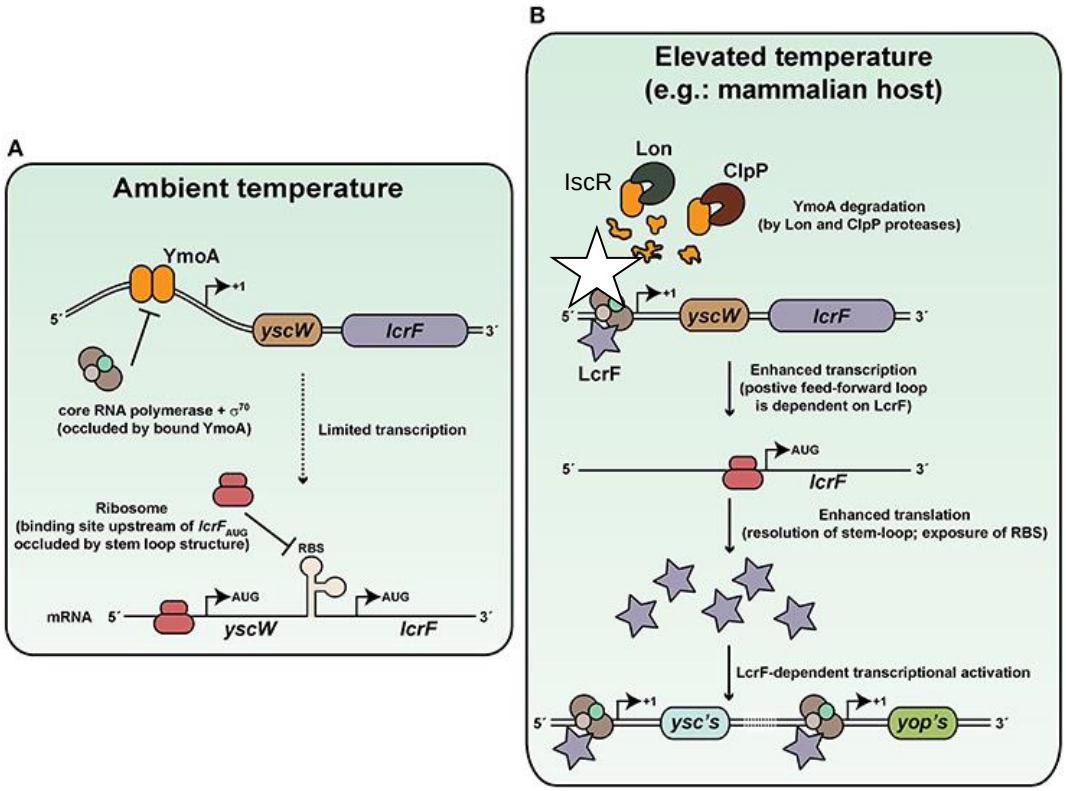

Figure 4.2 The T3S System is subject to thermo-dependent regulation

At ambient temperatures (A), YmoA blocks transcription of the *yscW-lcrF* operon through chromatin compaction. *lcrF* translation is blocked by formation of a 5' RNA thermometer which stops the formation of the ribosome complex. At elevated temperatures such as in the host (B) ClpXP and Lon proteases degrade YmoA, liberating the *yscW* promoter. The RNA thermometer melts, enabling the ribosome to target the RBS. IscR is believed to work upstream of the *yscW* promoter to enhance transcription. Adapted from (S. Chen et al., 2016)

T3S is also regulated by QS in *Yersinia* spp. QS was first linked to the regulation of T3S in *Y. pestis*, as the addition of exogenous *N*-octanoyl-homoserine lactone (C8) or *N*-(3-oxooctanoyl)-homoserine lactone (oxo-c8) led to a reduction in the virulence factor LcrQ (Gelhaus, Rozak, Nierman, *et al*., 2009), although this relied on high, non-physiological concentrations of AHLs. In *Y. pseudotuberculosis*, QS was linked to T3S through the regulation of motility and biofilm formation on *C. elegans* (Atkinson *et al*., 2008). Further links between QS and T3S have been identified through the repression of auto-aggregation as an increased aggregation phenotype is seen in an *ypsI/ytbI* QS synthase mutant,

suggesting that QS is a repressor of auto-aggregation and therefore a repressor of T3S (Barratt, 2018).

Previous studies on the regulation of T3S by IscR have employed RNA-seq analysis, and whilst this is an extremely powerful tool that provides an overall view of the transcriptome at any given timepoint, bioreporters can be used to monitor individual bacterial gene expression in a more targeted manner. Bioluminescent reporters allow the quantification of gene expression in real time, often with little effect on the host system. As very few non-marine bacteria exhibit bioluminescence naturally there is minimal background signal, offering high sensitivity. The source of *lux* in this study is *Photorhabdus luminescens*, where *lux* genes are arranged into the *luxCDABE* operon. *LuxAB* codes for luciferase and *luxCDE* codes for the fatty acid reductase complex responsible for synthesizing long chain fatty aldehydes as substrates for the luminescence reaction (Meighen, 1991). Use of the *lux* cassette from *P. luminescens* is preferred to other species due to its higher thermal stability (up to 45^{o}C) and *in situ* generation of the aldehyde meaning that the addition of substrate is not necessary (Meighen, 1991). By using the *lux* genes as reporters of gene expression, the strength and regulation of transcription from various promoters can be monitored in parent and mutant backgrounds.

4.1.1 Aims of this Chapter

There is not yet a clear picture of the full extent of the role IscR has in T3S regulation and whilst it appears to act through master regulator Lcrf, given the multi-faceted regulation of T3S, it is possible that IscR acts at more than one target promoter site. As a regulator of T3S, IscR also stands out as a potential therapeutic target in order to reduce virulence and minimise the pressure to acquire resistance. Therefore, a broader understanding of the regulatory network could be invaluable.

In order to elucidate more of this network, the work described in this chapter describes how promoter:*lux* fusions were used to examine the expression of key genes to determine the impact of IscR on the:

- *yscW-lcrF* promoter
- *lcrF* specific promoter
- expression of *ymoA*

A phenotypic link between IscR, QS and T3S is described in Chapter 3. To determine whether IscR acts on the QS system at a transcriptional level, promoter:*lux* fusions were also used to investigate whether:

- IscR regulates expression of the QS response regulator genes, *ypsR* and *ytbR*
- IscR regulates expression of the AHL synthase genes, *ypsI* and *ytbI*

4.2 Results

4.2.1 Does IscR regulate T3S via LcrF in *Y. pseudotuberculosis*?

T3S is controlled by the master regulator LcrF. The *lcrF* gene is part of an operon with *yscW* that previously was believed to be under the control of a single promoter (Böhme, Steinmann, Kortmann, Seekircher, Heroven, Berger, Pisano, Thiermann, *et al*., 2012). This promoter is repressed by YmoA and exhibits temperature sensitivity. Previously, our group identified a second, LcrF specific, promoter with weaker expression which was also found to be temperature sensitive and under YmoA repression (Slater, 2017). Promoter:*lux* fusions of these regions were used to determine whether IscR regulates T3S through any of these promoters.

4.2.1.1 Expression from the *yscW-lcrF* promoter

It was previously reported (Miller *et al*., 2014) that IscR binds upstream of *yscW*, in the *yscW-lcrF* promoter, and hypothesised that this is the mechanism by which IscR regulates T3S. As we had previously constructed a *lux* fusion to this promoter, it was transformed into the parent, *iscR* mutant and genetically complemented backgrounds and expression analysed. Published RNA-seq data were derived from experiments carried out on strains grown for 3 h at 37ºC in a minimal low calcium medium to induce expression of the T3S system (Miller *et al*., 2014). However, our previous *lux* reporter assays all used YLB, a rich medium with high calcium levels. Therefore, for comparison, *yscW-lcrF* promoter expression was investigated using both YLB and YLB-MOX (which contains a calcium chelator and so lacks free calcium) at both 22ºC and 37ºC.

Figure 4.3 shows that no expression was observed from the parent at 22ºC, in line with previous studies (Slater, 2017). However, very low levels of expression were observed in the *iscR* mutant at 22ºC, which was partially complemented by a plasmid based functional copy of *iscR.* At 37ºC a ~2 fold increase in expression in an *iscR* knockout strain compared

with the parent strain was observed, which was reduced to wild type by genetic complementation YLB-MOX conditions but not YLB. This confirms that *iscR* regulates expression of *lcrF* via the *yscW-lcrF* promoter. However, Miller *et al*. (2014) found the opposite of this, and in an *iscR* mutant a reduction in transcription of *lcrF* was observed. The calcium concentrations of the medium made no difference to the overall trend for expression levels at either temperature. However, the kinetics of expression, with regards to magnitude and the timing of switching off, were completely different. At 37^{o}C with YLB-MOX, conditions which trigger T3S expression, expression increases rapidly for a short space of time for all strains, whereas with high calcium the increase in expression is gradual and continues to increase for IscR after this time. This suggests that expression from this promoter is calcium dependent.

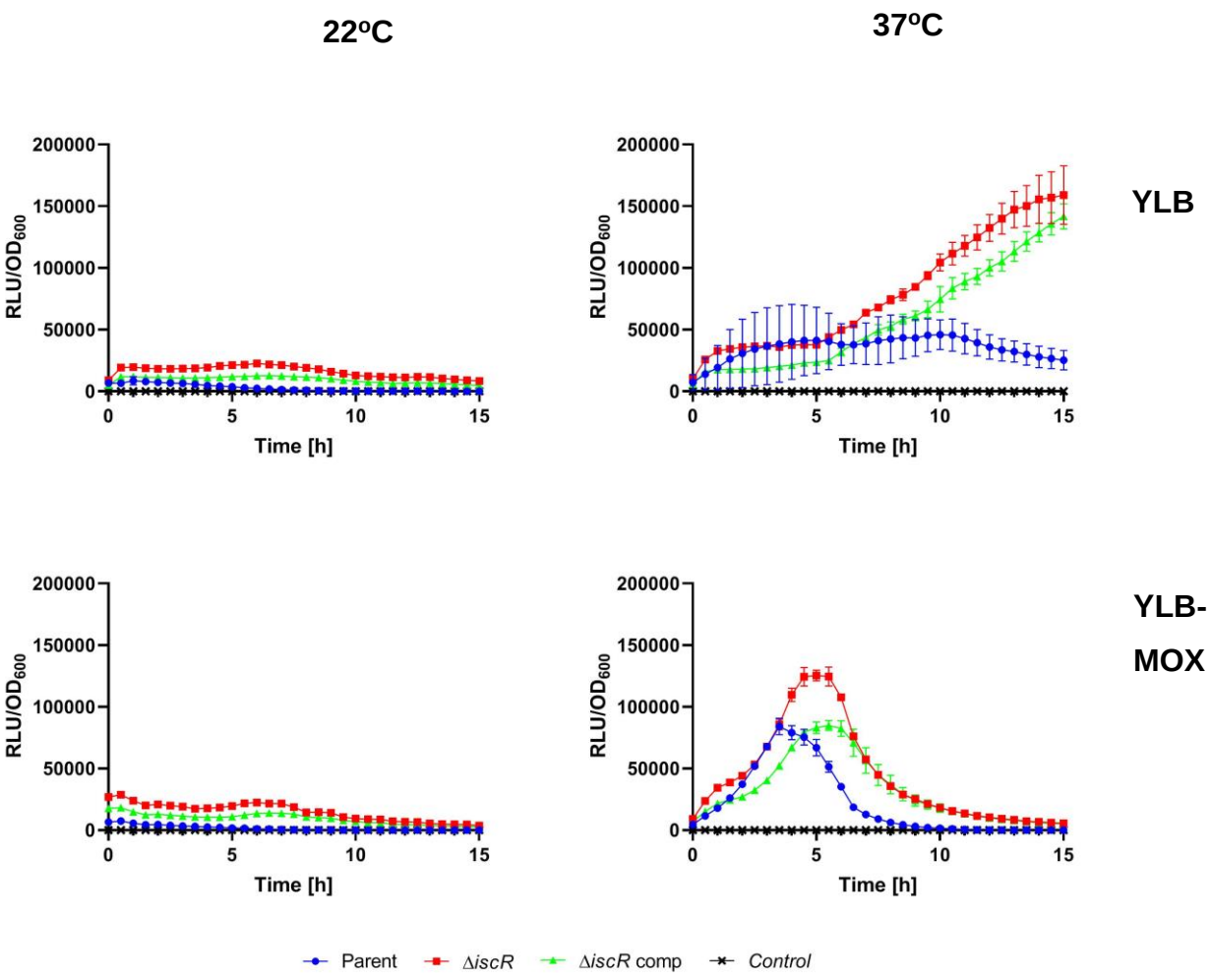

Figure 4.3 Transcription from the *yscW-lcrF* promoter region.

Expression from the *yscW-lcrF* promoter region was determined by promoter:*lux* fusions. No expression from this promoter was observed at 22ºC in the parent in contrast with the *iscR* mutant. At 37ºC expression was greater from this promoter in the *iscR* mutant. This was restored to wild type by complementation with plasmid-borne *iscR*. The presence or absence of calcium (YLB or YLB-MOX) changed the expression profiles, with low calcium (YLB-MOX) resulting in a quicker but shorter lived expression. Results are representative of 4 independent repeats. YLB only was ran as a control.

4.2.1.2 Expression from the *lcrF* specific promoter

To determine whether *iscR* also acted on the *lcrF* specific promoter, the bioluminescence of P_{lcrf}::*lux* was studied in the parent, *iscR* mutant and genetically complemented backgrounds (Figure 4.3). As previously reported, no expression was observed at 22ºC in the parent strain and, in contrast to the *yscW-lcrF* reporter, this remained the same when observed in the *iscR* mutant. This was expected as *lcrF* is not expressed at this temperature. At 37ºC, expression was ~2 fold lower in the *iscR* mutant in the presence of MOX, and this was restored to parental levels by genetic complementation. This result is at odds with the knowledge that an *iscR* mutant has reduced T3S activity and reduced levels of LcrF mRNA (Miller *et al*., 2014). If IscR positively regulates *lcrF* expression as this promoter fusion suggests, an *iscR* mutant would be expected to show an increase in T3S, subject to other limiting factors in the system. However, this is a secondary promoter, and overall expression is substantially much weaker (~100 fold) than from the *yscW-lcrF* promoter, so it is unlikely to have a sigificant effect on *lcrF* expression when *iscR* is acting on both promoters. Again, the presence of MOX and consequential low calcium levels changed the expression profile from this promoter. As with *yscW-lcrF*, expression with Mox from the *lcrF* specific promoter shows the same early and sharp induction, which is short lived.

These results reinforce work previously done by our group that suggest the presence of a novel, *lcrF* specific, promoter (Slater, 2017). Previous work on this promoter demonstrated very low levels of expression, often between 10 and 100 fold lower than observed with other reporters (Slater, 2017). However, this is the first time this promoter has been assayed in low calcium availability medium and, as can be seen in Figure 4.3, expression is much higher in these conditions. This highlights a potential role for this second promoter in the later stages of T3S expression, when the calcium blockade is removed and Yops are secreted, which would explain why its expression is dependent on low calcium concentrations.

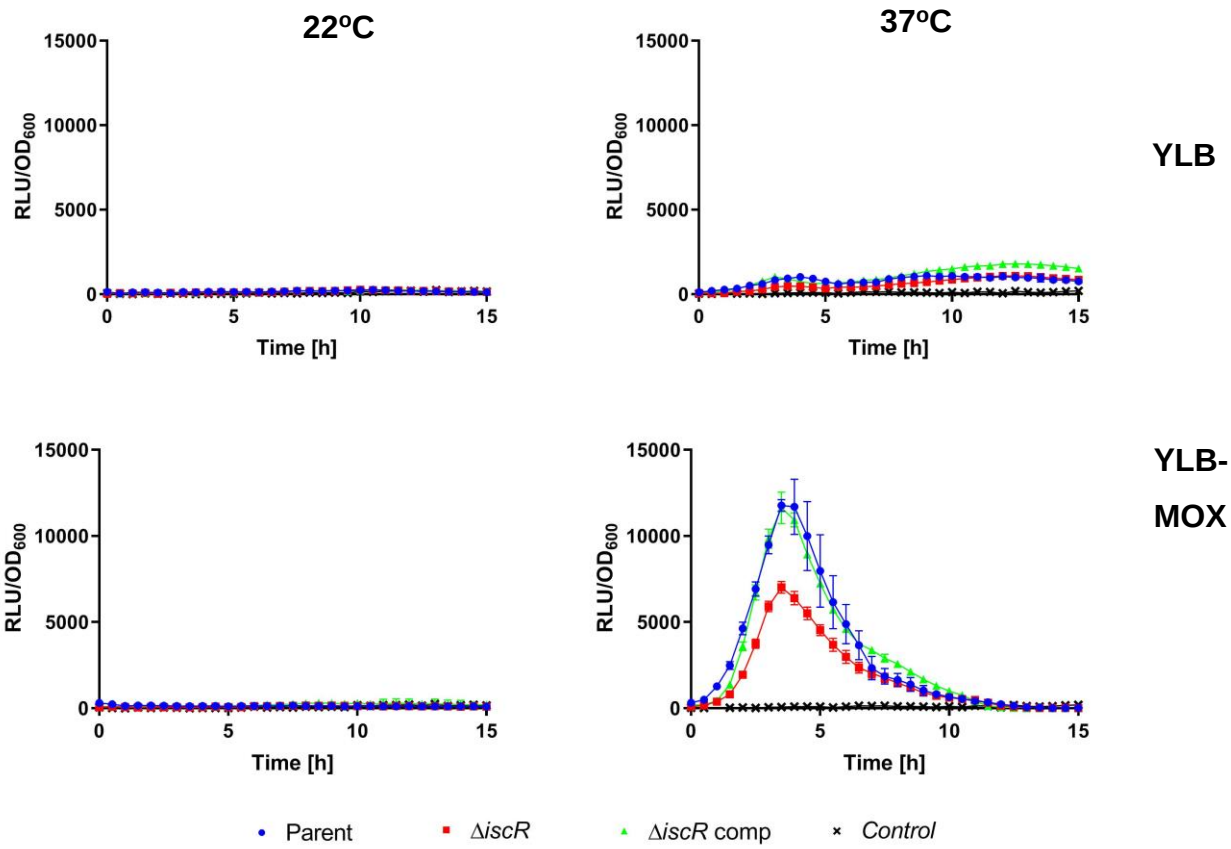

Figure 4.4 Transcription from the *lcrF* specific promoter.

Expression from the *lcrF* specific promoter region was determined using promoter:*lux* fusions. No expression from this promoter is observed at 22ºC. At 37ºC expression is reduced in the *iscR* mutant relative to the parent. This is restored by complementation with plasmid-borne *iscR*. The absence of available calcium (YLB-MOX) greatly increased expression levels from this promoter for all strains and resulted in different kinetics, with a short and brief period of expression instead of a longer, lower level. Results represent 3 independent repeats. YLB only was ran as a control.

4.2.1.3 IscR does not regulate expression of *ymoA*

To explore whether *iscR* could further influence *lcrF* levels via *ymoA*, which regulates LcrF expression through both *yscW-lcrF* and the *lcrF* promoters, the expression of *ymoA* was investigated in parent and *iscR* mutant backgrounds (Figure 4.4) No difference was observed between the strains, suggesting that IscR does not act transcriptionally on *ymoA*. Results in YLB and YLB-MOX were the same (data not shown).

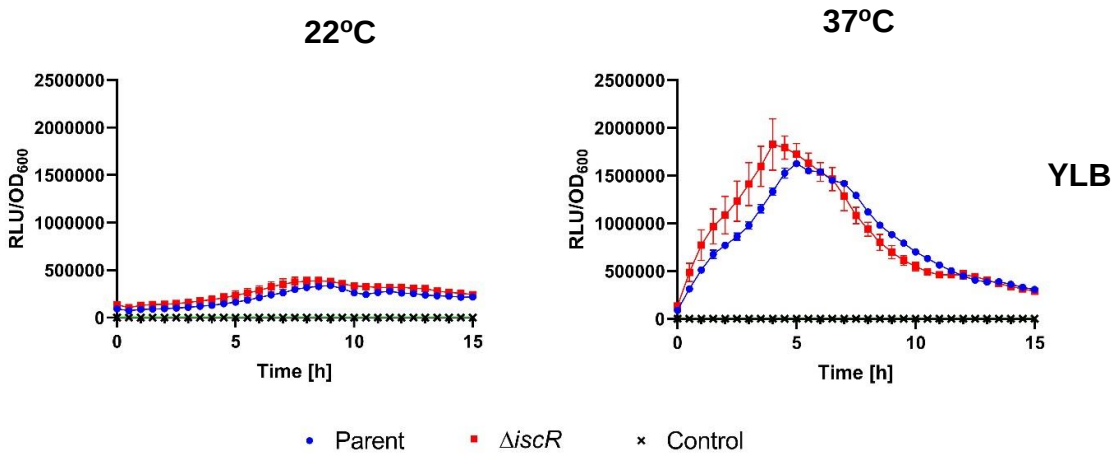

Figure 4.5 Transcription from the *ymoA* promoter.

Expression from the *ymoA* promoter region was determined using promoter:*lux* fusions. No difference in expression was observed between parent and *iscR* mutant at 22°C or 37°C. (n=3) YLB only was ran as a control.

4.2.2 Does IscR regulate T3S through QS in *Y. pseudotuberculosis*?

Figure 3.11 (Chapter 3 Section 2) showed that the defect in Yop secretion attributed to IscR deletion was not observed when response regulator genes, *ytbR* and *ypsR*, had been knocked out, although the presence of either R gene alone was enough to retain this phenotype. This suggests that the IscR-dependent regulation of T3S may be QS dependent. Promoter:*lux* fusions were therefore used to determine whether IscR directly regulates the expression of the QS system regulator genes (*ypsR* and *ytbR) or* AHL synthases (*ypsI* and *ytbI*).

4.2.2.1 Expression of *ypsR* and *ytbR* is reduced in an *iscR* mutant

To examine the impact of IscR on expression of the QS system response regulators YpsR and YtbR, P_{ypsR}::*lux* and P_{ytbR}::*lux* fusions were introduced into parent, *iscR* mutant and complemented strains and expression quantified as a function of growth at 22ºC and 37ºC. As previously, expression was studied in YLB or YLB containing a calcium chelator (YLB or YLB-MOX) but this made no difference to expression patterns (data not shown). Figure 4.5 shows that expression from both the *ypsR* and *ytbR* promoter regions was reduced in the absence of IscR at both 22ºC and 37ºC. This suggests that IscR positively regulates the expression of the response regulators in both QS systems. However, complementation with a plasmid-borne copy of *iscR* did not restore the expression of *ypsR* to parental levels, and only partially complemented for *ytbR.*

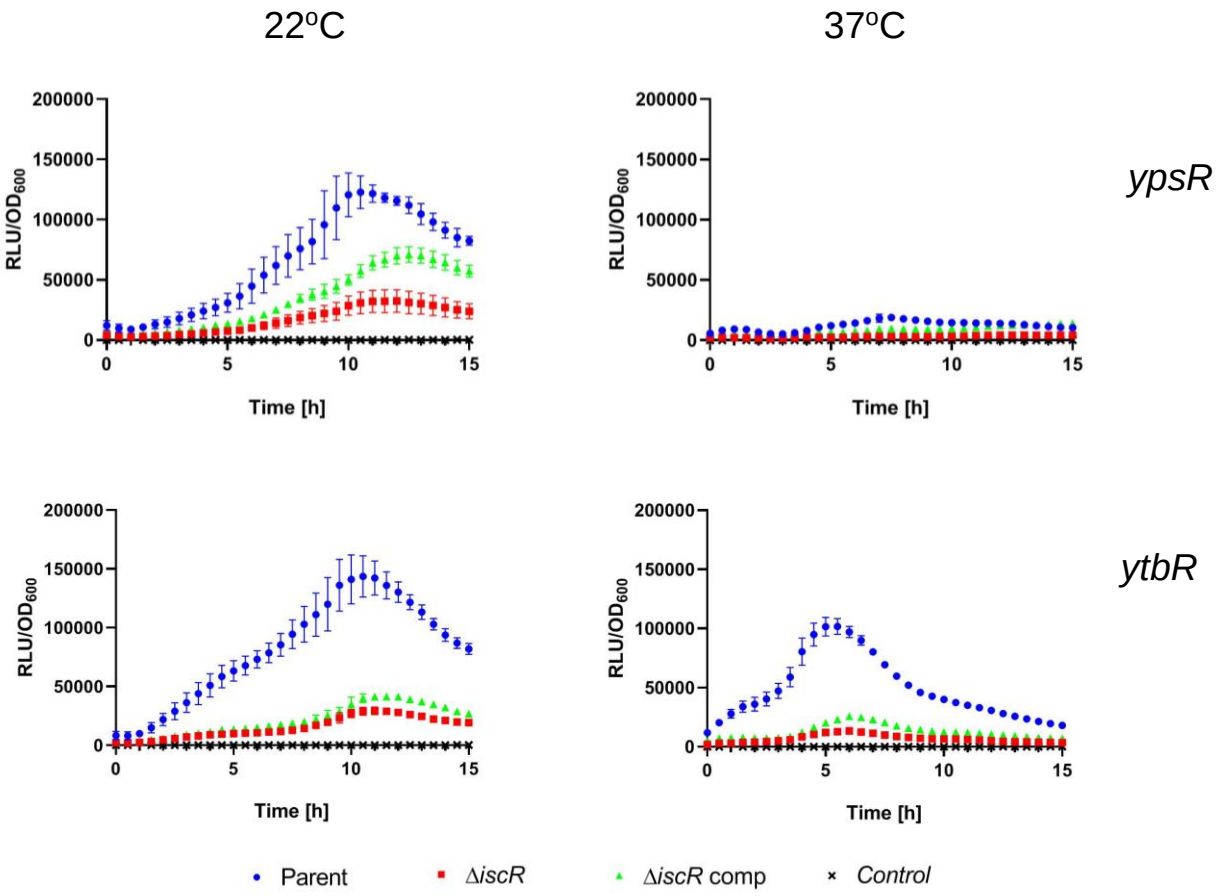

Figure 4.6 Impact of *iscR* on transcription of *ypsR* and *ytbR* promoters.

Expression of *ypsR ytbR* was investigated using promoter:*lux* fusions. At both 22ºC and 37ºC a large reduction in expression from both promoters is observed in the *iscR* mutant background. (N=3) YLB only was ran as a control.

4.2.2.2 IscR does not regulate the expression of *ytbI* or *ypsI*

To examine the impact of IscR on the AHL synthases YpsI and YtbI, P_{ypsI}::*lux* and P_{ytbI}::*lux* fusions were introduced into parent, *iscR* mutant and complemented strains and expression studied at 22ºC and 37ºC. Figure 4.7 shows that no difference was observed in the expression from either promoter between parent and *iscR* mutant backgrounds. Interestingly, when a plasmid based copy of IscR was introduced, expression from the *ytbI* promoter was increased significantly beyond that of the parent strain.

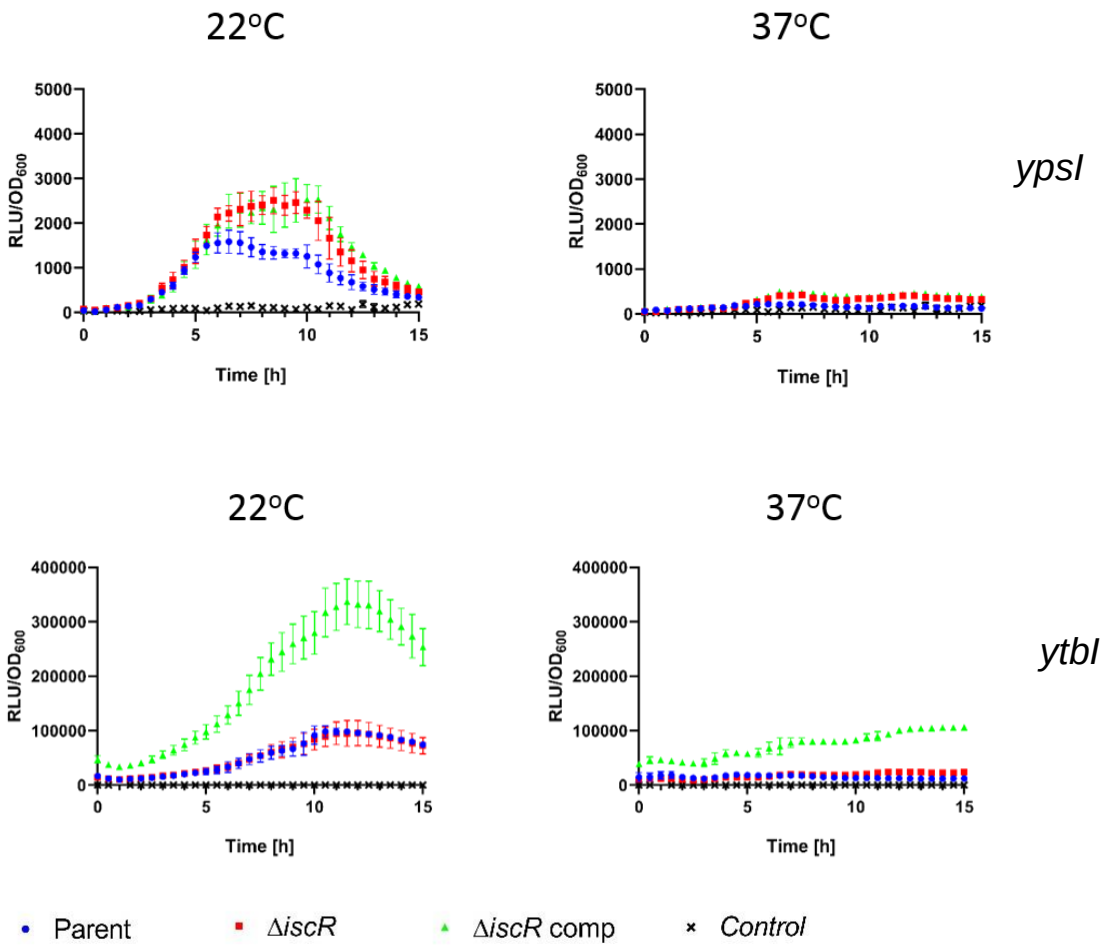

Figure 4.7 Impact of *iscR* on transcription of *ypsI* and *ytbI*.

Expression of *ypsI* and *ytbI* was determined using promoter:*lux* fusions. At both 22°C and 37°C no significant difference was observed between expression in parental and *iscR* mutant backgrounds. When complemented with IscR on low copy number vector pHG327, expression of *ytbI* is significantly increased. (N=3) YLB only was ran as a control.

4.3 Discussion

The results presented in this chapter explored the regulation of genes involved in T3S and QS by IscR and found that:

- IscR negatively regulates expression from the *yscW-lcrF* promoter
- IscR positively regulates expression from the *lcrF* specific promoter
- IscR has no effect on *ymoA* expression

- IscR positively regulates expression of *ypsR* at 22^{o}C and 37 ^{o}C and *ytbR* at 22^{o}C
- IscR has no effect on the expression of *ypsI* or *ytbI*

Promoter fusions showed that IscR negatively regulates the expression of LcrF through binding to the *yscW-lcrF* promoter, leading to increased expression in an *iscR* mutant. In contrast, expression from the *lcrF* specific promoter was around 2 fold lower in the *iscR* mutant. Whilst this does not fit with the knowledge that T3S is reduced in the absence of IscR, it is important to note that expression from this promoter is around 100 fold weaker than for *yscW-lcrF,* and so it is unlikely that action on this promoter would alter LcrF levels when IscR is acting on both. IscR is sensitive to the environment and binds to different DNA motifs depending on its Fe-S status, therefore it is possible that IscR is capable of activating or repressing LcrF expression depending on the presence of the cluster, allowing iron availability to influence expression of T3S. Bioinformatic analysis on the *lcrF* specific promoter, to see if there is a type 1 or type 2 iscR motif present that would explain this regulation would be a good next step. This study has explored the effect of complete deletion of IscR, but for future experiments it may be beneficial to have an apo-locked IscR strain, to further explore the effect of iron on IscR's regulatory activities.

Both LcrF promoters are under the control of the temperature sensitive YmoA (Böhme, Steinmann, Kortmann, Seekircher, Heroven, Berger, Pisano, Thiermann, *et al*., 2012) so promoter fusions were used to see if IscR indirectly regulated the expression of LcrF and Yop secretion via action on YmoA. IscR did not affect the expression from the YmoA promoter, suggesting that the regulation of LcrF expression by IscR is direct, through binding to the two previously discussed promoter regions.

One of the interesting things about these results was the effect of the presence of a calcium chelator on the expression profiles from LcrF promoters. The presence of Mox at 37^{o}C lead to much quicker peak in expression for both *yscW-lcrF* and *lcrF* promoters, both peaking after around 5 hours and expression being almost completely gone by 10 hours.

This highlights a benefit of fusion data over RNA seq, as the later only offers a snapshot of gene expression at a specific time and conditions. The expression of LcrF may be increased in low calcium and at 37ºC, as these are T3S inducing conditions and indirect factors, such as the presence of Yops, may be driving expression from these promoters. The sharp fall in expression after the initial peak could be due to the energetics of the system, as it could begin to shut down as the substrate for Lux, $FMNH_2$, is depleted. Before conclusions can be drawn about the changes in expression, it must first be ruled out that Mox does not affect the luciferase enzyme itself and this is the artefact we are seeing. A good test to do would be to run these assays with fusions of a constitutively active promoter, and see if Mox changes these expression profiles.

Chapter 3 previously identified a phenotypic link between IscR, QS and the regulation of T3S, with data suggesting that IscR's regulation of T3S is in some way linked and dependent on a functioning QS system. To explore this further, promoter fusions were used to see if IscR directly regulates the expression of QS genes. At 22ºC expression of *ypsR* and *ytbR* was reduced in the *iscR* mutant, and *ytbR* was also reduced at 37ºC. No change in expression of either AHL synthase was identified. These results indicate that IscR positively regulates both QS systems in *Y. pseudotuberculosis*, via direct regulation of the response regulator genes.

With complex systems there are often reciprocal regulatory relationships, and it would have been good to see if LcrF, YmoA or any QS genes regulate the expression of IscR. To this aim, promoter-fusions of the *iscR* promoter were designed and constructed however this strategy could not be completed. Difficulties arose due to the large size of the *luxCDABA* operon, when attempting to ligate to such a small promoter, and ligation and transformation efficiency was very low. A possible work around for this in the future could be switching to a nano-lux strategy, which is a smaller modified *lux* system. Additionally, other reporter genes could be considered, such as fluorescent proteins like GFP.

5 Overall Conclusions

A protein once believed to be exclusively involved in Fe-S biogenesis, IscR is now receieving greater attention as a global regulator of gene expression in many bacteria. Recently, IscR has been linked to virulence and T3S in *Yersinia* pseudotuberculosis (Miller *et al*., 2014) and this study set out to expland on this knowledge, characterising the role of IscR in *Yersinia.*

IscR was confirmed to regulate secretion of Yops in *Y. pseudotuberculosis*, and promoter:*lux* fusions provided evidence that this regulation may be multifaceted, through direct action on both identified *lcrF* promoters, with IscR capable of either activating or inhibiting expression of LcrF. This may be based on the Fe-S status of IscR, allowing environmental conditions such as iron concentration to influence the regulation of T3S *via* IscR.

As QS is also a regulator of T3S, with decreased Yop secretion seen in AHL synthases and response regulator mutants (Atkinson *et al*., 2011), whether QS is involved in how IscR regulates T3S was also explored. Phenotypic analysis found that the IscR associated Yop secretion defect was dependent on the presence of QS response regulator genes. Additionally, promoter:*lux* fusions showed that IscR positively regulates the expression of both response regulators. Together this suggests that IscR regulation of T3S is QS system dependent, specifically *via* direct regulation of *ypsR* and *ytbR*.

QS-mediated phenotypes identified so far in *Yersinia* include T3S, swimming motility, aggregation and biofilm formation on *C. elegans* and glass (Atkinson *et al*., 2008; 2011; Wiechmann, 2015; Barratt, 2018). At 22ºC swimming motility is activated as the flagellar master regulon *flhDC* is activated and the sigma factor *fliA* is downregulated by QS (Atkinson *et al*., 2008). Additionally, biofilm formation on *C. elegans* is promoted by FlhDC and QS, and is inhibited by assembly of the T3S system in environmental conditions in an AHL synthase mutant. This suggests a link between T3S and biofilm formation *via* QS. Together, it is clear that QS related phenotypes form a complex and inter-dependent

regulatory network. After a link between IscR, T3S and QS was identified, this study aimed to investigate the place of IscR in this network.

IscR was implicated in non-YadA dependent auto-aggregation in *Y. pseudotuberculosis*, as aggregation was reduced in this mutant. This was first hypothesised to be solely because of the reduction in secreted Yops as observed in previous T3S mutants (Barratt, 2018). However, triple mutants of *iscR* in QS backgrounds showed that the aggregation levels did not correlate with the levels of Yops secreted in these strains, suggesting a regulatory role for IscR in auto-aggregation separate from both T3S and QS.

The biofilm phenotype of *iscR* mutants proved to be interesting and varied depending on the model used. On *C. elegans*, IscR did not affect the levels or distribution of biofilm produced in *Y. pseudotuberculosis* or *Y. pestis*. However, on abiotic models at 22^{o}C IscR appeared to reduce biofilm levels significantly from that of the parent, and this was independent of the QS mediated reduction in biofilm levels. To offer a different approach, and with the aim of furthering research into transmission of *Y. pestis* by insect vectors, this study further developed a model for feeding and infection of *P. corporis*, with steps taken to optimise the imaging process to analyse biofilm levels. Preliminary data suggests that the *iscR* mutant is much more virulent to human body lice, though whether this is due to increased biofilm colonisation of the gut or additional factors remains to be determined. Though it was not achieved in time for this study, this model is now ready to be used with *Y. pestis* under CL3 conditions, and offers an exciting new approach to researching *Y. pestis* biofilms and transmission.

The decision to work with a fully virulent strain of *Y. pestis* posed many challenges throughout this project. Limitations on working hours and laboratory access, along with additional safety measures adding significant time onto otherwise simple assays, meant that time was always limited. There was also the added complications of GMO licences, which limited the amount and type of cloning that could be achieved. Protocols had to be

constantly redesigned and approved to make appropriate for CL3 work, and this took up a lot of time during this study. Whilst the body of this work focuses on *Y. pseudotuberculosis*, this has laid the ground work for taking these assays into *Y. pestis*. Preliminary data looking at T3S associated growth arrest suggests a role for IscR in T3S in *Y. pestis*, and with the protocols in place to remove pPst this can be soon studied. Despite these difficulties, the decision to work with all three plasmids offers the most biologically relevant results, particularly as the presence of pCD1 and the T3S system and effectors is so crucial to this study. Working with an attenuated strain lacking this plasmid would be far easier and quicker, but it would be difficult to gain a complete picture of IscR and translate any results into an active model of infection or transmission.

Despite the issues encountered during this project the results so far have cemented the role of IscR as a novel member of the regulatory network associated with virulence in *Yersinia*. A summary of the network so far, along with pathways yet to be determined, is shown in Figure 5.1.

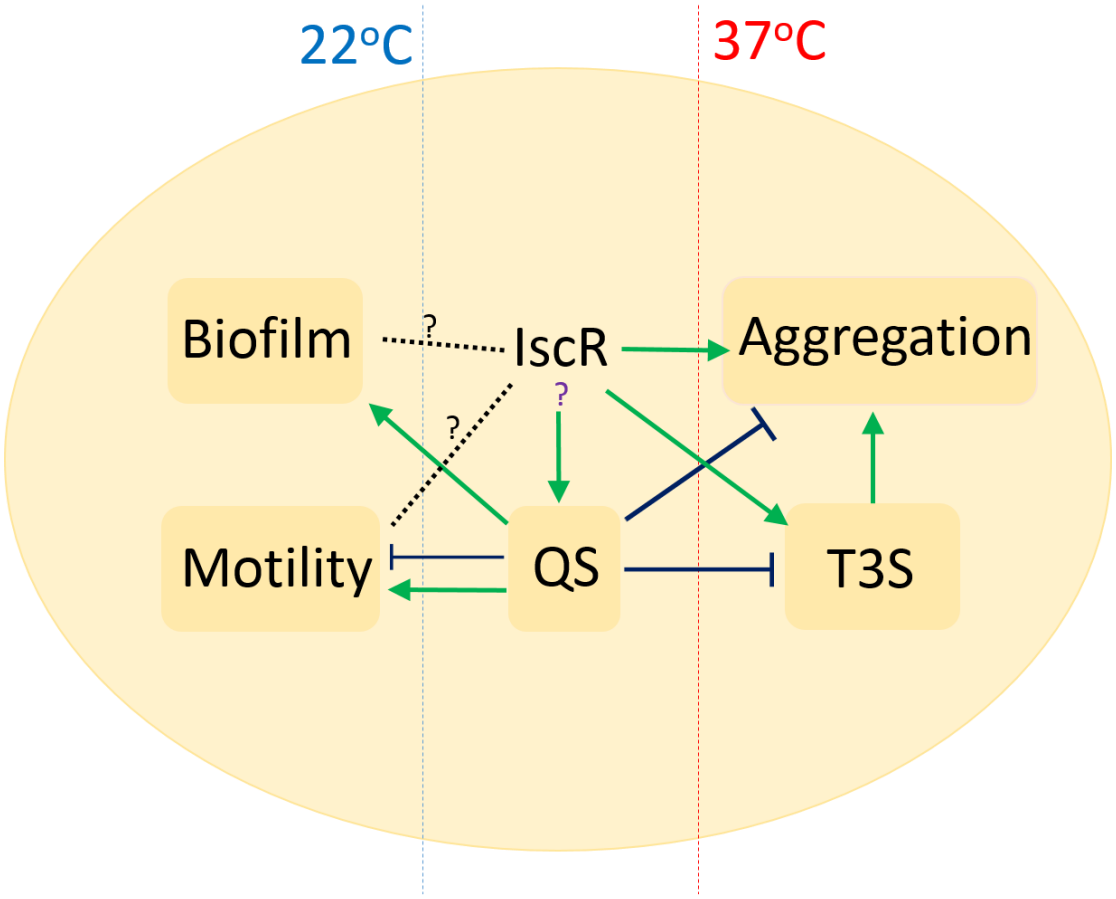

Figure 5.1 Regulation of phenotypes by IscR and QS at 22°C and 37°C.

IscR activates T3S, aggregation and QS. It is not known whether the regulation of QS by IscR is reciprocal. Nor is it clear if IscR regulates biofilms or motility. QS negatively regulates T3S and aggregation and posively regulates biofilms, *via* motility.

6 References

Achtman, Mark, Giovanna Morelli, Peixuan Zhu, Thierry Wirth, Ines Diehl, Barica Kusecek, Amy J Vogler, et al. (2004). Microevolution and History of the Plague Bacillus, Yersinia Pestis. *Proceedings of the National Academy of Sciences of the United States of America* **101** (51): 17837–42.

Achtman, Mark, Kerstin Zurth, Giovanna Morelli, Gabriela Torrea, Annie Guiyoule, and Elisabeth Carniel. (1999). Yersinia Pestis, the Cause of Plague, Is a Recently Emerged Clone of Yersinia Pseudotuberculosis. *Proceedings of the National Academy of Sciences of the United States of America* **96** (24): 14043–48.

Agrain, Céline, Isabelle Callebaut, Laure Journet, Isabel Sorg, Cécile Paroz, Luís Jaime Mota, and Guy R Cornelis. (2005). Characterization of a Type III Secretion Substrate Specificity Switch (T3S4) Domain in YscP from Yersinia Enterocolitica. *Molecular Microbiology* **56** (1): 54–67.

AM, Kolodziejek, Sinclair DJ, Seo KS, Schnider DR, Deobald CF, Rohde HN, Viall AK, et al. (2007). Phenotypic Characterization of OmpX, an Ail Homologue of Yersinia Pestis KIM. *Microbiology (Reading, England)* **153** (Pt 9).

Atkinson, Steve, Chien-Yi Chang, Hannah L Patrick, Catherine M F Buckley, Yao Wang, R Elizabeth Sockett, Miguel Cámara, and Paul Williams. (2008). Functional Interplay between the Yersinia Pseudotuberculosis YpsRI and YtbRI Quorum Sensing Systems Modulates Swimming Motility by Controlling Expression of FlhDC and FliA. *Molecular Microbiology* **69** (1): 137–51.

Atkinson, Steve, Chien-yi Chang, R Elizabeth Sockett, Miguel Cámara, Paul Williams, and Miguel Ca. (2006). Quorum Sensing in Yersinia Enterocolitica Controls Swimming and Swarming Motility Quorum Sensing in Yersinia Enterocolitica Controls Swimming and Swarming Motility. *Journal of Bacteriology* **188** (4): 1451–61.

Atkinson, Steve, Robert J. Goldstone, George W P Joshua, Chien Yi Chang, Hannah L. Patrick, Miguel C??mara, Brendan W. Wren, and Paul Williams. (2011). Biofilm Development on Caenorhabditis Elegans by Yersinia Is Facilitated by Quorum Sensing-Dependent Repression of Type III Secretion. *PLoS Pathogens* **7** (1).

Atkinson, Steve, John P Throup, G. S A B Stewart, and Paul Williams. (1999). A Hierarchical Quorum-Sensing System in Yersinia Pseudotuberculosis Is Involved in the Regulation of Motility and Clumping. *Molecular Microbiology* **33** (6): 1267–77.

Atkinson, Steve, and Paul Williams. (2009). Quorum Sensing and Social Networking in the Microbial World. *Journal of the Royal Society, Interface / the Royal Society* **6** (40): 959–78.

Atkinson, Steve, Paul Williams, Steve Atkinson, and Paul Williams. (2016). Yersinia Virulence Factors - a Sophisticated Arsenal for Combating Host Defences. *F1000Research* **5** (June):

1370.

Bacot, A W, and C J Martin. (1915). LXXXI. Further Notes on the Mechanism of the Transmission of Plague by Fleas. *Reports on Plague Investigations in India*, 423–39.

Balligand, G, Y Laroche, and G Cornelis. (1985). Genetic Analysis of Virulence Plasmid from a Serogroup 9 Yersinia Enterocolitica Strain: Role of Outer Membrane Protein P1 in Resistance to Human Serum and Autoagglutination. *Infection and Immunity* **48** (3): 782–86.

Barratt, Natalie Alice. (2018). The Type III Secretion System and Its Role in the Multicellular Behaviour of Yersinia Species, no. April.

Bartra, Sara Schesser, Katie L Styer, Deanna M O'Bryant, Matthew L Nilles, B Joseph Hinnebusch, Alejandro Aballay, and Gregory V Plano. (2008). Resistance of Yersinia Pestis to Complement-Dependent Killing Is Mediated by the Ail Outer Membrane Protein. *Infection and Immunity* **76** (2): 612–22.

Ben-Efraim, S, M Aronson, and L Bichowsky-Slomnicki. (1961). NEW ANTIGENIC COMPONENT OF PASTEURELLA PESTIS FORMED UNDER SPECIFIED CONDITIONS OF PH AND TEMPERATURE. *Journal of Bacteriology* **81** (5): 704–14.

Bercovier, Hervé, H. H. Mollaret, Jean Michel Alonso, J. Brault, G. Richard Fanning, Arnold G. Steigerwalt, and Don J. Brenner. (1980). Intra- and Interspecies Relatedness of Yersinia Pestis by DNA Hybridization and Its Relationship to Yersinia Pseudotuberculosis. *Current Microbiology* **4** (4): 225–29.

Bertani, G. (1951). Studies on Lysogenesis. I. The Mode of Phage Liberation by Lysogenic Escherichia Coli. *Journal of Bacteriology* **62** (3): 293–300.

Blaylock, Bill, Kelly E Riordan, Dominique M Missiakas, and Olaf Schneewind. (2006). Characterization of the Yersinia Enterocolitica Type III Secretion ATPase YscN and Its Regulator, YscL. *Journal of Bacteriology* **188** (10): 3525–34.

Bliska, James B, Xiaoying Wang, Gloria I Viboud, and Igor E Brodsky. (2013). Modulation of Innate Immune Responses by Yersinia Type III Secretion System Translocators and Effectors. *Cellular Microbiology*.

Bobrov, Alexander G, Scott W Bearden, Jacqueline D Fetherston, Arwa Abu Khweek, Kenneth D Parrish, and Robert D Perry. (2007). Functional Quorum Sensing Systems Affect Biofilm Formation and Protein Expression in Yersinia Pestis. *Advances in Experimental Medicine and Biology* **603**: 178–91.

Bobrov, Alexander G, Olga Kirillina, Stanislav Forman, Dietrich Mack, and Robert D Perry. (2008). Insights into Yersinia Pestis Biofilm Development: Topology and Co-Interaction of Hms Inner Membrane Proteins Involved in Exopolysaccharide Production. *Environmental Microbiology* **10**

(6): 1419–32.

Böhme, Katja, Rebekka Steinmann, Jens Kortmann, Stephanie Seekircher, Ann Kathrin Heroven, Evelin Berger, Fabio Pisano, Tanja Thiermann, et al. (2012). Concerted Actions of a Thermo-Labile Regulator and a Unique Intergenic RNA Thermosensor Control Yersinia Virulence. Edited by Ralph R. Isberg. *PLoS Pathogens* **8** (2): e1002518.

———. (2012). Concerted Actions of a Thermo-Labile Regulator and a Unique Intergenic RNA Thermosensor Control Yersinia Virulence. Edited by Ralph R. Isberg. *PLoS Pathogens* **8** (2): e1002518.

Bölin, I, A Forsberg, L Norlander, M Skurnik, and H Wolf-Watz. (1988). Identification and Mapping of the Temperature-Inducible, Plasmid-Encoded Proteins of Yersinia Spp. *Infection and Immunity* **56** (2): 343–48.

Bottone, Edward J. (1997). Yersinia Enterocolitica: The Charisma Continues. *Clinical Microbiology Reviews*. American Society for Microbiology (ASM).

Boyd, A. P., I. Lambermont, and G. R. Cornelis. (2000). Competition between the Yops of Yersinia Enterocolitica for Delivery into Eukaryotic Cells: Role of the SycE Chaperone Binding Domain of YopE. *Journal of Bacteriology* **182** (17): 4811–21.

Brannon, John R., David L. Burk, Jean Mathieu Leclerc, Jenny Lee Thomassin, Andrea Portt, Albert M. Berghuis, Samantha Gruenheid, and Hervé Le Moual. (2015). Inhibition of Outer Membrane Proteases of the Omptin Family by Aprotinin. *Infection and Immunity* **83** (6): 2300–2311.

Brubaker, R R. n.d. The Vwa+ Virulence Factor of Yersiniae: The Molecular Basis of the Attendant Nutritional Requirement for Ca++. *Reviews of Infectious Diseases* **5 Suppl 4**: S748-58.

Brubaker, Robert R. (1991). Factors Promoting Acute and Chronic Diseases Caused by Yersiniae. *CLINICAL MICROBIOLOGY REVIEWS* **4** (3): 309–24.

Burghout, P., F. Beckers, E. de Wit, R. van Boxtel, G. R. Cornelis, J. Tommassen, and M. Koster. (2004). Role of the Pilot Protein YscW in the Biogenesis of the YscC Secretin in Yersinia Enterocolitica. *Journal of Bacteriology* **186** (16): 5366–75.

Bzymek, Krzysztof P, Brent Y Hamaoka, and Partho Ghosh. (2012). Two Translation Products of Yersinia YscQ Assemble to Form a Complex Essential to Type III Secretion. *Biochemistry* **51** (8): 1669–77.

Carter, P B, R J Zahorchak, and R R Brubaker. (1980). Plague Virulence Antigens from Yersinia Enterocolitica. *Infection and Immunity* **28** (2): 638–40.

Cassat, James E, and Eric P Skaar. (2013). Iron in Infection and Immunity. *Cell Host & Microbe* **13** (5): 509–19.

Chen, Peter E, Christopher Cook, Andrew C Stewart, Niranjan Nagarajan, Dan D Sommer, Mihai Pop, Brendan Thomason, et al. (2010). Genomic Characterization of the Yersinia Genus. *Genome Biology* **11** (1): 1–18.

Chen, Shiyun, Karl M Thompson, and Matthew S Francis. (2016). Environmental Regulation of Yersinia Pathophysiology. *Frontiers in Cellular and Infection Microbiology* **6** (January): 25.

Chen, Xin, Stephan Schauder, Noelle Potier, Alain Van Dorsselaer, István Pelczer, Bonnie L. Bassler, and Frederick M. Hughson. (2002). Structural Identification of a Bacterial Quorum-Sensing Signal Containing Boron. *Nature* **415** (6871): 545–49.

Chhabra, Siri Ram, Bodo Philipp, Leo Eberl, Michael Givskov, Paul Williams, and Miguel Cámara. n.d. Extracellular Communication in Bacteria, 279–315.

Choi, Yongwook, Gregory E. Sims, Sean Murphy, Jason R. Miller, and Agnes P. Chan. (2012). Predicting the Functional Effect of Amino Acid Substitutions and Indels. Edited by Alexandre G. de Brevern. *PLoS ONE* **7** (10): e46688.

Clark, M Ann, Barry H Hirst, and Mark A Jepson. (1998). M-Cell Surface □1 Integrin Expression and Invasin-Mediated Targeting of Yersinia Pseudotuberculosis to Mouse Peyer's Patch M Cells. *INFECTION AND IMMUNITY* **66** (3): 1237–43.

Cohn, Samuel K. (2008). Epidemiology of the Black Death and Successive Waves of Plague. *Medical History. Supplement*, no. 27: 74–100.

Cornelis, G R. (1993). Role of the Transcription Activator VirF and the Histone-like Protein YmoA in the Thermoregulation of Virulence Functions in Yersiniae. *Zentralblatt Fur Bakteriologie : International Journal of Medical Microbiology* **278** (2–3): 149–64.

Cornelis, G R, T Biot, C Lambert de Rouvroit, T Michiels, B Mulder, C Sluiters, M P Sory, M Van Bouchaute, and J C Vanooteghem. (1989). The Yersinia Yop Regulon. *Molecular Microbiology* **3** (10): 1455–59.

Cornelis, G R, A Boland, a P Boyd, C Geuijen, M Iriarte, C Neyt, M P Sory, and I Stainier. (1998). The Virulence Plasmid of Yersinia, an Antihost Genome. *Microbiology and Molecular Biology Reviews : MMBR* **62** (4): 1315–52.

Cornelis, G R, C Sluiters, I Delor, D Geib, K Kaniga, C Lambert de Rouvroit, M P Sory, J C Vanooteghem, and T Michiels. (1991). YmoA, a Yersinia Enterocolitica Chromosomal Gene Modulating the Expression of Virulence Functions. *Molecular Microbiology* **5** (5): 1023–34.

Cornelis, G R, and H Wolf-Watz. (1997). The Yersinia Yop Virulon: A Bacterial System for Subverting Eukaryotic Cells. *Molecular Microbiology* **23** (5): 861–67.

Cornelis, Guy R. (2006). The Type III Secretion Injectisome. *Nature Reviews. Microbiology* **4** (11):

811–25.

Costerton, J W, Z Lewandowski, D E Caldwell, D R Korber, and H M Lappin-Scott. (1995). Microbial Biofilms. *Annual Review of Microbiology* **49**: 711–45.

Costerton, J W, P S Stewart, and E P Greenberg. (1999). Bacterial Biofilms: A Common Cause of Persistent Infections. *Science (New York, N.Y.)* **284** (5418): 1318–22.

Crook, Larry D., and Bruce Tempest. (1992). Plague: A Clinical Review of 27 Cases. *Archives of Internal Medicine* **152** (6): 1253–56.

Darby, Creg. (2008). Uniquely Insidious: Yersinia Pestis Biofilms. *Trends in Microbiology* **16** (4): 158–64.

Darby, Creg, Jennifer W. Hsu, Nafisa Ghori, and Stanley Falkow. (2002). Caenorhabditis Elegans: Plague Bacteria Biofilm Blocks Food Intake. *Nature* **417** (6886): 243–44.

DEGEN, J. L., T. H. BUGGE, and J. D. GOGUEN. (2007). Fibrin and Fibrinolysis in Infection and Host Defense. *Journal of Thrombosis and Haemostasis* **5** (s1): 24–31.

Deng, Wen, Valerie Burland, Guy Plunkett, Adam Boutin, George F. Mayhew, Paul Liss, Nicole T. Perna, et al. (2002). Genome Sequence of Yersinia Pestis KIM. *Journal of Bacteriology* **184** (16): 4601–11.

Dewoody, Rebecca S, Peter M Merritt, and Melanie M Marketon. (2013). Regulation of the Yersinia Type III Secretion System: Traffic Control. *Frontiers in Cellular and Infection Microbiology* **3** (February): 4.

Diepold, Andreas, Ulrich Wiesand, and Guy R Cornelis. (2011). The Assembly of the Export Apparatus (YscR,S,T,U,V) of the Yersinia Type III Secretion Apparatus Occurs Independently of Other Structural Components and Involves the Formation of an YscV Oligomer. *Molecular Microbiology* **82** (2): 502–14.

Doll, J M, P S Zeitz, P Ettestad, A L Bucholtz, T Davis, and K Gage. (1994). Cat-Transmitted Fatal Pneumonic Plague in a Person Who Traveled from Colorado to Arizona. *The American Journal of Tropical Medicine and Hygiene* **51** (1): 109–14.

Drali, Rezak, Jean Christophe Shako, Bernard Davoust, Georges Diatta, and Didier Raoult. (2015). A New Clade of African Body and Head Lice Infected by Bartonella Quintana and Yersinia Pestis-Democratic Republic of the Congo. *American Journal of Tropical Medicine and Hygiene* **93** (5): 990–93.

Du, Yidong, Roland Rosqvist, and Ake Forsberg. (2002). Role of Fraction 1 Antigen of Yersinia Pestis in Inhibition of Phagocytosis. *Infection and Immunity* **70** (3): 1453–60.

Eisen, Rebecca J., and Kenneth L. Gage. (2009). Adaptive Strategies of *Yersinia Pestis* to Persist

during Inter-Epizootic and Epizootic Periods. *Veterinary Research* **40** (2): 01.

Elton, Linzy. (2018). The Role of NagC in Yersinia Pestis and Yersinia Pseudotuberculosis Biofilm Development and Insect Transmission, no. September.

Epstein, H, and D Shakes. (1995). Caenorhabditis Elegans: Modern Biologcal Analysis of an Organism. *Methods in Cell Biology* **48**: 395–436.

Fällman, M., C. Persson, K. Schesser, and H. Wolf-Watz. (1998). Bidirectional Signaling between Yersinia and Its Target Cell. *Folia Microbiologica* **43** (3): 263–73.

Felek, Suleyman, and Eric S Krukonis. (2009). The Yersinia Pestis Ail Protein Mediates Binding and Yop Delivery to Host Cells Required for Plague Virulence. *Infection and Immunity* **77** (2): 825–36.

Felek, Suleyman, Tiffany M. Tsang, and Eric S. Krukonis. (2010). Three Yersinia Pestis Adhesins Facilitate Yop Delivery to Eukaryotic Cells and Contribute to Plague Virulence. *Infection and Immunity* **78** (10): 4134–50.

Ferber, D. M., and R. R. Brubaker. (1981). Plasmids in Yersinia Pestis. *Infection and Immunity* **31** (2): 839–41.

Ferber, D M, and R R Brubaker. (1979). Mode of Action of Pesticin: N-Acetylglucosaminidase Activity. *Journal of Bacteriology* **139** (2): 495–501.

Fields, K A, M L Nilles, C Cowan, and S C Straley. (1999). Virulence Role of V Antigen of Yersinia Pestis at the Bacterial Surface. *Infection and Immunity* **67** (10): 5395–5408.

Finegold, M. J., J. J. Petery, R. F. Berendt, and H. R. Adams. (1968). Studies on the Pathogenesis of Plague. Blood Coagulation and Tissue Responses of Macaca Mulatta Following Exposure to Aerosols of Pasteurella Pestis. *American Journal of Pathology* **53** (1): 99–114.

Flemming, Hans Curt, and Jost Wingender. (2010). The Biofilm Matrix. *Nature Reviews Microbiology*. Nat Rev Microbiol.

Forman, Stanislav, James T Paulley, Jacqueline D Fetherston, Yi-Qiang Cheng, and Robert D Perry. (2010). Yersinia Ironomics: Comparison of Iron Transporters among Yersinia Pestis Biotypes and Its Nearest Neighbor, Yersinia Pseudotuberculosis. *Biometals : An International Journal on the Role of Metal Ions in Biology, Biochemistry, and Medicine* **23** (2): 275–94.

Galindo, Cristi L., Jason A. Rosenzweig, Michelle L. Kirtley, Ashok K. Chopra, Cristi L. Galindo, Jason A. Rosenzweig, Michelle L. Kirtley, and Ashok K. Chopra. (2011). Pathogenesis of Y. Enterocolitica and Y. Pseudotuberculosis in Human Yersiniosis. *Journal of Pathogens* **2011**: 1–16.

Gelhaus, H. Carl, David A. Rozak, William C. Nierman, Dan Chen, John J. Varga, Mojgan Zadeh,

Ricky L. Ulrich, Jeffrey J. Adamovicz, and Jeffrey J Adamovicz. (2009). Exogenous Yersinia Pestis Quorum Sensing Molecules N-Octanoyl-Homoserine Lactone and N-(3-Oxooctanoyl)-Homoserine Lactone Regulate the LcrV Virulence Factor. *Microbial Pathogenesis* **46** (5): 283–87.

Gemski, P, Janet R Lazere, T Casey, and J A Wohlhieter '. (1980). Presence of a Virulence-Associated Plasmid in Yersinia Pseudotuberculosis. *INFECTION AND IMMUNITY* **28** (3): 1044–47.

Giel, Jennifer L., Dmitry Rodionov, Mingzhu Liu, Frederick R. Blattner, and Patricia J. Kiley. (2006a). IscR-Dependent Gene Expression Links Iron-Sulphur Cluster Assembly to the Control of O2-Regulated Genes in Escherichia Coli. *Molecular Microbiology* **60** (4): 1058–75.

———. (2006b). IscR-Dependent Gene Expression Links Iron-Sulphur Cluster Assembly to the Control of O2-Regulated Genes in Escherichia Coli. *Molecular Microbiology* **60** (4): 1058–75.

Gijsegem, F Van, C Gough, C Zischek, E Niqueux, M Arlat, S Genin, P Barberis, S German, P Castello, and C Boucher. (1995). The Hrp Gene Locus of Pseudomonas Solanacearum, Which Controls the Production of a Type III Secretion System, Encodes Eight Proteins Related to Components of the Bacterial Flagellar Biogenesis Complex. *Molecular Microbiology* **15** (6): 1095–1114.

Gil, Rosario, and Amparo Latorre. (2012). Factors behind Junk DNA in Bacteria. *Genes*. Multidisciplinary Digital Publishing Institute (MDPI).

Goldstone, Robert J. (2012). Investigating the Relationship between Quorum Sensing, Motility, and the Type 3 Secretion System of Yersinia Pseudotuberculosis, no. September.

Gophna, Uri, Eliora Z Ron, and Dan Graur. (2003). Bacterial Type III Secretion Systems Are Ancient and Evolved by Multiple Horizontal-Transfer Events. *Gene* **312** (July): 151–63.

Goure, Julien, Alexandrine Pastor, Eric Faudry, Jacqueline Chabert, Andréa Dessen, and Ina Attree. (2004). The V Antigen of Pseudomonas Aeruginosa Is Required for Assembly of the Functional PopB/PopD Translocation Pore in Host Cell Membranes. *Infection and Immunity* **72** (8): 4741–50.

Grutzkau, A, C Hanski, H Hahn, and E 0 Riecken. (1990). Involvement of M Cells in the Bacterial Invasion of Peyer's Patches: A Common Mechanism Shared by Yersinia Enterocolitica and Other Enteroinvasive Bacteria. *Gut* **31**: 1011–15.

Hall, David H. (1995). Electron Microscopy and Three-Dimensional Image Reconstruction. *Methods in Cell Biology* **48** (C): 395–436.

Hinnebusch, B. Joseph. (1997). Bubonic Plague: A Molecular Genetic Case History of the Emergence of an Infectious Disease. *Journal of Molecular Medicine*.

Hinnebusch, B J, and D L Erickson. (2008). Yersinia Pestis Biofilm in the Flea Vector and Its Role in the Transmission of Plague. *Current Topics in Microbiology and Immunology* **322**: 229–48.

Hinnebusch, B J, E R Fischer, and T G Schwan. (1998). Evaluation of the Role of the Yersinia Pestis Plasminogen Activator and Other Plasmid-Encoded Factors in Temperature-Dependent Blockage of the Flea. *The Journal of Infectious Diseases* **178** (5): 1406–15.

Hinnebusch, B J, R D Perry, T G Schwan, A.W. BACOT, A.W. BACOT, V.A. BIBIKOVA, P.T. BREY, et al. (1996). Role of the Yersinia Pestis Hemin Storage (Hms) Locus in the Transmission of Plague by Fleas. *Science (New York, N.Y.)* **273** (5273): 367–70.

Hinnebusch, B Joseph, Amy E Rudolph, Peter Cherepanov, Jack E Dixon, Tom G Schwan, Ake Forsberg, R. R. Brubaker, et al. (2002). Role of Yersinia Murine Toxin in Survival of Yersinia Pestis in the Midgut of the Flea Vector. *Science (New York, N.Y.)* **296** (5568): 733–35.

Hoang, T T, R R Karkhoff-Schweizer, A J Kutchma, and H P Schweizer. (1998). A Broad-Host-Range Flp-FRT Recombination System for Site-Specific Excision of Chromosomally-Located DNA Sequences: Application for Isolation of Unmarked Pseudomonas Aeruginosa Mutants. *Gene* **212** (1): 77–86.

Hobman, Jon L, and Lisa C Crossman. (2015). Bacterial Antimicrobial Metal Ion Resistance. *Journal of Medical Microbiology* **64** (Pt 5): 471–97.

Hoe, Nancy P, and Jon D Goguen. (1993). Temperature Sensing in Yersinia Pestis: Translation of the LcrF Activator Protein Is Thermally Regulated. *Journal of Bacteriology* **175** (24): 7901–9.

Hoiczyk, E, and G Blobel. (2001). Polymerization of a Single Protein of the Pathogen Yersinia Enterocolitica into Needles Punctures Eukaryotic Cells. *Proceedings of the National Academy of Sciences of the United States of America* **98** (8): 4669–74.

Hornung, J M, H A Jones, and R D Perry. (1996). The Hmu Locus of Yersinia Pestis Is Essential for Utilization of Free Haemin and Haem--Protein Complexes as Iron Sources. *Molecular Microbiology* **20** (4): 725–39.

Houhamdi, Linda, Pierre-Edouard Fournier, Rong Fang, Hubert Lepidi, and Didier Raoult. (2002). An Experimental Model of Human Body Louse Infection with Rickettsia Prowazekii . *The Journal of Infectious Diseases* **186** (11): 1639–46.

Houhamdi, Linda, Hubert Lepidi, Michel Drancourt, and Didier Raoult. (2006). Experimental Model to Evaluate the Human Body Louse as a Vector of Plague. *The Journal of Infectious Diseases* **194** (11): 1589–96.

Houppert, Andrew S, Elizabeth Kwiatkowski, Elizabeth M Glass, Kristin L DeBord, Peter M Merritt, Olaf Schneewind, and Melanie M Marketon. (2012). Identification of Chromosomal Genes in Yersinia Pestis That Influence Type III Secretion and Delivery of Yops into Target Cells. *PloS*

One **7** (3): e34039.

Hu, P C, and R R Brubaker. (1974). Characterization of Pesticin. Separation of Antibacterial Activities. *The Journal of Biological Chemistry* **249** (15): 4749–53.

Huang, Xiao-Zhe, and Luther E Lindler. (2004). The PH 6 Antigen Is an Antiphagocytic Factor Produced by Yersinia Pestis Independent of Yersinia Outer Proteins and Capsule Antigen. *Infection and Immunity* **72** (12): 7212–19.

Ibrahim, A., B M Goebel, W. Liesack, M. Griffiths, and E. Stackebrandt. (1993). The Phylogeny of the Genus Yersinia Based on 16S RDNA Sequences. *FEMS Microbiol.Lett.* **114** (0378-1097 (Print) LA-eng PT-Journal Article RN-0 (RNA, Bacterial) RN-0 (RNA, Ribosomal, 16S) SB-IM): 173–77.

Inglesby, Thomas V., David T. Dennis, Donald A. Henderson, John G. Bartlett, Michael S. Ascher, Edward Eitzen, Anne D. Fine, et al. (2000). Plague as a Biological Weapon. *JAMA* **283** (17): 2281.

Isherwood, Karen Elizabeth. n.d. Quorum Sensing in Yersinia Pestis.

Istivan, Taghrid S, and Peter J Coloe. n.d. Phospholipase A in Gram-Negative Bacteria and Its Role in Pathogenesis.

Jackson, Michael W, Eugenia Silva-Herzog, and Gregory V Plano. (2004). The ATP-Dependent ClpXP and Lon Proteases Regulate Expression of the Yersinia Pestis Type III Secretion System via Regulated Proteolysis of YmoA, a Small Histone-like Protein. *Molecular Microbiology* **54** (5): 1364–78.

Jaroschinsky, Monique, Constanze Pinske, and R. Gary Sawers. (2017). Differential Effects of Isc Operon Mutations on the Biosynthesis and Activity of Key Anaerobic Metalloenzymes in Escherichia Coli. *Microbiology (United Kingdom)* **163** (6): 878–90.

Joshua, G. W.P., C. Guthrie-Irons, A. V. Karlyshev, and Brendan W. Wren. (2006). Biofilm Formation in Campylobacter Jejuni. *Microbiology* **152** (2): 387–96.

Joshua, G W P, A V Karlyshev, M P Smith, K E Isherwood, R W Titball, and B W Wren. (2003). A Caenorhabditis Elegans Model of Yersinia Infection: Biofilm Formation on a Biotic Surface. *Microbiology (Reading, England)* **149** (Pt 11): 3221–29.

Journet, Laure, Céline Agrain, Petr Broz, and Guy R Cornelis. (2003). The Needle Length of Bacterial Injectisomes Is Determined by a Molecular Ruler. *Science (New York, N.Y.)* **302** (5651): 1757–60.

Ke, Yuehua, Zeliang Chen, and Ruifu Yang. (2013). Yersinia Pestis: Mechanisms of Entry into and Resistance to the Host Cell. *Frontiers in Cellular and Infection Microbiology* **3**: 106.

KIENLE, Z., L. EMODY, C. SVANBORG, and P. W. O'TOOLE. (1992). Adhesive Properties Conferred by the Plasminogen Activator of Yersinia Pestis. *Journal of General Microbiology* **138** (8): 1679–87.

Kim, Seol-Hee, Bo-Young Lee, Gee W Lau, and You-Hee Cho. (2009). IscR Modulates Catalase A (KatA) Activity, Peroxide Resistance and Full Virulence of Pseudomonas Aeruginosa PA14. *Journal of Microbiology and Biotechnology* **19** (12): 1520–26.

King, Jessica M, Sara Schesser Bartra, Gregory Plano, and Timothy L Yahr. (2013). ExsA and LcrF Recognize Similar Consensus Binding Sites, but Differences in Their Oligomeric State Influence Interactions with Promoter DNA. *Journal of Bacteriology* **195** (24): 5639–50.

Kirwan, J Paul, Ty A Gould, Herbert P Schweizer, Scott W Bearden, Robert C Murphy, and Mair E A Churchill. (2006). Quorum-Sensing Signal Synthesis by the Yersinia Pestis Acyl-Homoserine Lactone Synthase YspI. *Journal of Bacteriology* **188** (2): 784–88.

Koornhof, H. J., R. A. Smego, and M Nicol. (1999). Yersiniosis II: The Pathogenesis of Yersinia Infections. *European Journal of Clinical Microbiology and Infectious Diseases*.

Koster, M, W Bitter, H de Cock, A Allaoui, G R Cornelis, and J Tommassen. (1997). The Outer Membrane Component, YscC, of the Yop Secretion Machinery of Yersinia Enterocolitica Forms a Ring-Shaped Multimeric Complex. *Molecular Microbiology* **26** (4): 789–97.

Kugeler, Kiersten J, J Erin Staples, Alison F Hinckley, Kenneth L Gage, and Paul S Mead. (2015). Epidemiology of Human Plague in the United States, 1900-2012. *Emerging Infectious Diseases* **21** (1): 16–22.

Lähteenmäki, Kaarina, Maini Kukkonen, and Timo K Korhonen. (2001). The Pla Surface Protease/Adhesin of *Yersinia Pestis* Mediates Bacterial Invasion into Human Endothelial Cells. *FEBS Letters* **504** (1–2): 69–72.

Laird, W. J., and D. C. Cavanaugh. (1980). Correlation of Autoagglutination and Virulence of Yersiniae. *Journal of Clinical Microbiology* **11** (4): 430–32.

Lamont, Iain L., Paul A. Beare, Urs Ochsner, Adriana I. Vasil, and Michael L. Vasil. (2002). Siderophore-Mediated Signaling Regulates Virulence Factor Production in Pseudomonas Aeruginosa. *Proceedings of the National Academy of Sciences of the United States of America* **99** (10): 7072–77.

Laroche, Y., M. van Bouchaute, and G. Cornelis. (1984). A Restriction Map of Virulence Plasmid PVYE439-80 from a Serogroup 9 Yersinia Enterocolitica Strain. *Plasmid* **12** (1): 67–70.

Lavander, Moa, Solveig K Ericsson, Jeanette E Bröms, and Ake Forsberg. (2006). The Twin Arginine Translocation System Is Essential for Virulence of Yersinia Pseudotuberculosis. *Infection and Immunity* **74** (3): 1768–76.

Lee, Wei Lin, Jonathan M Grimes, and Robert C Robinson. (2015). Yersinia Effector YopO Uses Actin as Bait to Phosphorylate Proteins That Regulate Actin Polymerization. *Nature Structural & Molecular Biology* **22** (3): 248–55.

Lennox, E S. (1955). Transduction of Linked Genetic Characters of the Host by Bacteriophage P1. *Virology* **1** (2): 190–206.

Lim, Jong Gyu, and Sang Ho Choi. (2014). IscR Is a Global Regulator Essential for Pathogenesis of Vibrio Vulnificus and Induced by Host Cells. *Infection and Immunity* **82** (2): 569–78.

Lindler, L E, and B D Tall. (1993). Yersinia Pestis PH 6 Antigen Forms Fimbriae and Is Induced by Intracellular Association with Macrophages. *Molecular Microbiology* **8** (2): 311–24.

Louden, Brian C., Daniel Haarmann, and Aaron Lynne. (2011). Use of Blue Agar CAS Assay for Siderophore Detection. *Journal of Microbiology & Biology Education* **12** (1): 51–53.

MacNab, R. M. (1996). *Flagella and Motility. In Escherichia Coli and Salmonella Typhimurium.*

Makoveichuk, Elena, Peter Cherepanov, Susanne Lundberg, Ake Forsberg, and Gunilla Olivecrona. (2003). PH6 Antigen of Yersinia Pestis Interacts with Plasma Lipoproteins and Cell Membranes. *Journal of Lipid Research* **44** (2): 320–30.

Martínez-Chavarría, Luary C., and Viveka Vadyvaloo. (2015). Yersinia Pestis and Yersinia Pseudotuberculosis Infection: A Regulatory RNA Perspective. *Frontiers in Microbiology*. Frontiers Media S.A.

Matz, Carsten, and Staffan Kjelleberg. (2005). Off the Hook - How Bacteria Survive Protozoan Grazing. *Trends in Microbiology* **13** (7): 302–7.

McDonald, Christine, Panayiotis O Vacratsis, James B Bliska, and Jack E Dixon. (2003). The Yersinia Virulence Factor YopM Forms a Novel Protein Complex with Two Cellular Kinases. *The Journal of Biological Chemistry* **278** (20): 18514–23.

Mehigh, Richard J., Allen K. Sample, and Robert R. Brubaker. (1989). Expression of the Low Calcium Response in Yersinia Pestis. *Microbial Pathogenesis* **6** (3): 203–17.

Meighen, E A. (1991). Molecular Biology of Bacterial Bioluminescence. *Microbiological Reviews* **55** (1): 123–42.

Miethke, Marcus, and Mohamed A. Marahiel. (2007). Siderophore-Based Iron Acquisition and Pathogen Control. *Microbiology and Molecular Biology Reviews* **71** (3): 413–51.

Miller, Halie K., Laura Kwuan, Leah Schwiesow, David L. Bernick, Erin Mettert, Hector A. Ramirez, James M. Ragle, et al. (2014). IscR Is Essential for Yersinia Pseudotuberculosis Type III Secretion and Virulence. *PLoS Pathogens* **10** (6).

Miller, V L, K B Beer, G Heusipp, B M Young, and M R Wachtel. (2001). Identification of Regions of Ail Required for the Invasion and Serum Resistance Phenotypes. *Molecular Microbiology* **41** (5): 1053–62.

Miller, V L, J B Bliska, and S Falkow. (1990). Nucleotide Sequence of the Yersinia Enterocolitica Ail Gene and Characterization of the Ail Protein Product. *Journal of Bacteriology* **172** (2): 1062–69.

Miller, V L, and S Falkow. (1988). Evidence for Two Genetic Loci in Yersinia Enterocolitica That Can Promote Invasion of Epithelial Cells. *Infection and Immunity* **56** (5): 1242–48.

Milton, D L, R O'Toole, P Horstedt, and H Wolf-Watz. (1996). Flagellin A Is Essential for the Virulence of Vibrio Anguillarum. *Journal of Bacteriology* **178** (5): 1310–19.

Mueller, C. A., P. Broz, and G. R. Cornelis. (2008). The Type III Secretion System Tip Complex and Translocon. *Molecular Microbiology*. Blackwell Publishing Ltd.

Mueller, Catherine A, Petr Broz, Shirley A Müller, Philippe Ringler, Françoise Erne-Brand, Isabel Sorg, Marina Kuhn, Andreas Engel, and Guy R Cornelis. (2005). The V-Antigen of Yersinia Forms a Distinct Structure at the Tip of Injectisome Needles. *Science (New York, N.Y.)* **310** (5748): 674–76.

Mühlenkamp, Melanie, Philipp Oberhettinger, Jack C Leo, Dirk Linke, and Monika S Schütz. (2015). Yersinia Adhesin A (YadA) – Beauty & Beast. *International Journal of Medical Microbiology* **305**: 252–58.

Ni, B., Z. Du, Z. Guo, Y. Zhang, and R. Yang. (2008). Curing of Four Different Plasmids in *Yersinia Pestis* Using Plasmid Incompatibility. *Letters in Applied Microbiology* **47** (4): 235–40.

Nishimura, A, M Morita, Y Nishimura, and Y Sugino. (1990). A Rapid and Highly Efficient Method for Preparation of Competent Escherichia Coli Cells. *Nucleic Acids Research* **18** (20): 6169.

Norrander, Jan, Tomas Kempe, and Joachim Messing. (1983). Construction of Improved M13 Vectors Using Oligodeoxynucleotide-Directed Mutagenesis. *Gene* **26** (1): 101–6.

Olson, Nathan D., Steven P. Lund, Rebecca E. Colman, Jeffrey T. Foster, Jason W. Sahl, James M. Schupp, Paul Keim, Jayne B. Morrow, Marc L. Salit, and Justin M. Zook. (2015). Best Practices for Evaluating Single Nucleotide Variant Calling Methods for Microbial Genomics. *Frontiers in Genetics*. Frontiers Media S.A.

Ono, Shusuke, Martin D Goldberg, Tjelvar Olsson, Diego Esposito, Jay C D Hinton, and John E Ladbury. (2005). H-NS Is a Part of a Thermally Controlled Mechanism for Bacterial Gene Regulation. *The Biochemical Journal* **391** (Pt 2): 203–13.

Orth, K, L E Palmer, Z Q Bao, S Stewart, A E Rudolph, J B Bliska, and J E Dixon. (1999). Inhibition

of the Mitogen-Activated Protein Kinase Kinase Superfamily by a Yersinia Effector. *Science (New York, N.Y.)* **285** (5435): 1920–23.

Ortori, Catharine A., Steve Atkinson, Siri Ram Chhabra, Miguel Cámara, Paul Williams, and David A. Barrett. (2007a). Comprehensive Profiling of N-Acylhomoserine Lactones Produced by Yersinia Pseudotuberculosis Using Liquid Chromatography Coupled to Hybrid Quadrupole–Linear Ion Trap Mass Spectrometry. *Analytical and Bioanalytical Chemistry* **387** (2): 497–511.

Ortori, Catharine A, Steve Atkinson, Siri Ram Chhabra, Miguel Cámara, Paul Williams, and David A Barrett. (2007b). Comprehensive Profiling of N-Acylhomoserine Lactones Produced by Yersinia Pseudotuberculosis Using Liquid Chromatography Coupled to Hybrid Quadrupole-Linear Ion Trap Mass Spectrometry. *Analytical and Bioanalytical Chemistry* **387** (2): 497–511.

Paerregaard, A., F. Espersen, and M. Skurnik. (1991). Role of the Yersinia Outer Membrane Protein YadA in Adhesion to Rabbit Intestinal Tissue and Rabbit Intestinal Brush Border Membrane Vesicles. *APMIS* **99** (3): 226–32.

Parkhill, J, B W Wren, N R Thomson, R W Titball, M T Holden, M B Prentice, M Sebaihia, et al. (2001). Genome Sequence of Yersinia Pestis, the Causative Agent of Plaque. *Nature* **413** (6855): 523–27.

Pawel-Rammingen, U Von, M V Telepnev, G Schmidt, K Aktories, H Wolf-Watz, and R Rosqvist. (2000). GAP Activity of the Yersinia YopE Cytotoxin Specifically Targets the Rho Pathway: A Mechanism for Disruption of Actin Microfilament Structure. *Molecular Microbiology* **36** (3): 737–48.

Payne, D, D Tatham, E D Williamson, and R W Titball. (1998). The PH 6 Antigen of Yersinia Pestis Binds to Beta1-Linked Galactosyl Residues in Glycosphingolipids. *Infection and Immunity* **66** (9): 4545–48.

Payne, P L, and S C Straley. (1999). YscP of Yersinia Pestis Is a Secreted Component of the Yop Secretion System. *Journal of Bacteriology* **181** (9): 2852–62.

Pearson, James P., Christian Van Delden, and Barbara H. Iglewski. (1999). Active Efflux and Diffusion Are Involved in Transport of Pseudomonas Aeruginosa Cell-to-Cell Signals. *Journal of Bacteriology* **181** (4): 1203–10.

Pechous, Roger D., Vijay Sivaraman, Nikolas M. Stasulli, and William E. Goldman. (2016). Pneumonic Plague: The Darker Side of Yersinia Pestis. *Trends in Microbiology*. Elsevier Ltd.

Pérez-Miranda, S., N. Cabirol, R. George-Téllez, L. S. Zamudio-Rivera, and F. J. Fernández. (2007). O-CAS, a Fast and Universal Method for Siderophore Detection. *Journal of Microbiological Methods* **70** (1): 127–31.

Perry, R. D., and J. D. Fetherston. (1997). Yersinia Pestis - Etiological Agent of Plague. *Clinical*

Microbiology Reviews **10**: 35–66.

Perry, Robert D, Ildefonso Mier, and Jacqueline D Fetherston. (2007). Roles of the Yfe and Feo Transporters of Yersinia Pestis in Iron Uptake and Intracellular Growth. *Biometals : An International Journal on the Role of Metal Ions in Biology, Biochemistry, and Medicine* **20** (3–4): 699–703.

Plumbridge, J. (1995). Co-Ordinated Regulation of Amino Sugar Biosynthesis and Degradation: The NagC Repressor Acts as Both an Activator and a Repressor for the Transcription of the GlmUS Operon and Requires Two Separated NagC Binding Sites. *The EMBO Journal* **14** (16): 3958–65.

Portnoy, D. A., and S. Falkow. (1981). Virulence-Associated Plasmids from Yersinia Enterocolitica and Yersinia Pestis. *Journal of Bacteriology* **148** (3): 877–83.

Portnoy, D. A., S. L. Moseley, and S. Falkow. (1981). Characterization of Plasmids and Plasmid-Associated Determinants of Yersinia Enterocolitica Pathogenesis. *Infection and Immunity* **31** (2): 775–82.

Rakin, A, E Boolgakowa, and J Heesemann. (1996). Structural and Functional Organization of the Yersinia Pestis Bacteriocin Pesticin Gene Cluster. *Microbiology (Reading, England)*, December, 3415–24.

Rakin, Alexander, Lukas Schneider, and Olga Podladchikova. (2012). Hunger for Iron: The Alternative Siderophore Iron Scavenging Systems in Highly Virulent Yersinia. *Frontiers in Cellular and Infection Microbiology* **2**: 151.

Rasch, Maria, Jens Bo Andersen, Kristian Fog Nielsen, Lars Ravn Flodgaard, Henrik Christensen, Michael Givskov, and Lone Gram. (2005). Involvement of Bacterial Quorum-Sensing Signals in Spoilage of Bean Sprouts. *Applied and Environmental Microbiology* **71** (6): 3321–30.

Riley, G, and S Toma. (1989). Detection of Pathogenic Yersinia Enterocolitica by Using Congo Red-Magnesium Oxalate Agar Medium. *Journal of Clinical Microbiology* **27** (1): 213–14.

Rodda, Stuart J. (1996). T-Cell Epitope Mapping with Synthetic Peptides and Peripheral Blood Mononuclear Cells. In *Epitope Mapping Protocols*, 66:363–72. New Jersey: Humana Press.

Romsang, Adisak, Jintana Duang-Nkern, Panithi Leesukon, Kritsakorn Saninjuk, Paiboon Vattanaviboon, and Skorn Mongkolsuk. (2014). The Iron-Sulphur Cluster Biosynthesis Regulator IscR Contributes to Iron Homeostasis and Resistance to Oxidants in Pseudomonas Aeruginosa. *PloS One* **9** (1): e86763.

Rosqvist, Roland, Mikael Skurnik, and Hans Wolf-Watz. (1988a). Increased Virulence of Yersinia Pseudotuberculosis by Two Independent Mutations. *Nature* **334** (6182): 522–25.

———. (1988b). Increased Virulence of Yersinia Pseudotuberculosis by Two Independent Mutations. *Nature* **334** (6182): 522–25.

Ross, Julia A, and Gregory V Plano. (2011). A C-Terminal Region of Yersinia Pestis YscD Binds the Outer Membrane Secretin YscC. *Journal of Bacteriology* **193** (9): 2276–89.

Rossi, M S, J D Fetherston, S Létoffé, E Carniel, R D Perry, and J M Ghigo. (2001). Identification and Characterization of the Hemophore-Dependent Heme Acquisition System of Yersinia Pestis. *Infection and Immunity* **69** (11): 6707–17.

Sample, Allen K., Janet M. Fowler, and Robert R. Brubaker. (1987a). Modulation of the Low-Calcium Response in Yersinia Pestis via Plasmid-Plasmid Interaction. *Microbial Pathogenesis* **2** (6): 443–53.

———. (1987b). Modulation of the Low-Calcium Response in Yersinia Pestis via Plasmid-Plasmid Interaction. *Microbial Pathogenesis* **2** (6): 443–53.

Santos, Joana A., Pedro José Barbosa Pereira, and Sandra Macedo-Ribeiro. (2015). What a Difference a Cluster Makes: The Multifaceted Roles of IscR in Gene Regulation and DNA Recognition. *Biochimica et Biophysica Acta - Proteins and Proteomics* **1854** (9): 1101–12.

SCHAR, M, and K F MEYER. (1956). Studies on Immunization against Plague. XV. The Pathophysiologic Action of the Toxin of Pasteurella Pestis in Experimental Animals. *Schweizerische Zeitschrift Für Pathologie Und Bakteriologie. Revue Suisse de Pathologie et de Bactériologie* **19** (1): 51–70.

Schmidt, Herbert, and Michael Hensel. (2004). Pathogenicity Islands in Bacterial Pathogenesis. *Clinical Microbiology Reviews* **17** (1): 14–56.

Schmiel, D H, E Wagar, L Karamanou, D Weeks, and V L Miller. (1998). Phospholipase A of Yersinia Enterocolitica Contributes to Pathogenesis in a Mouse Model. *Infection and Immunity* **66** (8): 3941–51.

Schwartz, C J, J L Giel, T Patschkowski, C Luther, F J Ruzicka, H Beinert, and P J Kiley. (2001). IscR, an Fe-S Cluster-Containing Transcription Factor, Represses Expression of Escherichia Coli Genes Encoding Fe-S Cluster Assembly Proteins. *Proceedings of the National Academy of Sciences of the United States of America* **98** (26): 14895–900.

Schwiesow, Leah, Hanh Lam, Petra Dersch, and Victoria Auerbuch. (2016). Yersinia Type III Secretion System Master Regulator LcrF. *Journal of Bacteriology*. American Society for Microbiology.

Schwiesow, Leah, Erin Mettert, Yahan Wei, Halie K. Miller, Natalia G. Herrera, David Balderas, Patricia J. Kiley, and Victoria Auerbuch. (2018). Control of Hmu Heme Uptake Genes in Yersinia Pseudotuberculosis in Response to Iron Sources. *Frontiers in Cellular and Infection*

Microbiology **8** (FEB): 47.

Schwyn, B, and J B Neilands. (1987). Universal Chemical Assay for the Detection and Determination of Siderophores. *Analytical Biochemistry* **160** (1): 47–56.

Shen, Richard, Jian-Bing Fan, Derek Campbell, Weihua Chang, Jing Chen, Dennis Doucet, Jo Yeakley, et al. (2005). High-Throughput SNP Genotyping on Universal Bead Arrays. *Mutation Research* **573** (1–2): 70–82.

Silva-Herzog, Eugenia, Franco Ferracci, Michael W Jackson, Sabrina S Joseph, and Gregory V Plano. (2008). Membrane Localization and Topology of the Yersinia Pestis YscJ Lipoprotein. *Microbiology (Reading, England)* **154** (Pt 2): 593–607.

Simon, R., U. Priefer, and A. Pühler. (1983). A Broad Host Range Mobilization System for In Vivo Genetic Engineering: Transposon Mutagenesis in Gram Negative Bacteria. *Bio/Technology* **1** (9): 784–91.

Skurnik, M, I Bölin, H Heikkinen, S Piha, and H Wolf-Watz. (1984). Virulence Plasmid-Associated Autoagglutination in Yersinia Spp. *Journal of Bacteriology* **158** (3): 1033.

Slater, Amy. (2017). Unraveling the Regulatory Relationship between Quorum Sensing and the Type III Secretion System in Yersinia Pseudotuberculosis. University of Nottingham.

Somprasong, N., T. Jittawuttipoka, J. Duang-nkern, A. Romsang, P. Chaiyen, H. P. Schweizer, P. Vattanaviboon, and S. Mongkolsuk. (2012). Pseudomonas Aeruginosa Thiol Peroxidase Protects against Hydrogen Peroxide Toxicity and Displays Atypical Patterns of Gene Regulation. *Journal of Bacteriology* **194** (15): 3904–12.

Stewart, G. S A B, S Libinsky-Mink, C G Jackson, A Cassel, and J Kuhn. (1986). PHG165: A PBR322 Copy Number Derivative of PUC8 for Cloning and Expression. *Plasmid* **15**: 172–81.

Straley, Susan C., Gregory V. Plano, Elźbieta Skrzypek, Pryce L. Haddix, and Kenneth A. Fields. (1993). Regulation by Ca^{2+} in the Yersinia Low-Ca^{2+} Response. *Molecular Microbiology* **8** (6): 1005–10.

Sun, Wei, David Six, Xiaoying Kuang, Kenneth L. Roland, Christian R.H. Raetz, and Roy Curtiss. (2011). A Live Attenuated Strain of Yersinia Pestis KIM as a Vaccine against Plague. *Vaccine* **29** (16): 2986–98.

Sun, Yi-Cheng, Alexandra Koumoutsi, and Creg Darby. (2009). The Response Regulator PhoP Negatively Regulates Yersinia Pseudotuberculosis and Yersinia Pestis Biofilms. *FEMS Microbiology Letters* **290** (1): 85–90.

Suomalainen, Marjo, Johanna Haiko, Maini Kukkonen, Timo K. Korhonen, Kaarina Lähteenmäki, Ritva Virkola, Benita Westerlund-Wikström, Leandro Lobo, and Päivi Ramu. (2007). Using

Every Trick in the Book: The Pla Surface Protease of Yersinia Pestis. In *Advances in Experimental Medicine and Biology*, 603:268–78. Springer New York.

Swift, S, Karen Elizabeth. Isherwood, Steve Atkinson, P.C Oystom, and G.S. Stewart. (1999). *Quorum Sensing in Aeromonas and Yersinia*. *Microbial Signalling and Communication Cambridge University Press*.

Tan, Li, and Creg Darby. (2004). A Movable Surface: Formation of Yersinia Sp. Biofilms on Motile Caenorhabditis Elegans. *Journal of Bacteriology* **186** (15): 5087–92.

Troisfontaines, Paul, and Guy R Cornelis. (2005). Type III Secretion: More Systems than You Think. *Physiology (Bethesda, Md.)* **20**: 326–39.

Trosky, Jennifer E., Amy D B Liverman, and Kim Orth. (2008). Yersinia Outer Proteins: Yops. *Cellular Microbiology*.

Tsang, Tiffany M, Suleyman Felek, and Eric S Krukonis. (2010). Ail Binding to Fibronectin Facilitates Yersinia Pestis Binding to Host Cells and Yop Delivery. *Infection and Immunity* **78** (8): 3358–68.

Viboud, Gloria I, and James B Bliska. (2005). Yersinia Outer Proteins: Role in Modulation of Host Cell Signaling Responses and Pathogenesis. *Annual Review of Microbiology* **59**: 69–89.

Wattiau, P., and G. R. Cornelis. (1994). Identification of DNA Sequences Recognized by VirF, the Transcriptional Activator of the Yersinia Yop Regulon. *Journal of Bacteriology* **176** (13): 3878–84.

Wessman, Garner E., and Donna J. Miller. (1966). BIOCHEMICAL AND PHYSICAL CHANGES IN SHAKEN SUSPENSIONS OF PASTEURELLA PESTIS. *Applied Microbiology*. Vol. 14. American Society for Microbiology (ASM).

Wiechmann, Anja. (2015). Quorum Sensing and the Regulation of Multicellular Behaviour in Yersinia Pseudotuberculosis. University of Nottingham.

Williams, Paul. (2007). Quorum Sensing, Communication and Cross-Kingdom Signalling in the Bacterial World. *Microbiology* **153** (12): 3923–38.

Winzer, Klaus, Kim R. Hardie, Nicola Burgess, Neil Doherty, David Kirke, Matthew T.G. Holden, Rob Linforth, et al. (2002). LuxS: Its Role in Central Metabolism and the in Vitro Synthesis of 4-Hydroxy-5-Methyl-3(2H)-Furanone. *Microbiology* **148** (4): 909–22.

Wu, Yun, and Wayne Outten. (2009). IscR Controls Iron-Dependent Biofilm Formation in Escherichia Colic by Regulating Type I Fimbria Expression. *Journal of Bacteriology* **191** (4): 1248–57.

Xavier, Karina B., and Bonnie L. Bassler. (2003). LuxS Quorum Sensing: More than Just a Numbers

Game. *Current Opinion in Microbiology*. Elsevier Ltd.

Yang, Y, J J Merriam, J P Mueller, and R R Isberg. (1996). The Psa Locus Is Responsible for Thermoinducible Binding of Yersinia Pseudotuberculosis to Cultured Cells. *Infection and Immunity* **64** (7): 2483–89.

Yates, Edwin A., Bodo Philipp, Catherine Buckley, Steve Atkinson, Siri Ram Chhabra, R. Elizabeth Sockett, Morris Goldner, et al. (2002). N-Acylhomoserine Lactones Undergo Lactonolysis in a PH-, Temperature-, and Acyl Chain Length-Dependent Manner during Growth of Yersinia Pseudotuberculosis and Pseudomonas Aeruginosa. *Infection and Immunity* **70** (10): 5635–46.

Yip, Calvin K, and Natalie C J Strynadka. (2006). New Structural Insights into the Bacterial Type III Secretion System. *Trends in Biochemical Sciences*.

Zavialov, Anton V, Jenny Berglund, Alexander F Pudney, Laura J Fooks, Tara M Ibrahim, Sheila MacIntyre, and Stefan D Knight. (2003). Structure and Biogenesis of the Capsular F1 Antigen from Yersinia Pestis: Preserved Folding Energy Drives Fiber Formation. *Cell* **113** (5): 587–96.

Zhou, Dongsheng, and Ruifu Yang. (2011). Formation and Regulation of Yersinia Biofilms. *Protein and Cell*.

Zietz, Björn P., and Hartmut Dunkelberg. (2004). The History of the Plague and the Research on the Causative Agent Yersinia Pestis. *International Journal of Hygiene and Environmental Health* **207** (2): 165–78.

7 Appendix

7.1 Variant Calling

Table 7.1 SNPs in the genome of *Y. pestis* parent plasmid pCD1 compared to the reference sequence identified by Illumina sequencing.

Nucleotide positions refer to NCBI reference sequence NZ_CP009972.1.

Nucleotide Position	Base Change	Codon Change	Mutation Type	Amino Acid Substitution	Gene	Max Frequency %
29956	TTTAGA - CTCAGG	-	-	-	Non-coding	52
30021	C - T	Cat/Tat	Missense	His27Tyr		51

Table 7.2 SNPs in the genome of *Y. pestis* parent compared to the reference sequence identified by Illumina sequencing.

Nucleotide positions refer to NCBI reference sequence NZ_CP009973.1.

Nucleotide Position	Base Change	Codon Change	Mutation Type	Amino Acid Substitution	Gene	Max Frequency %
16	AC - A				Non-coding	100
150946	C - A	acG/acT	Silent		pckA	100
351821	T - G	caT/caG	Missense	H617Q	YPO0342	100
757473	A - AT				Non-coding	40.59
917155	A - G	Agt/Ggt	Missense	S60G	YPO0837	100
1234971	G - GA				Non-coding	97.96

1245196	T - C	tAc/tGc	Missense	Y57C	tnp	60.98
1383648	G - A	tGc/tAc	Missense	C57Y	tnp	35.71
1939828	T - G	gcA/gcC	Silent		YPO1701	100
1939841	A - G	cTt/cCt	Missense	L555P	YPO1701	100
2052197	T - C				Non-coding	11.11
2273616	G - C	aCg/aGg	Missense	T50R	YPO2000	100
2554169	A - G				Non-coding	43.75
3058095	G - A	gaG/gaA	Silent		YPO2725	25
3058116	C - A	acC/acA	Silent		YPO2725	21.43
3058149	G - A	gaG/gaA	Silent		YPO2725	25
3058167	G - A	gaG/gaA	Silent		YPO2725	36.36
3058260	C - A	acC/acA	Silent		YPO2725	38.46
3058293	G - A	gaG/gaA	Silent		YPO2725	33.33
3201494	T - G	ctT/ctG	Silent		YPO2866	11.54
3201872	C - T	gaC/gaT	Silent		YPO2867	12
3201891	G - A	Ggt/Agt	Missense	G109S	YPO2867	16
3428103	T - C	tAc/tGc	Missense	Y57C	tnp	70.45
3608932	T - C	gAc/gGc	Missense	D109G	gmhA	100
3647867	C - T	gCt/gTt	Missense	A347V	pssA	100
3655609	T - C	Aaa/Gaa	Missense	K553E	clpB	100
3886839	T - C	gaA/gaG	Silent		ibeB	100
3955442	A - G				Non-coding	14.71
3955518	A - C				Non-coding	10.87
4000717	AG - A				Non-coding	28.24
4136713	AG - A				Non-coding	47.47
4390026	G - GC				Non-coding	100

4440607	T - G	acA/acC	Silent		YPO3944	15.48
4624135	C - G	cCc/cGc	Missense	P391R	trmE	100

7.2 PIPS Reflective Statement

Professional Internship at Framework for the Replacement of Animals in Medical Experiments (FRAME)

To fulfil the criteria for a Biotechnology and Biological Science Research Council funded Doctoral Training Partnership PhD studentship, in addition to the process of training that happens through the first six-months of laboratory rotations, I also undertook a three-month professional internship at FRAME where I worked alongside their Scientific Liaison Officer. FRAME is an independent charity with the ultimate aim of the replacement of animals in medical experiments. They focus on promoting and researching new, ethical and valid scientific methods that will replace the need for laboratory animals in scientific research, education and testing. Where the use of animals is still necessary, FRAME champion the reduction of numbers and refinement of methods to minimise suffering. They also fund the FRAME alternatives laboratory, who directly research these alternatives. For my placement I worked alongside FRAMEs Scientific Liaison Officer, who oversees the day-to-day running of the charity. My particular focus was on public engagement and creating content for the FRAME website.

The activities I was involved in included:

- Writing about the research of the FRAME alternatives laboratory for the general public
- Liaising with researchers for relevant publications, images and arranging meetings
- Preparing a variety of written material for the FRAME website including blog posts surrounding the wider issues animals in science
- Attending a symposium and talks about animals in science and the principles of the 3Rs
- Identifying potential corporate sponsors for the upcoming FRAME symposium

The skills I developed during this project included:

- Enhanced written communication skills to a wide audience
- An understanding of motivations and values of the charity
- An understanding of the process of obtaining sponsors and funding as a charity
- Project management skills and an ability to manage multiple projects simultaneously
- Greater understanding of animal experiments and the principles and implementation of the 3R's
- Greater understanding of mammalian cell-based research

I am incredibly grateful for FRAME for the fantastic opportunity to work with them, in particular Amy Beale and Andrew Bennett who coordinated my project.